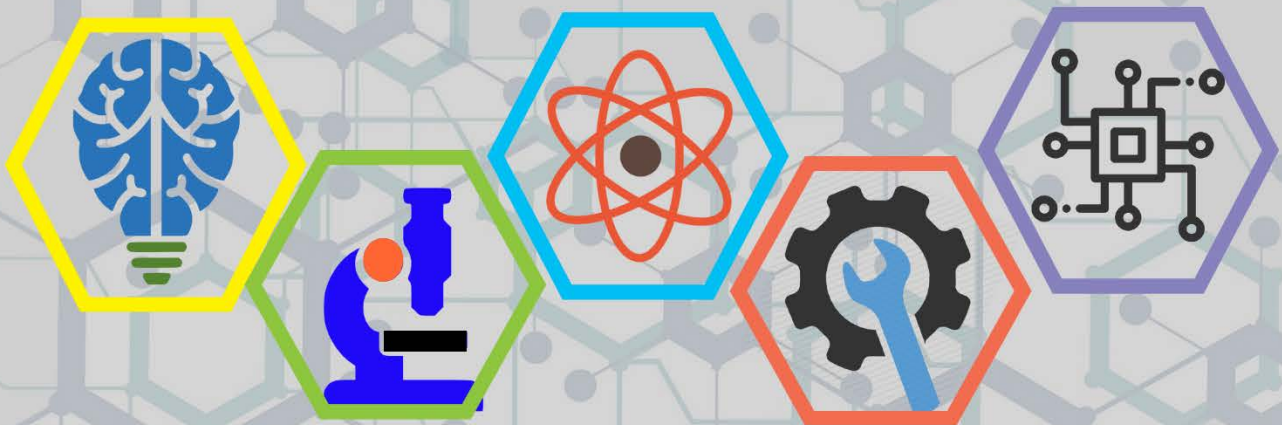


ISSN: 2687-2153

IJEIR

International Journal of Engineering & Innovative Research



Volume: 2 Issue: 2

International Journal of Engineering and Innovative Research (IJEIR)

Year: 2020

Volume: 2

Issue: 2

Editor in Chief

Dr. Ahmet Ali SÜZEN
Isparta University of Applied Sciences

Editorial Board Secretaries

Osman CEYLAN
Isparta University of Applied Sciences

Ziya YILDIZ
Isparta University of Applied Sciences

Correspondence Address

International Journal of Engineering and Innovative Research (IJEIR)
Secretaries Office
Isparta University of Applied Sciences
Uluborlu Selahattin Karasoy Vocatioal School
Uluborlu / Isparta / Turkey

Phone and e-mail

Tel: +90 0246 531 26 21 - 0246 531 26 22

E-mail: ijeirturkey@gmail.com

e-ISSN: 2687-2153

International Journal of Engineering and Innovative Research (IJEIR)

Year: 2020

Volume: 2

Issue: 2

Editorial Board

Prof. Dr. Narita Md Norwawi Universiti Sains Islam Malaysia University- MALAYSIAN
Prof. Dr. Shivam Mishra Dr. A.P.J. Abdul Kalam Technical University- INDIA
Prof. Dr. Fu Jianzhong Zhejiang University – CHINA
Prof. Dr.Hans-Jörg Trnka Fusszentrum Wien – AUSTRIA
Assoc. Prof Dr. Deniz KILINÇ İzmir Bakırçay University - TURKEY
Asst. Prof. Dr. Burhan DUMAN Applied Sciences University of Isparta - TURKEY
Dr. Merve VAROL ARISOY Mehmet Akif Ersoy University - TURKEY

Advisory Board

Prof. Dr. Kamaruzzaman Seman Universiti Sains Islam Malaysia University- MALAYSIAN
Prof. Dr. David HUI University of New Orleans- USA
Prof. Dr. Vladimir Jotsov University of Library Studies and IT - BULGARIA
Assoc. Prof Dr. Madihah MOHD SAUDI Universiti Sains Islam Malaysia - MALAYSIA
Assoc. Prof Dr. Azni Haslizan Ab Halim Universiti Sains Islam Malaysia - MALAYSIA
Asst. Prof. Dr. Ali Dinç American University of Middle East - KUWAIT
Dr. Fotis Kokkoras Technological Educational Inst. of Thessaly – GREECE

Reviewers for this issue

Roya ASADI
Aniekan IKPE
Koray ÖZSOY
Kate UKPE
Tahya TOMA
Gülhan INCE

Olufemi ONI
Ali Tekin GÜNER
Ali Riza MOTORCU
Önder KIZILKAN
İhsan PENÇE
Cengiz ÖZEL

International Journal of Engineering and Innovative Research (IJEIR)

Year: 2020

Volume: 2

Issue: 2

CONTENTS

PAGE

Research Articles

Angular solar relations analysis of a flat plate solar collector in Benin City metropolis

Eghosa OMO-OGHOGHO, Aniekan IKPE.....67-77

POLAR SIMULATION OF SUBSONIC FLOW AROUND NACA 4610 AIRFOIL IN HORIZONTAL AXIS WIND TURBINE

Ekom ETUK, R. S. EBHOJIAYE, Patrick AMÍOLEMHEN.....78-91

A STUDY OF THIN PLATE VIBRATION USING HOMOTOPY PERTUBATION ALGORITHM

Falade KAZEEM IYANDA, Tiamiyu ABD'GAFAR, Tolufase EMMANUEL.....92-101

TÜRKİYE'NİN AKDENİZ BÖLGESİNE AİT RÜZGÂR EKSERJİSİNİN ÇOK KATMANLI YAPAY SİNİR AĞI İLE MODELLENMESİ

Durmuş Fatih MENGİ, Sedat METLEK.....102-120

Analysis of a simulated flat plate solar collector system using solidworks flow simulator interface

Eghosa OMO-OGHOGHO, Godwin SADIJERE.....121-128

THREE-DIMENSIONAL MODAL ANALYSIS OF BEAMS WITH TRIANGULAR AND HEXAGONAL CROSS SECTIONS USING DIFFERENT CERAMIC MATERIALS

Savaş EVRAN.....129-136

DETERMINATION OF ATTITUDES AND QUALIFICATIONS OF CIVIL ENGINEERING STUDENTS FOR USE OF PACKAGE PROGRAM

Melda ALKAN ÇAKIROĞLU.....137-147



ANGULAR SOLAR RELATIONS ANALYSIS OF A FLAT PLATE SOLAR COLLECTOR IN BENIN CITY METROPOLIS

Eghosa Omo-Oghogho^{1*} , Ikpe Aniekan Essienubong¹

¹ Department of Mechanical Engineering, University of Benin, P.M.B 1154, Benin City, Nigeria.

*Corresponding Author: eghosa.omo-oghogho@uniben.edu

(Received: 26.04.2020; Revised: 20.05.2020; Accepted: 15.06.2020)

ABSTRACT: The sun is one of the major sources of energy, the distance, position and rotation of the sun and the earth are obtained for proper collector design. The declination angles, zenith angles, solar azimuth angles and the incident angles of Benin City, Edo State were obtained considering the ambient conditions, longitude and latitudes of site under consideration. This was achieved through experimental investigation using a prototype designed flat plate solar collector system. Average declination angle of 14.6675, average zenith Angles of the sun of 22.1850, average incidence angle of 21.7650, average solar Azimuth angle of 77.0625 and average ratio of beam radiation of 1.0875 were obtained respectively. As a result of this, the average radiation on a tilted surface were obtained to be 1025.3258w/m² for enhanced flat plate solar collector design.

Keywords: Flat Plate Solar Collector, Tilt Angle, Declination Angle, Zenith Angles of The Sun, Solar Azimuth Angle, Incidence Angle, Ratio of Beam Radiation

1. INTRODUCTION

The annual amount of solar radiation received by the earth varies due to the changeable distance between the earth and the sun. The Earth- Sun distance has a minimum value of 1.471×10^{11} m which is called, perihelion, on December 21 and a maximum value of 1.512×10^{11} m which is called, aphelion, on June 21 [1]. The average distance between the earth and the sun that is called astronomical unit (AU) is 1.419×10^{11} m. The earth revolves around itself within an axis that has tilted angle of 23.45° with respect to its orbital plane axis [2]. This angle is the cause of the changeable solar radiation throughout the year.

Solar energy is a form of renewable energy that can be used in one form or another. This research work shows that a lot depends on the position and distance between the sun and the rotation of the earth.

Nielsen [3] gave an expression for determination of the global horizontal solar radiation intensity in nth hours of the day. Bena and Fuller [4], Sharma, Chen and Nguyen [5] and Iloeje [6] indicated that solar energy trapped by solar dryers is now commonly used globally in drying and preservation of agricultural products. The uses of helio-electrical devices, which trap solar radiation on horizontal plane, are increasing world-wide.

The total energy output of the sun is about 3.8×10^{20} MW which is equal to 63 MW/m² of the sun's surface. Although the energy radiates in all directions relative to its location, only a small fraction of about 1.7 Kw of the total radiation emitted is intercepted by the earth [7]. Hanif et

al. [8] analyzed the energy, exergy and efficiency of a flat plate solar air heater based on five different air mass flow rates of 0.5 (Natural), 1.31, 2.11, 2.72 and 3.03 kgs^{-1} under three different tilt angles of 25, 35 and 50°. From the results obtained, the solar collector performance better at air mass flow rate of 3.03 kgs^{-1} under tilt of 35°. At maximum air mass flow rate of 3.03 kgs^{-1} and optimum tilt angle of 35°, the maximum energetic efficiency of 51%, minimum exergetic efficiency of 24% as well as maximum overall efficiency of 71% were obtained.

Dare et al. [9] investigated the efficiency and insolation of flat plate solar collectors considering selected locations in the six geopolitical zones of Nigeria at different tilts. Performance of a flat plate collector in relation to heat transfer fluid in the absorber was examined using Standard Equation known as the Hottel -Whillier- Bliss Equation. The results obtained indicated that, as the incidence angle approaches 0°, insolation become maximum and as incidence angle approaches 90°, insolation becomes minimum.

To establish the dependence of first law efficiency, second law efficiency, orientation of flat plate collector, average temperature rise on the mass flow rate of water as well as the greenhouse effect, Swain et al. [10] experimentally investigated a solar water heater in technical collaboration with Welson Energy Systems which uses variable water flow rate ranging from 0.001-0.02 kgs^{-1} . The results revealed that the instantaneous efficiency increases with increase in mass flow rate while the second law efficiency decreased with increase in mass flow rate. The instantaneous efficiency and second law efficiency were observed to be more significant with greenhouse effect than it is without the greenhouse effect. Exergy loss was found to be more significant without greenhouse effect than it is with greenhouse effect. Skeiker [11] in an investigation of the optimum tilt angle for Syrian regions reported that the adjustment of solar collector tilt angle has the potential to increase the solar energy collection by 10%.

An empirical correlation of Erbs to determine the optimal tilt angle for Abu Dhabi was employed by Jafarkazemi and Saadabadi [12]. It was suggested that the tilt angle be adjusted for at least semi-annually. The difference between annual average optimum tilt angle and the latitude was obtained as 2-3° and azimuth was suggested close to the due south. This correlates with the findings of Soulayman and Hammoud [13], where the general correlation for mid latitudes was derived to determine the optimum tilt angle of solar collectors. Optimum tilt angle was observed to not exactly depend on the latitude and should be adjusted for the collector at least semi-annually. Also in a study conducted by Khorasanizadeh et al. [14] using several diffused radiation models and long term solar radiation data availed to determine the optimum tilt angle for a site located in Iran, semi-annual adjustment of surface tilt was suggested.

Ucar et al. [15] employed five different geometries in solar air collector to improve the performance of the heater using passive heat transfer enhancement techniques. Among the solar collectors tested, collector with absorber surface at 2° angle was found to be optimum. On the other hand, Jamil et al. [16] suggested at least a seasonal or monthly adjustment of tilt angle for optimum output based on their findings obtained from optimum tilt for solar collectors at two sites in India using measured solar radiation data. The tilt angle for several cities in Saudi Arabia was optimized by Kaddoura et al. [17] using MATLAB model. Adjustment of tilt angle of the solar collector was suggested as six times annually. For optimum tilt angle, frequent adjustments was suggested in the months near equinox, due to rapid change in the direction of the sun compared to solstices. Bhowmik and Amin [18] developed a novel technology to

improve the performance of the solar thermal collectors. To maximize the intensity of incident radiation, the reflector was allowed to change its angle with daytime. The radiations coming from the sun's energy were converted into heat which was transferred to a prototyped solar water heating system. Collector efficiency of around 10% was obtained using the reflector. A flat plate surface solar collector of dimension 0.5 m², hinged on a horizontal support at inclination from 0-90° was fabricated in Zaria, Kaduna State, Nigeria by Akachukwu [19]. Solar radiation and varying degrees of inclination were taken for each month of the year. The result showed that optimum angle of inclination of a flat plate for maximum collection of solar radiation intensities were 26.5, 24.5, 10.0, 19.5, 26.0, 30.0, 24.0, 21.0, 11.5, 19.5, 27.0 and 30.0°, in the months of January to December. An average annual increment of 4.23 % solar radiation intensity was achieved for flat surface located at the predicted optimum angle of inclination for each month when compared to the yearly average solar radiation intensity obtained from the same flat plate collector on horizontal position, and under the same condition.

The aim of this research is to effectively predict optimum angles of inclination and amount of solar energy gained, using Benin City, Edo State, Nigeria as the location of study.

2. MATERIALS AND METHOD

To carry out the experimentation using the designed flat plate solar collector, the amount of solar radiation, day, declination angle, zenith angle of the sun, azimuth angle and the angle of incidence on the inclined surface was determined. A particular day in each month was chosen (mid-month), this day has approximately the total solar radiation which is equal to the monthly mean value for that particular month [20]. To design a solar flat plate collector, the area was determined considering the temperature of fluid (water) expected and the expected solar radiation of the location. The heat requirement is a function of the mass flow rate and the time of heating. Figure 1 shows an isometric view of the flat plate solar collector experimental set-up tilted at 10° and has a water supply tank and a water discharge tank. The materials used in the flat plate solar collector setup are as follows: Wood used for casing, fibre (Polyurethane) used for insulation, aluminium painted black used for absorber plate, copper used for flow tube, transparent glass used for glazing cover, plastic used for water supply and discharged tank, plastic hose used for connecting the water tanks. The following initial conditions were considered for the flat plate solar collector system.

- i. Steady state system.
- ii. 26.1°C daily average water inlet temperature (Relates to ambient temperature obtained from the National Centre for Energy and Environment (NCEE), University of Benin, Edo State, Nigeria.
- iii. Active heating time of the water is estimated to be about 6 hours, within which the sun is actively present. Though daily peak temperature may vary with time.
- iv. 100°C absorber plate temperature.
- v. Average daily solar radiation $I = 1017.695W/m^2$ from NCEE, University of Benin.
- vi. Specific heating capacity of water $Cp = 4190J/kgK$.
- vii. Tilt angle of 10°
- viii. 300 litres capacity water tank was used to supply water to the solar collector. The tank was placed at 0.5m height from the collector inlet, thus creating the required pressure head for circulation of water in the system.

- ix. The surface azimuth angle is 0° (the collector is facing the south).
- x. The solar parameters are calculated with the sun one hour after noon i.e. 15° .

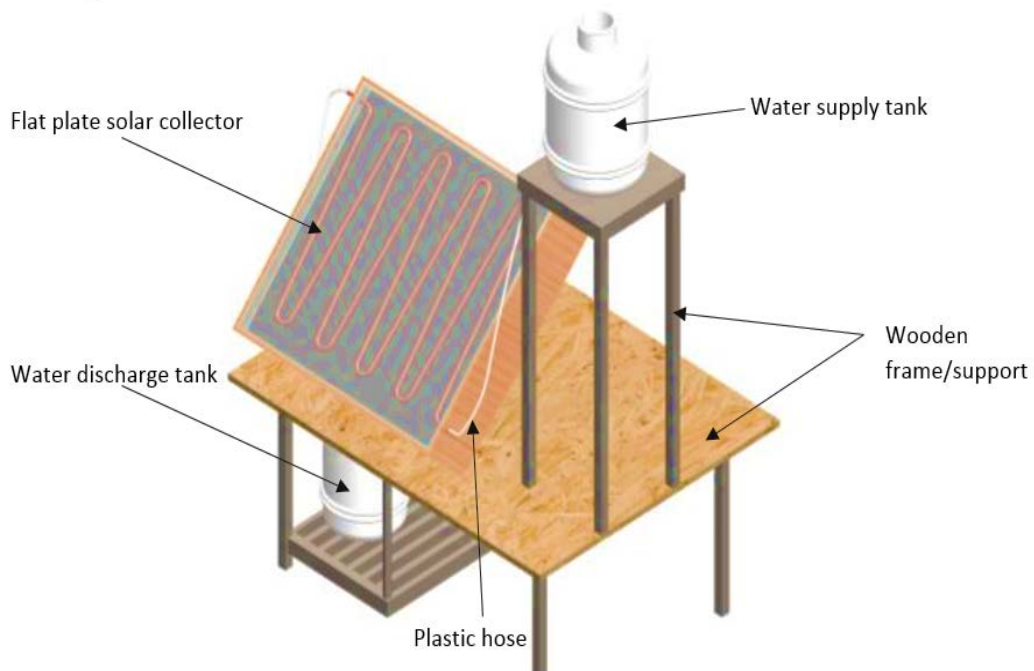


Figure 1. Flat plate solar collector setup.

2.1. Declination Angle

To effectively estimate the solar radiation of a tilted surface, there is need to know the angular position of the sun at solar noon, hence the determination of the declination angle considering the number of days. Declination angle varies and is calculated using the following relation:

$$\delta = 23.45 \sin\left(360 \frac{284+n}{365}\right) \tag{1}$$

where n is the no of days. For n , the mean day in each month was used.

For January $n=17$, from Table 1.

Table 1. Recommended average days of various months and values of n by months [21].

Months	Days of the month	Mid-month	N
January	I	17	17
February	31 + i	16	47
March	59 + i	16	75
April	90 + i	15	105
May	120 + i	15	135
June	151 + i	11	162
July	181 + i	17	198
August	212 + i	16	228
September	243 + i	15	258
October	273 + i	15	288
November	304 + i	14	318
December	334 + i	10	344

2.2. Zenith Angles of The Sun

The Zenith angle was estimated considering the angle between the vertical and the line to the sun, that is, the angle of incidence of beam radiation on a horizontal surface has to be known in order to effectively estimate the amount of solar radiation on a solar collector.

The zenith angle is given by

$$\cos \theta_z = \cos \phi \cos \delta \cos \omega + \sin \phi \sin \delta \quad (2)$$

Where, $\phi = 6.5438^\circ$ (*latitude of Benin City, Edo State, Nigeria*)

δ = declination angle.

ω = Hour angle. (15° was used because 1pm was considered as the time, during the system analysis)

2.3. Solar Azimuth Angle (γ_s)

The solar azimuth angle is estimated using the following relations:

$$\gamma_s = \text{sign}(\omega) \left| \cos^{-1} \left(\frac{\cos \theta_z \sin \phi - \sin \delta}{\sin \theta_z \cos \phi} \right) \right| \quad (3)$$

Where, Sign function is used to determine ω .

θ_z = Zenith angle.

ϕ = latitude of site.

δ = Declination angle.

2.4. Incidence Angle

The angle of incidence on the inclined surface is given by

$$\cos \theta = \cos \theta_z \cos \beta + \sin \theta_z \sin \beta \cos(\gamma_s - \gamma) \quad (\text{Duffie and Beckman, [21]}) \quad (4)$$

Where, θ = incidence angle.

β = tilted angle

$\gamma = 0$, because it is facing south.

θ_z = Zenith angle.

γ_s = Solar azimuth angle.

2.5. Radiation on Tilted Surface

The data collected from the National Centre for Energy and Environment [22] are related to the horizontal surface, for purposes of solar process design and performance calculations, it is often necessary to calculate the radiation on a tilted surface of a collector from measurements or estimates of solar radiation on a horizontal surface. The geometric factor R_b , is the ratio of beam radiation on the tilted surface to that on a horizontal surface and this can be estimated using the following relations.

$$R_b = \frac{\cos \theta}{\cos \theta_z} = \frac{G_{b,t}}{G_h} \quad (5)$$

Where, θ = angle of incidence.

θ_z = zenith angle respectively.

$G_{b,t}$ = radiation on tilted surface.

G_h = radiation on horizontal surface.

To utilize R_b the radiation on the horizontal surface was gotten from National Centre for Energy and Environment (NCEE), University of Benin, Edo State, Nigeria [22].

To determine the available energy in the solar collector, it is important to consider the equation for energy gained by the working fluid. This is given by Equation 6 [23],

$$Q_{use} = m_a C_p \Delta T \quad (6)$$

Equation for heat losses from the collector as the fluid flows from the solar collector to the atmosphere is expressed as [27]:

$$Q_{use} = A_{abs} Q_r [S_i - U_1 (\Delta T)] \quad (7)$$

The energy leaked from the solar collector is given by Equation 8 [24].

$$E_1 = \left\{ U_1 A_{abs} (T_{abs} - T_a) \left(1 - \frac{T_a}{T_{abs}} \right) \right\} \quad (8)$$

where S_i is the optical absorbed solar flux and U_1 is the heat lost by emittance, reflection and optical efficiency of glazing given by Equation 9 [25].

$$Q_R = \frac{m a C_p}{U_1 A_{abs}} \left[1 - \exp \left\{ \frac{-F \phi U_1 A_{abs}}{m a C_p} \right\} \right] \quad (9)$$

The energy destroyed by the solar collector is given by Equation 10 [26].

$$E_d = -m C_p T_a \frac{T_{out}}{T_{in}} E_d = -m C_p T_a \left\{ 1 n \left(\frac{T_{out}}{T_{in}} \right) - \left(\frac{T_{out} - T_{in}}{T_{abs}} \right) \right\} \quad (10)$$

where E_d is the heat lost energy due to absorber plate temperature difference with the fluids. It is the latent heat absorbed by the fluids in phase change. The exergy of the solar collector is given by Equation 11[27].

$$E_{out} = \left[\left\{ \left(m_a C_p (T_{out} - T_a) T_a \ln \frac{T_{out}}{T_a} \right) - \frac{m \Delta P_{out}}{\rho} \right\} + m_w C_p (T_w - T_a) \right] \quad (11)$$

The discharge flow rate of water expressed in m^3/sec is given by Equation 12

$$Q = \frac{\pi}{4} d^2 v \quad (12)$$

where d is the diameter of the collector pipe and v is the average velocity of fluid. In this case, the angle of incidence is given by Equation 13 [28].

$$\begin{aligned} \cos \theta = & \sin \phi (\sin \delta \cos \beta + \cos \delta \cos \gamma \cos \omega \sin \beta) + \cos \phi (\cos \delta \cos \omega \cos \beta - \\ & \sin \delta \cos \gamma \sin \beta) + \cos \delta \sin \gamma \sin \omega \sin \beta \end{aligned} \quad (13)$$

where δ is the Declination angle, n is no of day in the yea, β is the slope angle ϕ is the latitude of the location γ is the surface azimuth angle and ω is the hour angle. Tilt factor for beam radiation is given by Equation 14.

$$r_{rb} = \frac{\cos \theta}{\cos \theta_z} \quad (14)$$

$$\cos \theta_z = (\sin \phi * \sin \delta) + (\cos \phi * \cos \delta * \cos \omega) \quad (15)$$

Radiation shape factor for the diffused radiation is given by Equation 16 while the tilt factor for reflected radiation is given by Equation 17.

$$R_d = \frac{(1 + \cos \beta)}{2} \quad (16)$$

$$r_r = \frac{\rho(1 - \cos \beta)}{2} \quad (17)$$

Instantaneous efficiency is given by Equation 18 while exergy (e) is given by Equation 19

$$\eta_i = \frac{\dot{m} C_p (T_2 - T_1)}{I_t * A_p} \quad (18)$$

$$e = (h - h_o) - T_o(S - S_o) + \frac{v^2}{2} + gz \quad kJ/kg \quad (19)$$

3. RESULTS AND DISCUSSION

3.1. Angular Relations of Solar Radiation

The thermodynamic analysis was carried out considering some conditions, these conditions are ambient conditions, materials, the location of study and the mid-month in each month. The mid-months are recommended average days of various months and values of n by months. A particular day in each month was chosen (mid-month), this day has approximately the total solar radiation which is equal to the monthly mean value for that particular month.

3.1.1. Declination angle

Declination angle was estimated for a year considering the mid-month. Using Equation 1, the declination angle from January to December were gotten as follows.

Table 2. Declination angle from January to December for Benin City, Edo State.

Mid-Month	Latitude (ϕ)	No of Days(n)	Declination (d)
17 January 2018	6.5438	17	-20.91696257
16 February 2018		47	-12.95460809
16 March 2018		75	-2.417734805
15 April 2018		105	9.414893347
15 May 2018		135	18.79191752
11 June 2018		162	23.085911
17 July 2018		198	21.18369356
16 August 2018		228	13.45495968
15 September 2018		258	2.216886783
15 October 2018		288	-9.599397234
14 November 2018		318	-18.91195474
10 December 2018		344	-23.04962764

Table 2 shows the analysis of the declination angle from January to December for Benin City, Edo State, the mid-month, latitude and number of days were considered during the analysis. This analysis was carried out because the angle of declination is necessary to estimate for the angle of incidence which enables the radiation on a tiled surface to be known.

3.1.2. Zenith angle

The zenith angle was estimated for a period of one year and it was done using Equation 2 as follows.

Table 3. Zenith angle from January to December in Benin City, Edo State.

Mid-Month	Latitude (θ)	No of Days(n)	Zenith Angle (θ_z)
17 January 2018	6.5438	17	31.16223057
16 February 2018	6.5438	47	24.54156547
16 March 2018	6.5438	75	17.45151134
15 April 2018	6.5438	105	15.12726132
15 May 2018	6.5438	135	19.05767107
11 June 2018	6.5438	160	21.95626908
17 July 2018	6.5438	198	20.61477906
16 August 2018	6.5438	228	16.29885949
15 September 2018	6.5438	258	15.56579039
15 October 2018	6.5438	288	21.99881101
14 November 2018	6.5438	318	29.43745646
10 December 2018	6.5438	344	33.02824726

Table 3 shows the analysis of the Zenith angle from January to December for Benin City, Edo State, the mid-month, latitude, number of days and the hour angle were considered during the analysis. This analysis enables us to know the angle between the vertical and the line to the sun, that is, the angle of incidence of beam radiation on a horizontal surface.

3.1.3. Solar azimuth angle

The solar azimuth angle was estimated using Equations 3 and this was done for a period of one year. It is shown on Table 4.

Table 4. Solar Azimuth angle from January to December in Benin City, Edo State.

Mid-Month	Latitude (θ)	No of Days(n)	Declination (d)	Solar Azimuth Angle(γ_s)
17 January 2018	6.5438	17	-20.91696257	-27.81909576
16 February 2018	6.5438	47	-12.95460809	-37.39236626
16 March 2018	6.5438	75	-2.417734805	-59.57057582
15 April 2018	6.5438	105	9.414893347	101.9242569
15 May 2018	6.5438	135	18.79191752	131.374367
11 June 2018	6.5438	162	23.085911	140.4476725
17 July 2018	6.5438	198	21.18369356	136.7302372
16 August 2018	6.5438	228	13.45495968	116.2453433
15 September 2018	6.5438	258	2.216886783	74.53216113
15 October 2018	6.5438	288	-9.599397234	-42.94294037
14 November 2018	6.5438	318	-18.91195474	-29.88037461
10 December 2018	6.5438	344	-23.04962764	-25.9089543

Table 4 shows the analysis of the solar Azimuth angle from January to December for Benin City, Edo State, the mid-month, latitude, number of days, hour angle and declination were considered during the analysis. This analysis helps to show the angular displacement from south of the projection of beam radiation on the horizontal plane.

3.1.4. Incidence angle

The angle of incidence on an inclined surface was determined using Equation 4 as shown in Table 5.

Table 5. Incident angles from January to December of Benin City, Edo State.

Mid-Month	Latitude (θ)	No of Days(n)	Angle of Incidence
17 January 2018	6.5438	17	22.75053397
16 February 2018	6.5438	47	17.60890387
16 March 2018	6.5438	75	15.01592951
15 April 2018	6.5438	105	19.72562973
15 May 2018	6.5438	135	26.70224584
11 June 2018	6.5438	162	30.30883487
17 July 2018	6.5438	198	28.68973778
16 August 2018	6.5438	228	22.53011347
15 September 2018	6.5438	258	16.03038807
15 October 2018	6.5438	288	16.11188848
14 November 2018	6.5438	318	21.30486345
10 December 2018	6.5438	344	24.38399044

Table 5 shows the analysis of the incident angle from January to December for Benin City, Edo State, the mid-month, latitude and the number of days were considered during the analysis.

3.1.5. Ratio of beam radiation

The ratio of beam radiation is a geometric factor that deals with the ratio of beam radiation on the tilted surface to that on a horizontal surface. For the purposes of solar process design and performance calculations, it is often necessary to calculate the radiation on a tilted surface of a collector from measurements or estimates of solar radiation on a horizontal surface. The values on Table 6 were gotten using Equation 5.

Table 6. Ratio of beam radiation from January to December of Benin City, Edo State.

R_b	G_h (W/m²)	G_{b,t}(W/m²)
1.08	1017.695	1099.11
1.05	1017.695	1068.58
1.01	1017.695	1027.87
0.98	1017.695	997.34
0.95	1017.695	966.81
0.93	1017.695	946.46
0.94	1017.695	956.63
0.96	1017.695	976.98
0.99	1017.695	1007.52
1.04	1017.695	1058.40
1.07	1017.695	1088.93
1.09	1017.695	1109.28

Table 6 shows the analysis of the ratio of beam radiation from January to December for Benin City, Edo State, the Zenith angle and the angle of incidence were considered during the analysis. $G_{b,t}$ (W/m²) was gotten by multiplying R_b by the horizontal solar radiation which was gotten from National Centre for Energy and Environment (NCEE), University of Benin, Edo State Nigeria).

4. CONCLUSION

The estimation of the various angles which are declination angles, zenith angles, solar azimuth angles and the incident angles was geared towards obtaining the radiation on a tilted surface. It is necessary to obtain the radiation on a tiled surface because the flat plate collector is tilted at some angle to get optimum solar energy. The available solar radiation of the locations shows a positive availability of renewable energy in the form of solar energy and the angular solar relations were estimated for the months of more solar radiation and the positions in which the solar thermal system (experimental setup) can be placed for more solar energy absorption.

REFERENCES

- [1] Foster, Robert, Majed Ghassemi and Alma Cota. (2010): Solar energy: renewable energy and the environment. Boca Raton: CRC press.
- [2] Goswami, D. Yogi, Frank Kreith and Jan F. Kreider. (1999): Principles of solar engineering. 2nd. Philadelphia: Taylor & Francis.
- [3] Nielsen, R. 2005. Solar Radiation. <http://home.iprimus.com.au/niensens/>.
- [4] Bena, B. and R. J. Fuller. 2002. Natural convection solar dryer with biomass back up heater. Journal of Solar Energy, 72 (1): 75-83.
- [5] Sharma, A., C. R. Chen, and V. Nguyen. 2009. Solar energy drying systems: a review. *Renewable and Sustainable Energy Review*, 13(6-7):1185-1210.
- [6] Iloeje, O. C. 1993. Design, operation and performance of a solar rice dryer. In proc. 2nd Workshop on "SDTAI", Nsukka, Nigeria, 24-27 November.

- [7] Kreith, F. and Kreider, J. F. (1978) Principle of solar engineering.
- [8] Hanif, M., Khattak, M. K., Khan, M. and Ramzan, M. (2018) Energy, Exergy and Efficiency Analysis of a Flat Plate Solar Collector Used as Air Heater. *Sains Malaysiana* 47(5), 1061-1067.
- [9] Dare, A. A., Odunfa, K. M., Ajuka, L. O., Oyedepo, S. O. and Adeaga, O. A. (2017) Estimation of insolation of flat plate solar collectors in selected cities in Nigeria. *International Journal of Computational Engineering Research*, 7(12), 14-28.
- [10] Swain, B., Memon, S. A. and Achari, A. M. (2019) Parametric Analysis of Inclined Flat Plate Collector: A Review with Case Study. *International Journal of Applied Engineering Research* 14(7), 1658-1667.
- [11] Skeiker, K. (2009) Optimum tilt angle and orientation for solar collectors in Syria. *Energy Convers. Manag.*, 50(9), 2439–2448.
- [12] Jafarkazemi, F. and Saadabadi, S. A. (2013) Optimum tilt angle and orientation of solar surfaces in Abu Dhabi, UAE. *Renewable Energy*, 56, 44–49.
- [13] Soulayman, S. and Hammoud, M. (2016) Optimum tilt angle of solar collectors for building applications in mid-latitude zone. *Energy Conversion Management*, 124, 20–28.
- [14] Khorasanizadeh, H., Mohammadi, K. and Mostafaeipour, A. (2014) Establishing a diffuse solar radiation model for determining the optimum tilt angle of solar surfaces in Tabass, Iran. *Energy Convers. Manag.*, 78, 805–814.
- [15] Ucar, A. and Inall, M. (2006) Thermal and exergy analysis of solar air collectors with passive augmentation techniques. *Int. Commun. Heat Mass Transf.*, 33(10), 1281–1290.
- [16] Jamil, B., Siddiqui, A. T. and Akhtar, N. (2016) Estimation of solar radiation and optimum tilt angles for south-facing surfaces in Humid Subtropical Climatic Region of India. *Eng. Sci. Technol. an Int. J.*, 19(4), 1826–1835.
- [17] Kaddoura, T. O., Ramli, M. A. M. and Al-Turki, Y. A. (2016) on the estimation of the optimum tilt angle of PV panel in Saudi Arabia. *Renew. Sustain. Energy Rev.*, 65, 626–634.
- [18] Bhowmik, H. and Amin, R. (2017) Efficiency improvement of flat plate solar collector using reflector. *Energy Reports*, 3, 119–123
- [19] Akachukwu, B. E. (2011) Prediction of optimum angle of inclination for flat plate solar collector in Zaria, Nigeria. *Agricultural Engineering International: CIGR Journal*. 13(4), 1-11. 2011.
- [20] Klein, S.A (1977): Calculation of monthly average insolation on tilted surfaces, solar energy laboratory, University of Wisconsin-Madison, Madison, WI 53706, USA.
- [21] Duffie, J.A. and Beckman, W.A. (2013): *Solar Engineering of Thermal Processes*. John Wiley and Sons, inc., New York.
- [22] National Centre for Energy and Environment (NCEE) (2017), University of Benin, Edo State Nigeria.
- [23] Al-Sulaiman, F.A. 2014. Exergy analysis of parabolic trough solar collectors integrated with combined steam and organic Rankine cycles. *Energy Conversion and Management* 77: 441-449.
- [24] Calise, F., d'Accadia, M.D., Macaluso, A., Piacentino, A. & Vanoli, L. 2016. Exergetic and exergoeconomic analysis of a novel hybrid solar–geothermal polygeneration system producing energy and water. *Energy Conversion and Management* 115(1): 200-220.
- [25] Jafarkazemi, F. & Ahmadifard, E. 2013. Energetic and exergetic evaluation of flat plate solar collectors. *Renewable Energy* 56: 55-63.
- [26] Farahat, S., Sarhaddi, F. & Ajam, H. 2009. Exergetic optimization of flat plate solar collectors. *Renewable Energy* 34(3): 1169-1174.
- [27] Islam, S., Dincer, I. & Yalbas, B.S. 2015. Energetic and exergetic performance analysis of a solar energy-based integrated system for multi generation including thermoelectric generators. *Energy* 93: 1246-1258.
- [28] Kalogirou, S.A., Karellas, S., Badescu, V. & Braimakis, K. 2016. Exergy analysis on solar thermal systems: A better understanding of their sustainability. *Renewable Energy* 85: 1328-1333.



POLAR SIMULATION OF SUBSONIC FLOW AROUND NACA 4610 AIRFOIL IN HORIZONTAL AXIS WIND TURBINE

Etuk Ekom Mike^{1*}, Ebhojiaye Raphael Sylvester¹, Amiolemhen Patrick¹

¹University of Benin, Faculty of Engineering, Department of Production Engineering, Benin City, Nigeria.

*Corresponding Author: alwayssetuk@gmail.com

(Received: 06.05.2020; Revised: 25.05.2020; Accepted: 15.06.2020)

ABSTRACT: This study provide details on the characteristics of horizontal axis wind turbine airfoil under subsonic flow regime at distinct angle of attacks (AoA) using XFOIL. Using a fixed Mach number (Ma) of 1000,000 and Renolds number (Re), the XFOIL modelled cambered airfoil was simulated at various AoA including -10°, -5°, 0.0°, 5°, 10°, 15°, 22° and 25° to observe the variations in lift, drag, lift and drag coefficient and their effects on the overall wind turbine performance. It was observed that constant increase in AoA can prevent separation in airflow while continuous reduction in AoA can make airflow separation more pronounce, thereby, causing decrease in the rate at which the lift coefficient increases. A negative pitching moment coefficient was observed, indicating a nose-down moment which would reduce the angle of attack on the rotor blade. It was also found that the drag coefficient C_D varied proportionately with the AoA, and lower C_D values indicate less drag foces on the on the airfoil. The results indicated that the lift to drag ratio initially increase as the AoA increases upto a maximum point of 108.64, but as the AoA is increased further, the L/D ratio decreases until the stalling angle is reached. In summary, the rotor blade undergoes minimum drag at fairly low AoA while the lifting ability of the rotor is quite low at low AoA.

Keywords: Wind Turbine, Blade Foil, Drag Force, Aerodynamics, Lift Force, Renolds Number

1. INTRODUCTION

To achieve full range of optimal operating condition in a wind turbine blade, robust numerical and computational approach is required in addition to the design calculations. The outcome can be validated by comparing with experimental data for accuracy of results [1]. According to Bertagnolio et al. [2], experimental measurement and/or flow field simulation of airfoils are used as the basis for evaluating the aerodynamic behaviour of wind turbine blades. Alrobaian et al. [3] designed and fabricated a low cost open typed subsonic compressible flow wind tunnel and the flow field measured as wall pressure reading indicated a stable flow at Mach number of 0.6, 0.7, 0.8 and 0.9 respectively. Moreover, with approximately 80% area, the exit velocity was found to be constant. Winslow et al. [4] examined NACA 0009 and NACA 0012 airfoils for drag and lift performance as well as surface pressure and flow field characteristics. The result revealed that below Re of 10^6 , lift and drag characteristics were difficult to be assumed optimum or better but below Re of 10^5 , the cambered airfoils had better lift and drag characteristics. Arun and Surya [5] designed a horizontal axis wind turbine with two different airfoil sections including the straight and swept back pattern using QBlade. The straight blade design produced 250KW of power at peak wind speed of 36m/s while the swept back bade produced 310 KW of power at peak wind speed of 40m/s, indicating that the swept back blade design outperformed the straight blade pattern. Mohokar and Kale [6] employed QBlade in the

optimization of a wind turbine chord length. This was experimented on ten different blade designs by changing their chord lengths between the range of 30 and 120 mm at a fixed wind velocity of 11.5 m/s, and the result revealed that at 90 mm chord length, maximum power coefficient was obtained. Gantasala et al. [7] Numerically Investigated the Aeroelastic behaviour of a wind turbine with iced blades using FAST software. The outer third of the blade produced over 50% of the turbine's total power and severe icing in this part of the blade reduced the power output and aeroelastic damping of the blade's flapwise vibration modes. Increase in the blade mass due to ice lead to reduction in its natural frequencies. Symmetrical icing of the blades reduced the loads acting on the turbine components while asymmetrical icing of the blades induced loads and vibrations in the tower, hub, and nacelle assembly at a frequency synchronous to rotational speed of the turbine. Etuk et al. [8] examined the normal, radial, axial and tangential loading cycles undergone by wind turbine rotor blades and their effects on the displacement of the blade structure using QBlade finite element sub module. Geometry of the deformed blades were characterized by twisting and bending configuration at maximum strain deformation at frequencies up to 200 Hz. From the deflection values obtained, it was found that normal loading cycle would cause the highest level of structural damage on the rotor blade followed by radial, axial and tangential loading. The aim of this study is to provide an open source turbine calculation that is seamlessly integrated into XFOIL, an airfoil design and analysis tool/software. The motivation for this is to create a one solution for the design and aerodynamic computation of wind turbine blades. The integration in XFOIL enables the user to rapidly design custom airfoils and compute their polars, extrapolate the polar data to a range of 360°, and directly integrate them into a wind turbine simulation. By so doing, the procedures of exporting and importing foil and geometry data between different programs is avoided as well as the troubles involved. At the same time, the integration of the BEM and DMS code into XFOIL's sophisticated GUI will make this software accessible to a huge number of wind related applications without the usual command line interface software tools.

2. METHODS

The software XFOIL is programmed to analyse and compute the flow around subsonic isolated airfoils. It is a software used for the calculation of profile polars. The polars were generated starting from $\alpha = -10$ in first a negative direction up to 25 in a positive direction. For the design a NACA 4610 foil was used. An efficient wind rotor blade has many airfoil profiles blended at an angle of twist terminating at a circular flange. The airfoil parameters are presented in Table 1.

Table 1. NACA 4610 airfoil Design parameters.

Parameter	Value (%)	At (%)
Thickness	10	29
Camber	4	59.5
Points	99	
TE_{flap} (Deg)	0.00	
TE_x (Deg)	0.00	
TE_y (Deg)	0.00	

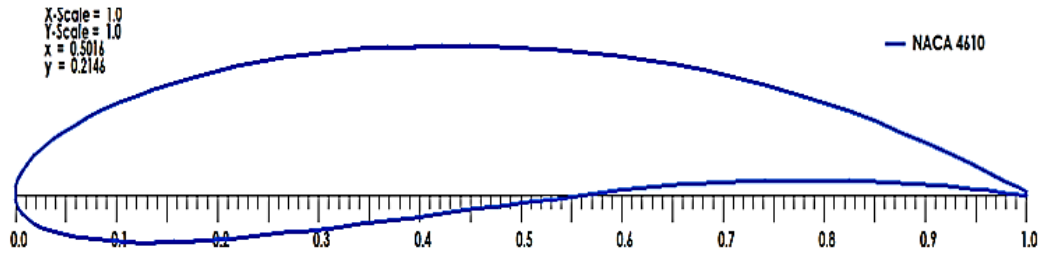


Figure 1. Diagram of the Blade Foil.

As shown in Figure 2, a circular foil with a drag coefficient of 1.2 was used for the root of the blade to enhance the blade structural strength. The parameters of the root foil are presented in Table 2. This part of the blade has low relative wind velocity as a result of its relatively small rotor radius but however carries the highest load [9]. The low wind velocity results in reduced aerodynamic lift, leading to large chord lengths. With this, the blade profile becomes excessively large at the rotor hub to enable it support the weight of the blade as well as the loads encountered during rotation.

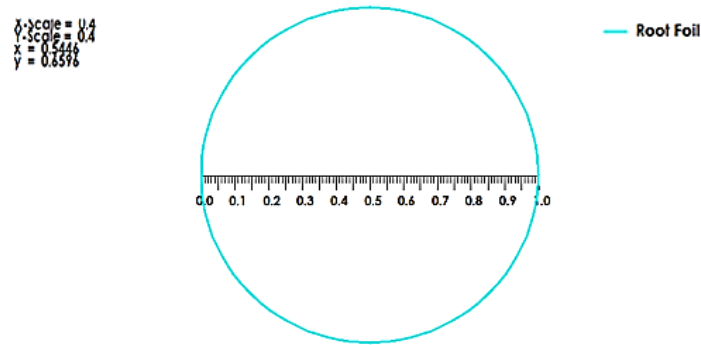


Figure 2. Airfoil for root of Blade.

Table 2. NACA 4610 root foil Design parameters.

Parameter	Value (%)	At (%)
Thickness	100	50
Camber	-0.00	99.90
Points	101	
TE _{flap} (Deg)	0.00	
TE _x (Deg)	0.00	
TE _y (Deg)	0.00	

The forces acting along the length of the blade s_i are obtained by $(p_i-p_0)s_i$. The lift (L) force and the drag (D) force per unit with of the blade alongside all the forces acting on the drag and lift direction can be obtained by integrating as follows:

$$L = \sum(p_1-p_0)s_1 * \sin(\theta_1 + \alpha) \tag{1}$$

$$D = \sum(p_1-p_0)s_1 * \cos(\theta_1 + \alpha) \tag{2}$$

Were p_1 and p_0 are the pressure points on the airfoil, θ is the angle of inclination against the blade chord and α is the angle of attack.

The lift and drag coefficient is given by Equation 3:

$$C_L = \frac{L}{(1/2)\rho U^2 c} \quad (3)$$

$$C_D = \frac{D}{(1/2)\rho U^2 c} \quad (4)$$

Where L is the lift force, D is the drag force, c is the chord length, ρ is the air density and U is the mainstream velocity. Pitching moment coefficient plays a vital role in understanding the principles of aerodynamic centre of an airfoil, and it is given by Equation 5:

$$C_m = \frac{M}{qSc} \quad (5)$$

The Reynolds number is given by Equation 6;

$$Re = \frac{cU}{\nu} \quad (6)$$

Where M is the pitching moment, q is the dynamic pressure, S is the wing area, c is the chord length of the airfoil and ν is the kinematic viscosity of air. The local pressure coefficient which is the difference between local static pressure and free-stream static pressure is given by Equation 7.

$$C_p = \frac{P - P_\infty}{\frac{1}{2}\rho_\infty U_\infty^2} \quad (7)$$

The total or stagnation upstream pressure which is the sum of the static and dynamic pressure at that point according to Bernoulli's equation is given by Equation 8;

$$P_T = P + \frac{1}{2}\rho_\infty U_\infty^2 \quad (8)$$

In terms of differential pressures, C_p can be written in the expression in Equation 9. In this case, C_p at the airfoil stagnation point is equal to unity [10].

$$C_p = \frac{P - P_\infty}{P_T - P_\infty} \quad (9)$$

2.1. Xfoil Design Module

The software is adequate for teaching, as it provides a 'hands on' feeling for HAWT and VAWT rotor design and shows all the fundamental relationships and concepts between twist, chord, foils, turbine control and the power curve in an easy and intuitive way. The GUI serves as a post processor to conducted rotor simulations as well and gives deep insight into all relevant blade and rotor variables for verification, to compare different rotor configurations, or even to study the numerical algorithm and the dependencies among the aerodynamic variables. In addition to that, the software at hand is flexible and user-friendly for wind turbine blade design. Hence, it can also act as a modular system for future implementations that can exploit the possibilities that a combination of manual and parametric airfoil design and analysis coupled with a blade design and simulation tool offers. The functionality of the BEM software includes the following features:

- i. extrapolation of XFOIL generated or imported polar data to 360° AoA
- ii. advanced blade design and optimization, including 3D visualization, using XFOIL generated or imported profiles
- iii. computation of wind turbine performance over wind speed range
- iv. manual selection of BEM and DMS correction algorithms
- v. manual selection of all relevant simulation parameters
- vi. data browsing and visualization as post processing
- vii. export functionality for all created simulation data

3. RESULTS AND DISCUSSION

During revolution which occurs at an angle of 360°, a wind turbine blade experiences much higher angles of attack than the wing of an airplane. For stall-regulated wind turbines, the flow phenomenon is even used as a means to limit the power produced. As stall is generally avoided in aerodynamics, the coefficients corresponding to high AoA are not of interest and therefore not available. Additionally, AoA in the post stall range may occur temporarily during the airfoil iteration procedures.

The lift and drag coefficients consequently have to be extrapolated for the whole 360° range of the AoA. In general, experimental pre-stall data ($\alpha \leq 15$) is available for common air foils and XFOIL is suitable to generate such data as well. For post stall data on the other hand, some further considerations are needed. With increasing AoA, the frontal area facing the airflow increases, too. As stall occurs, the foil dramatically stops producing lift, and the drag coefficient increases. Around 180, the trailing edge of the streamlined air foil faces the flow resulting in decreasing drag and higher lift again. Hence, the flow characteristics evolve from those of a thin, streamlined air foil to those of a blunt body and back during a 180 revolution of the blade. Polar that are either imported or as a result of an XFOIL analysis, can be extrapolated to the full 360° AoA range in the 360° polar extrapolation sub module.

Wind turbines are usually denoted by the wind speed across the rotor blade section relative to the speed of sound. This is therefore the air speed ratio to the speed of sound commonly known as Mark number. For Subsonic flow, Mark no. < 0.8 , transonic flow, Mark no. > 0.8 but < 1.2 , supersonic flow, Mark no. > 1.2 but < 5.0 and for hypersonic flow, Mark no. > 5.0 . The Mark number designated by QBlade software for the purpose of the simulation carried out in this study was 0.020 which falls within the specified range of values for subsonic flow. The difference in Mark number is due to the relative importance of compressible effects which can be neglected in subsonic flows but plays a vital role in the aforementioned flows. For subsonic flows, the air density is almost constant but decreasing the cross sectional area can result in increase in the flow velocity and decrease in pressure. Likewise increasing the area can result in decrease in the flow velocity and increase in pressure. However for higher speeds above subsonic range, some of the energy of the turbine rotors compresses the air and locally changes the air density. The compressibility effect alters the amount of resulting force on the rotors and becomes more pronounced as the speed increases near and beyond the speed of sound (330 m/s or 760 mph). As a result, small disturbances in the flow are transmitted to other parts of the wind turbine isentropically or with constant entropy but a sharp disturbance can generate shock waves that affects the aerodynamics (lift and drag) of the rotor blade.

Figures 3-10 represent results obtained from the polar simulation of the horizontal axis wind turbine blade at various degrees of Alpha. As shown in Figures 3-10, the simulated blade profiles were done using QBlade software which evaluated the blade profile and graphically

assigned a generated scale depending on the value representing the Alpha for each blade profile. In other words, the value representing Alpha (α) at each blade simulation phase is the angle of attack that determines the minimum, optimum and maximum drag or lift force. Table 3 shows summary of the polar simulation results extracted from the blade simulation profiles at different angles of attack.

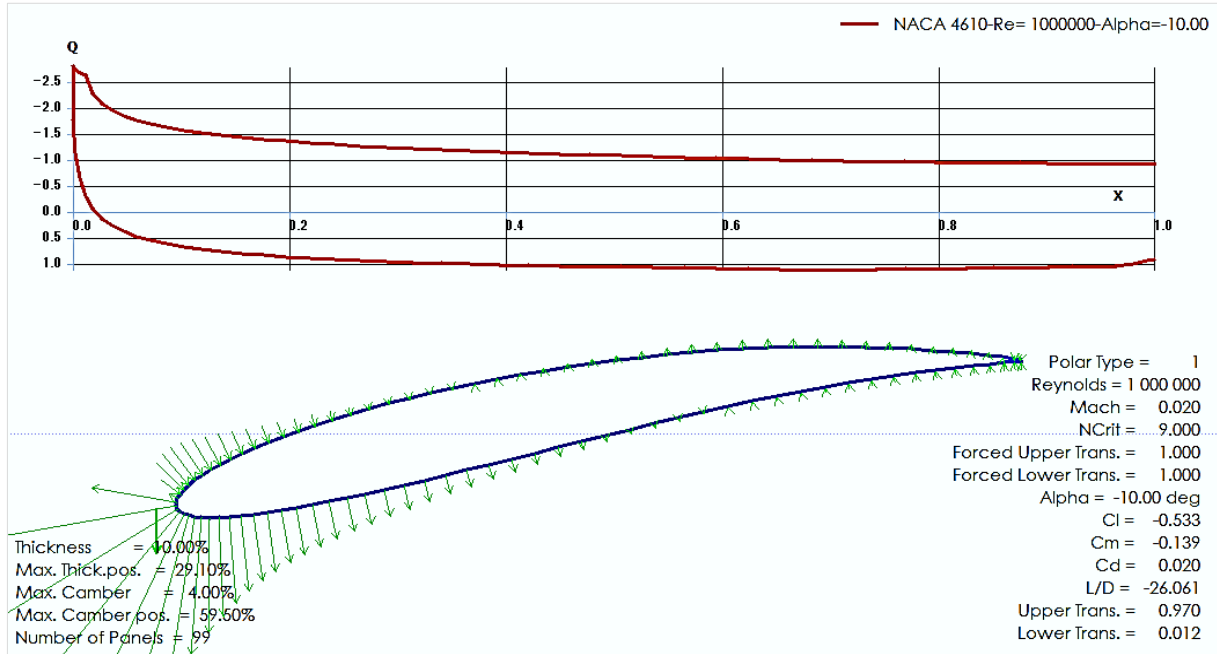


Figure 3. Blade Simulation Profile for AoA of -10 deg.

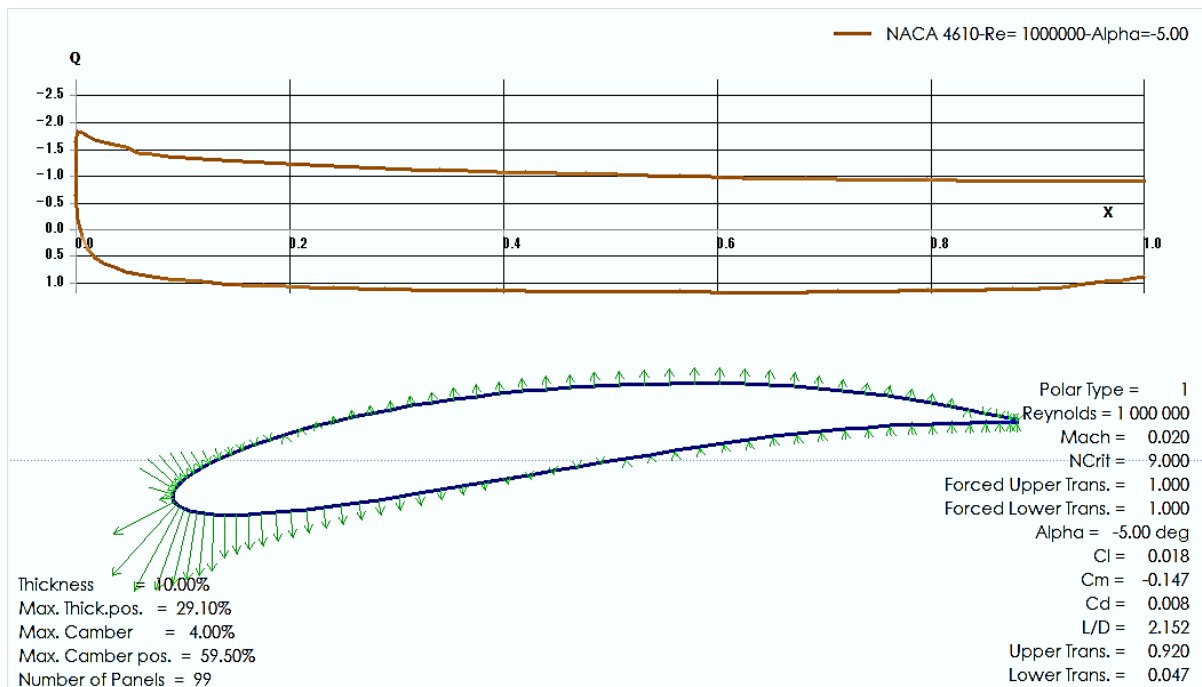


Figure 4. Blade Simulation Profile for AoA of -5.00 deg.

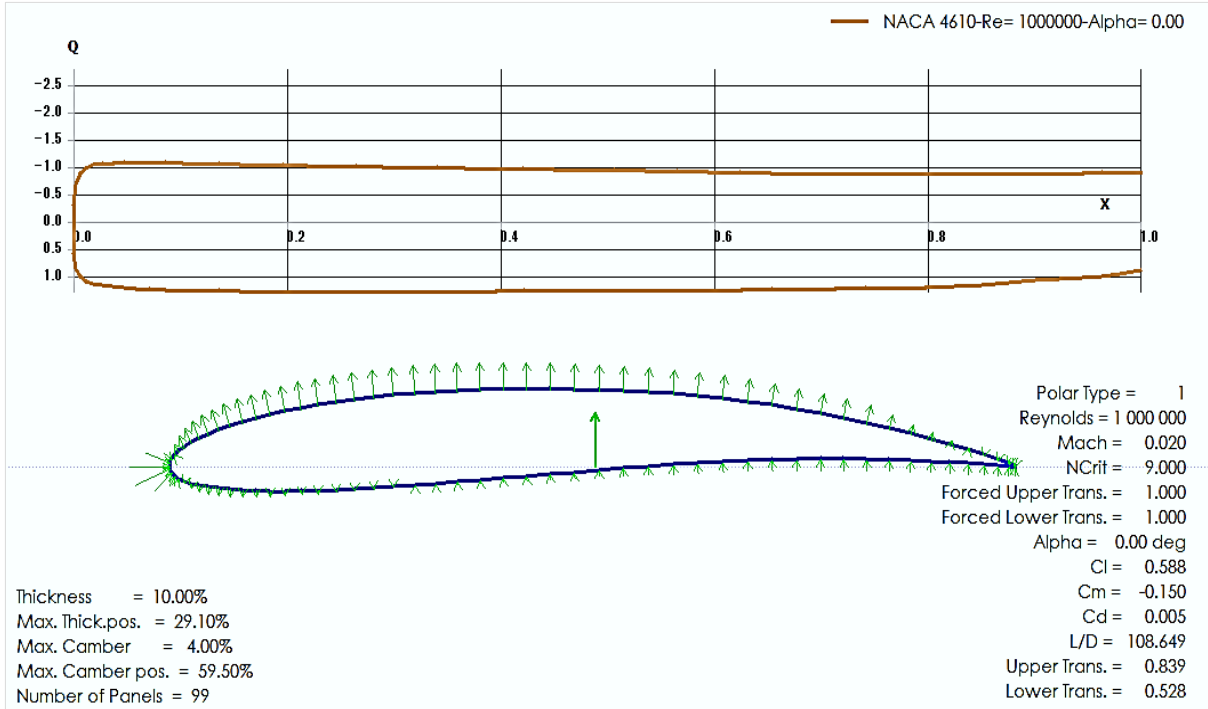


Figure 5. Blade Simulation Profile for AoA of 0.00deg.

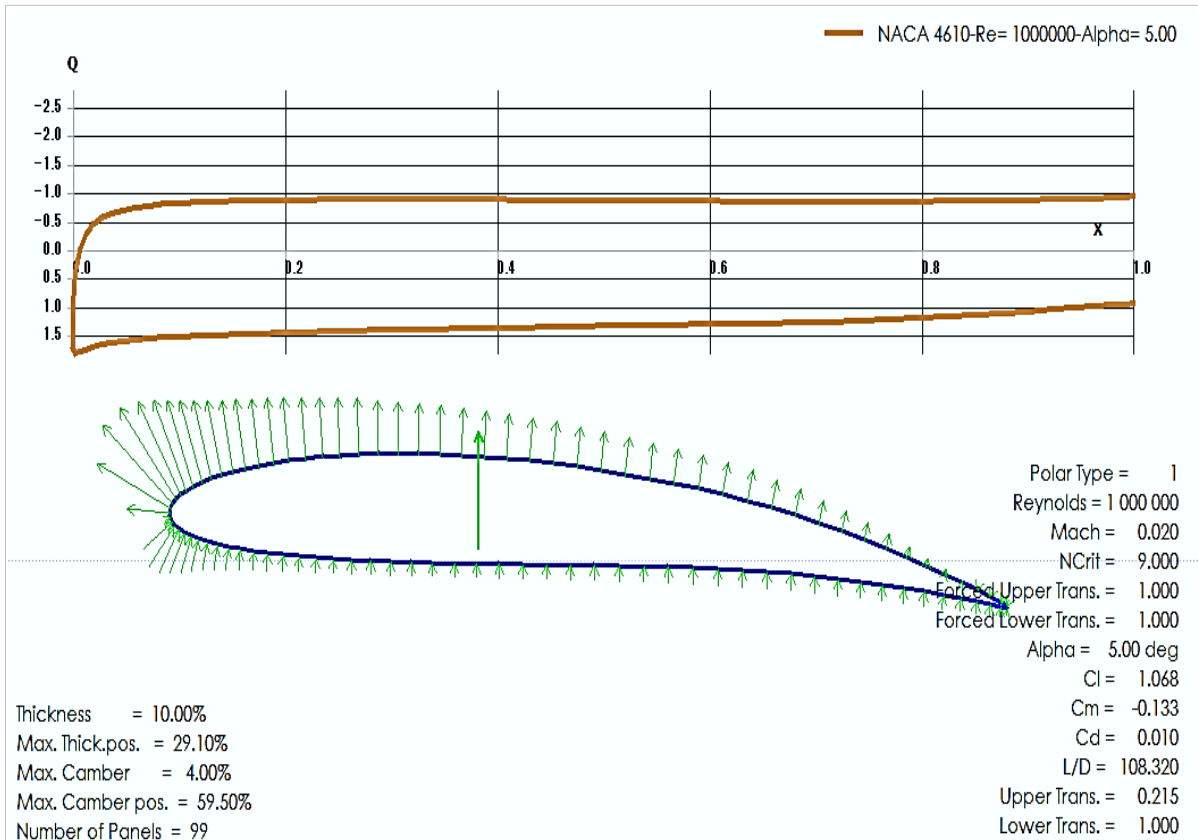


Figure 6. Blade Simulation Profile for AoA of 5.00deg.

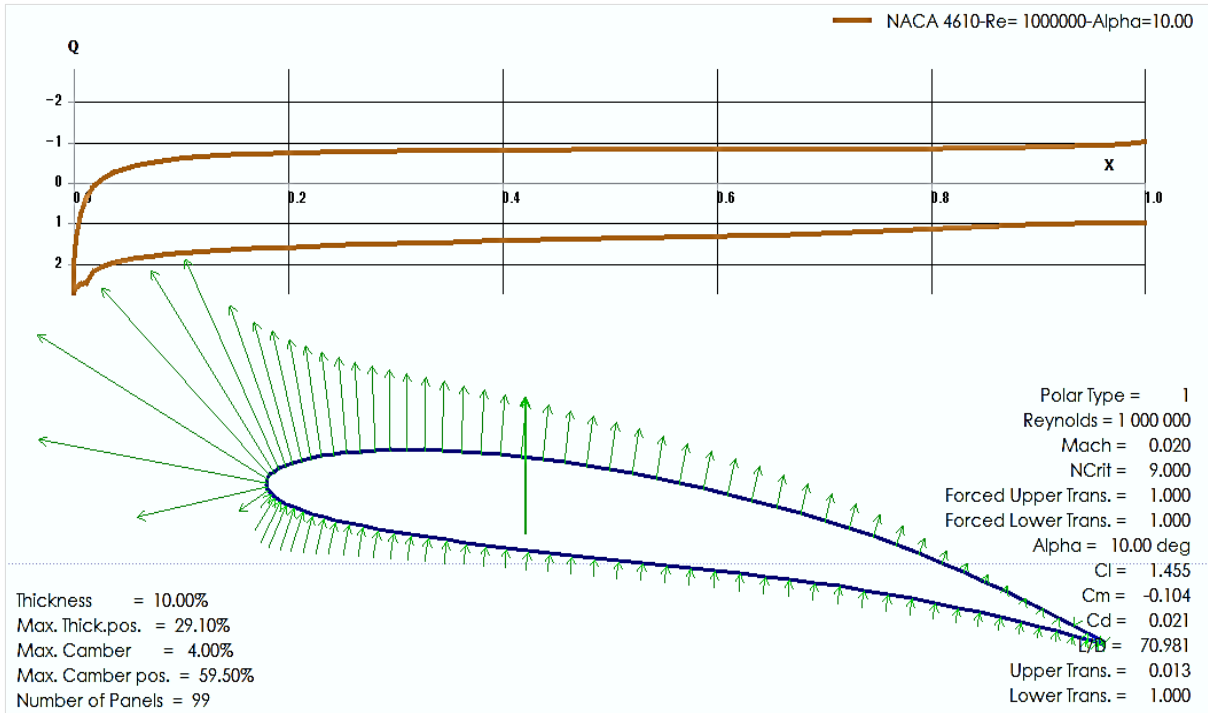


Figure 7. Blade Simulation Profile for AoA of 10.00deg.

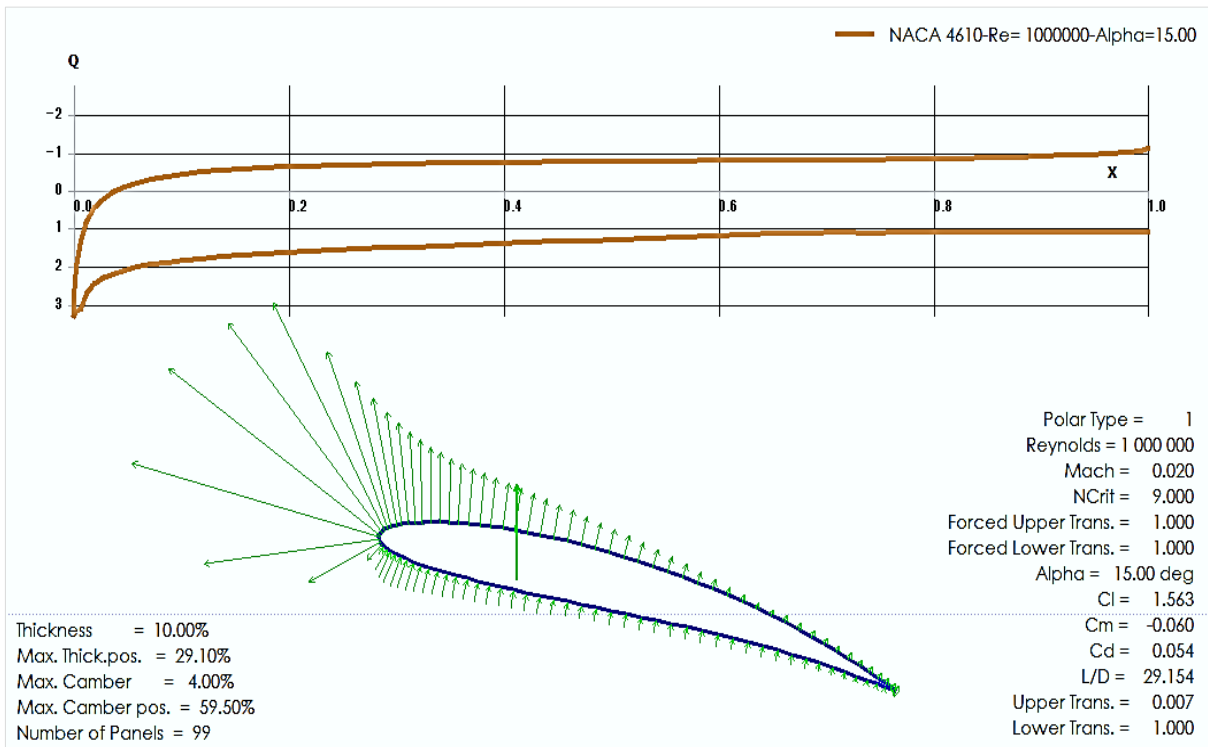


Figure 8. Blade Simulation Profile for AoA of 15.00deg.

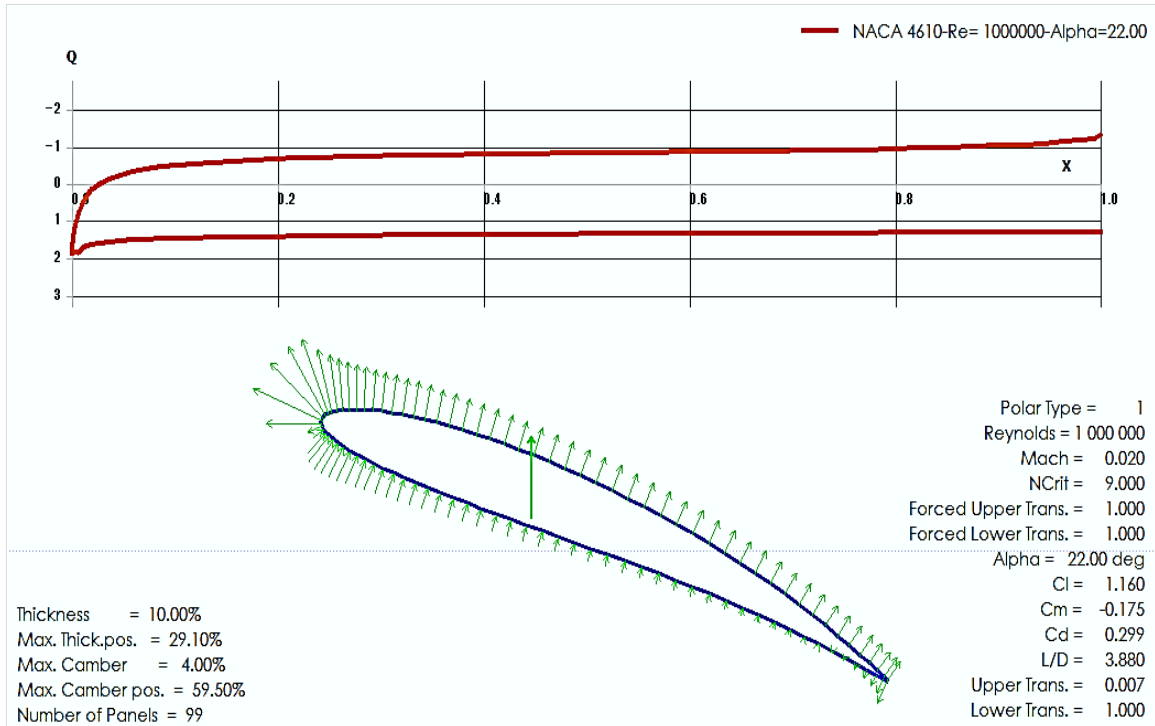


Figure 9. Blade Simulation Profile for AoA of 22deg.

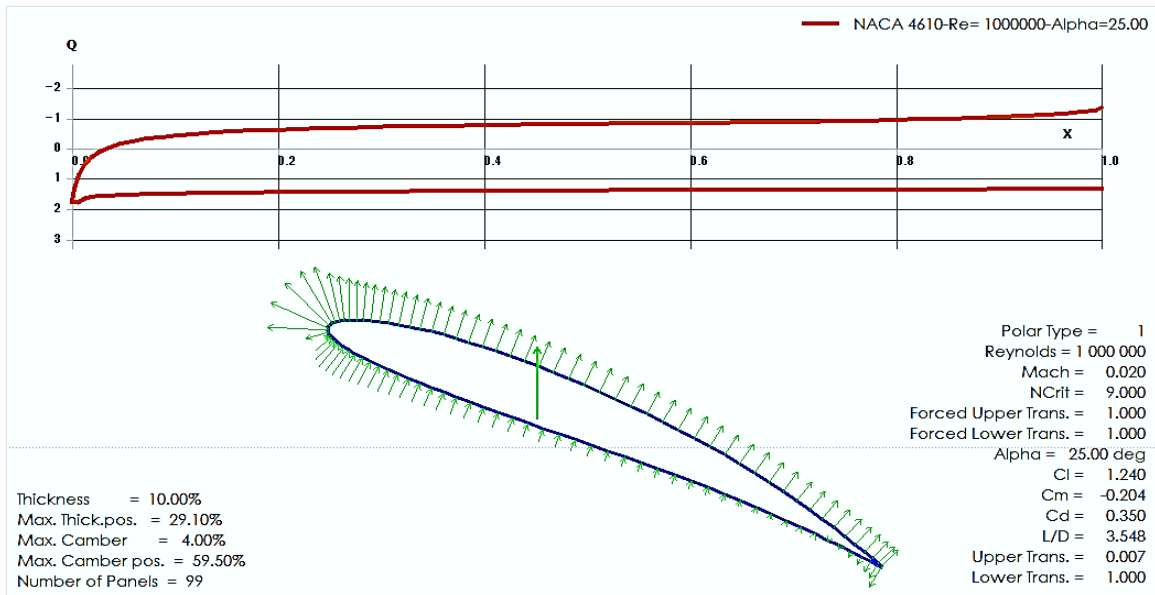


Figure 10. Blade Simulation Profile for AoA of 25.00deg.

Table 3. Summary of the Polar Simulation Results.

Alpha (deg)	Cl	Cm	Cd	L/d
-10	-0.533	-0.139	0.02	-26.061
-5	0.018	-0.147	0.008	2.152
0	0.588	-0.15	0.005	108.649
5	1.068	-0.133	0.01	108.32
10	1.455	-0.104	0.021	70.981
15	1.563	-0.06	0.054	29.154
22	1.16	-0.175	0.299	3.88
25	1.24	-0.204	0.35	3.548

Angle of attack (AoA) increases with increasing lift coefficient up to a certain maximum point, after which, the lift coefficient decreases and varies with increasing angle of attack. This can be observed in Figure 11, where the lift coefficient increases from -0.5 to a maximum point of 1.5 at AoA of 15° before reduction begins to occur. There was no separation of airflow in this case as the angle of attack increased continuously through the simulation. However, reduction in angle of attack indicates that separation of airflow from the upper surface of the blade becomes more pronounced, resulting in decrease in the rate at which the lift coefficient increases. The AoA which produces the highest lift coefficient is referred to as the critical angle of attack also known as the stall angle of attack. In operating conditions below the critical angle of attack, as the angle of attack decreases, the lift coefficient also decrease. Similarly above the critical angle of attack, as the angle of attack increases, the smoothness of airflow over the surface of the airfoil begins to lessen and the air begins to separate from the airfoil surface. Generally on most airfoil geometries, as the angle of attack increases, the flow separation point on the upper surface of the airfoil shifts from the trailing edge towards the leading edge. However, at critical angle of attack, separation in the upper surface flow is more pronounced and the airfoil produces its maximum lift coefficient, and further increase in the AoA can cause the upper surface flow to become fully separated with further reduction in the lift coefficient.

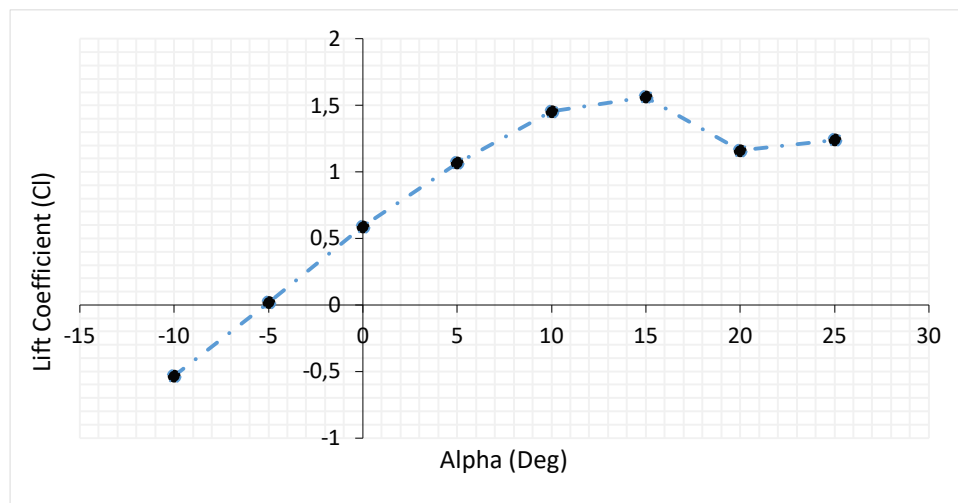


Figure 11. Graph of Lift Coefficient against Alpha.

Figure 12 represents a graph of pitching moment coefficient (C_m) against angle of attack. As graphically demonstrated in Figure 12, a negative pitching moment coefficient indicates a nose-down moment which reduces the angle of attack of the rotor blade in the absence of a control input. Such occurrence is of great advantage in the sense that the wind turbine may resort to a condition in the linear lift region (stable) rather than the stall or post stall region (unstable). In aerodynamics, the pitching moment on an airfoil is the moment or torque produced by the aerodynamic force acting on the airfoil when the aerodynamic force is considered to be acting on the aerodynamic centre of the airfoil rather than on the centre of pressure. By convention, the pitching moment is considered to be positive when it is found pitching the airfoil in the nose-up direction. However, conventional cambered airfoils supported at the aerodynamic centre pitch nose-down, causing the pitch moment coefficient of the airfoils to be negative like in the case presented in Figure 12. Camber represents the asymmetry between the two surfaces of an airfoil, with the upper surface of the airfoil usually being more convex (positive camber). It is commonly designed into an airfoil to minimize its lift coefficient which in turn minimizes the stalling speed of the wind turbine. Aerodynamic centre is the point on a chord line of the airfoil at which the pitching moment coefficient does not vary with AoA.

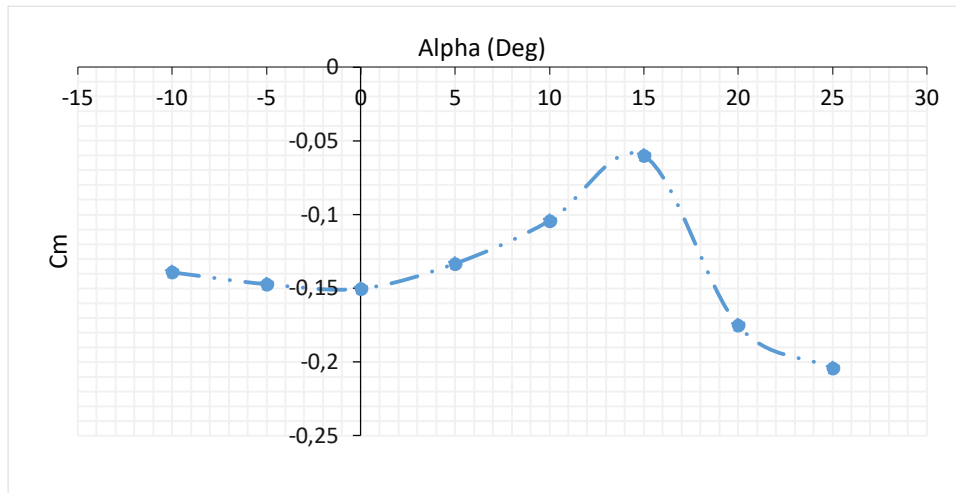


Figure 12. Graph of Pitching Moment coefficient (Cm) against Alpha.

Figure 13 represents a plot of drag coefficient against the angle of attack. Drag coefficient is a number that is used in modelling of complex dependencies of drag on shape, inclination as well as some conditions. It can be observed that at AoA of -10° , drag coefficient of 0.02 is produced, and this further shows a gradual decrease such that, at AoA of 0° , zero drag coefficient is observed. However, at AoA of 15° and 25° , drag coefficient of 0.054 and 0.35 are observed, indicating that the drag coefficient vary with the angle of attack. In similar study carried out by Tang et al. [11], drag coefficient of 0.058 and 0.059 were obtained for corrugated airfoil and NACA2408 airfoil at AoA of 2° . In the context of fluid dynamics, drag is referred to as the forces acting on a solid object in the direction of relative flow, usually in opposite direction to the flow. From aerodynamic point of view, drag forces acting on a body are due to the differences in pressure and viscous sharing stresses, and are therefore classified into two (2) components namely: frictional drag (viscous drag) and pressure drag (form drag). In other words, the airfoil is considered as a streamline body (like in the case of the rotor blade understudied in this research) if friction drag (viscous drag) dominates pressure drag but when pressure drag (form drag) dominates friction drag, such a body is known as blunt body.

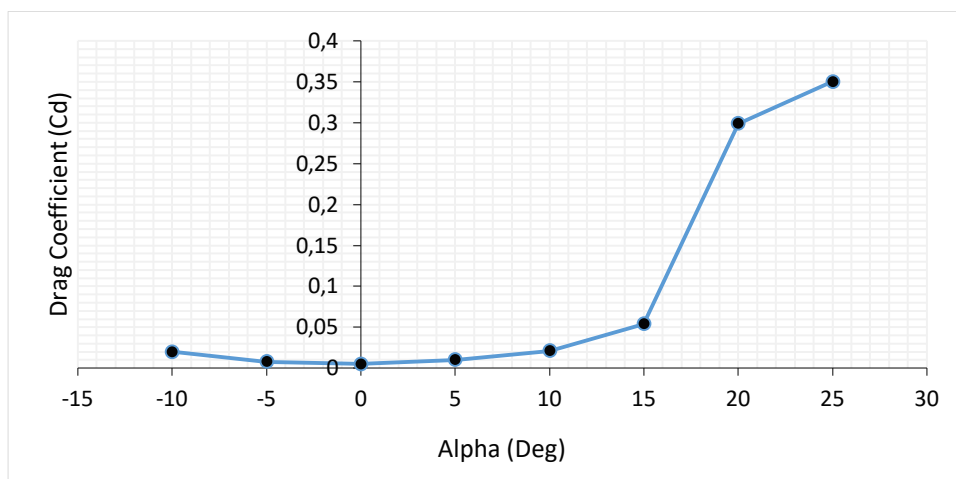


Figure 13. Graph of Drag Coefficient against Alpha.

Figure 14 represents a graph of lift to drag ratio (L/D) against angle of attack. L/D ratio in practical sense is a measure of how efficient an aerodynamic surface is generating lift force at the expense of drag force. It can be observed that at AoA of -10° , L/D ratio of -26.061 is produced, and this further shows a sharp increase such that, at AoA of -5° and 0° , L/D ratio of 2.152 and 108.64 is observed. This is followed by gradual decrease such that at progressive

angle of attacks at 5° , 10° , 15° and 25° , L/D ratios of 108.32, 70.98, 29.15 and 3.54 are produced in decreasing order. The sharp increase on the negative side of the plot and the gradual decline observed in the positive side of the plot indicates that the L/D ratio varies with a given angle of attack. This implies that for a normally cambered airfoil, as the AoA increases, the L/D increases rapidly to the maximum value which can be observed at 108.64 , but as the AoA is increased further, the L/D ratio decreases until the stalling angle is reached and even decreases further beyond that angle. For each AoA, the L/D ratio can be calculated by dividing C_L by C_D (or lift by drag). By so doing, a graph representing the variation of L/D ratio as a function of AoA can be plotted.

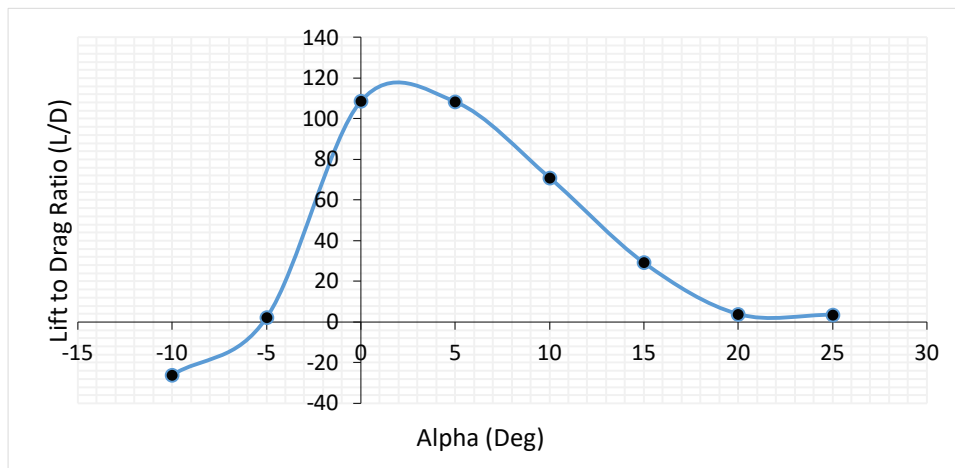


Figure 14. Graph of L/d against Alpha.

Drag polar represents the relationship between the lift and drag for wind turbine airfoils or objects exposed to fluid flow, expressed as a function of the drag coefficient dependent on the lift coefficient. Both coefficients are dependent on three (3) dimensionless variables namely: angle of attack, Reynolds number (Re) and Mach number (Ma). It may be described using mathematical equation or represented in a diagram (plotted in Figure 15) known as polar plot. While the lift coefficient increases from -0.533 to 0.588 , the drag coefficient is observed to decrease from 0.02 to 0.005 as shown in Figure 15. Further increase in the C_L from 0.588 , 1.068 , 1.455 and 1.563 is characterized by corresponding increase in the C_D from 0.005 , 0.01 and 0.021 , 0.054 respectively. The C_L and C_D values represented in this plot has a specific Re and Ma ($1,000,000$ and 0.020) as could be seen on the rotor blade simulation profiles in Figure 3-10, but the plot itself is obtained by varying AoA (from -10 deg to 25 deg) for each simulation phase and computing the C_L and C_D . The major reason why C_L is plotted against C_D is that for a wide range of AoA variation, there is trade-off between both coefficients such that, higher C_L requirement may lead to higher or lower C_D depending on the AoA. In scenarios where higher C_L is required, understanding how these variables are connected to each other is based on the drag polar diagram.

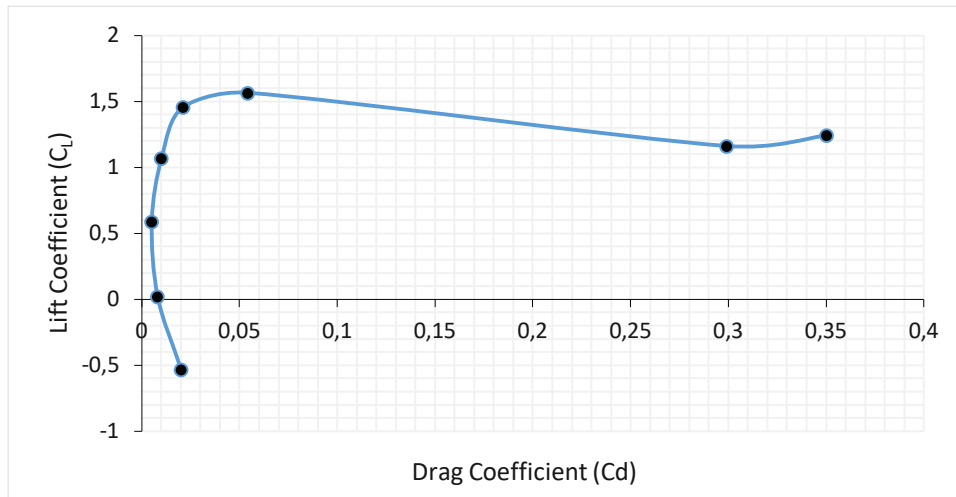


Figure 15. Graph of Lift Coefficient against Drag Coefficient.

4. CONCLUSIONS

In this study, Polar Simulation of Subsonic Flow around NACA 4610 Airfoil was successfully carried out using AIFOIL software. The cambered airfoil geometry had a specific Re and Ma (1,000,000 and 0.020) which were computed with different AoA. The simulation which considered angles of attack in the order of -10, -5, 0.0, 5, 10, 15, 22 and 25 degree indicated an increase or decrease in the lift, drag and lift to drag ratio of the rotor blade which in turn influences the aerodynamic performance in a negative or positive manner as well as the overall performance of the wind turbine. Moreover, the study also revealed that the rotor blade experiences minimum drag at fairly low AoA while its lifting capacity is also very low at low AoA. However, for selection of optimum operating data and in-depth understanding of the lift and drag characteristics at various AoA, wind turbine operators may try to simulate cambered airfoils at lower and higher Re and Ma to observe the airfoil behavior as well as the wind turbine performance.

REFERENCES

- [1] Duque, E. P. N., Burklund, M. D. and Johnson, W. (2003). Navier-stoke and Comprehensive Analysis Performance Predictions of the Nrel Phase Vi Experiment. 22nd ASME Wind Energy Symposium, Reno, Nevada, USA, January, 2003. American Institute of Aeronautic and Astronauts, 2003-0355.
- [2] Bertagnolio, F., Sorensen, N. N. and Rasmussen, F. (2004). New Insight into the Flow around a Wind Turbine Airfoil Section. Special Topic Conference, The Science of making Torque from Wind, Delft, 19-21 April 2004, The Netherlands.
- [3] Alrobaian, A. A., Khan, S. A., Asadullah, M., Ahmed, F. and Imtiyaz, A. (2018). A New Approach to Low-cost Open-typed Subsonic Compressible Flow Wind Tunnel for Academic Purpose. International Journal of Mechanical and Production Engineering Research and Development, 8(6), 383-394.
- [4] Winslow, J., Otsuka, H., Govindarajan, B. and Chopra, I. (2018). Basic Understanding of Airfoil Characteristics at Low Reynolds Numbers (104-105). Journal of Aircraft, 55(3), 1050-1061.
- [5] Arun, A. K. and Surya, J. (2019). A Comparison of the Straight Blade and Swept Back Blade Horizontal Axis Wind Turbine. SSRG International Journal of Mechanical Engineering, 2348-8360, 30-35.
- [6] Mohokar, A. and Kale, N. W. (2017). Development of the Performance of Small Horizontal Axis Wind Turbine Blade by Optimizing its Chord Using QBlade Software. International Journal of Advanced Engineering and Research Development, 4(11), 790-796.
- [7] Gantasala, S., Tabatabaei, N., Cervantes, M. and Aidanpaa, J. (2019). Numerical Investigation of the Aeroelastic Behaviour of a Wind Turbine with Iced Blades. Energies, 12(2422), 1-24.
- [8] Etuk, E. M., Ikpe, A. E. and Adoh, U. A. (2020). Design and Analysis of Displacement Models For Modular Horizontal Wind Turbine Blade Structure. Nigerian Journal of Technology, 39(1), 121-130.
- [9] Schubel, P. J. and Crossley, R. J. (2012). Wind Turbine Blade Design. Energies, 5, 3425-3449.

- [10] Kandil, M. A. F. and Elnady, A. O. (2017). Performance of GOE-387 Airfoil Using CDF. International Journal of Aerospace Sciences, 5(1), 1-7.
- [11] Tang, H., Lei, Y., Li, X. and Fu, Y. (2019). Numerical Investigation of the Aerodynamic Characteristics and Attitude Stability of aBio-Inspired Corrugated Airfoil for MAV or UAV Applications. Energies, 12(4021), 1-25.



International Journal of Engineering and Innovative Research

<http://dergipark.gov.tr/ijeir>

A STUDY OF THIN PLATE VIBRATION USING HOMOTOPY PERTUBATION ALGORITHM

Falade Kazeem Iyanda^{1*}, Tihamiyu Abd'gafar Tunde², Tolufase Emmanuel³

^{1*}Kano University of Science and Technology, Department of Mathematics, Wudil Kano State, Nigeria.

²Federal University of Technology, Department of Mathematics, Minna Niger State, Nigeria.

³Nigeria Police Academy, Department of Physics, Faculty of Science, Wudil Kano State, Nigeria.

*Corresponding Author: faladekazeem2016@kustwudil.edu.ng

(Received: 12.05.2020; Revised: 02.06.2020; Accepted: 16.06.2020)

ABSTRACT: In this paper, we apply homotopy perturbation method for the numerical solution of three dimensional second-order partial differential equation which occurred in a plate vibration behaviour. The MAPLE 18 Mathematical software was used to develop a four steps algorithm based on homotopy perturbation method (HPM). Three test cases are considered to verify the reliability and efficiency of the method. The suggested algorithm is quite efficient and practically well suited for use in these problems. The approximated solutions are in good agreement with analytical solutions for the tested problems Moreover, the approximate solutions obtained proved that the proposed method is easy, efficient, and accurate.

Keywords: Second-Order Partial Differential Equation, Homotopy Perturbation Method, MAPLE 18 Mathematical Software, Algorithm, Analytical Solutions.

1. INTRODUCTION

Modal analysis of plate vibration is important engineering analysis that relates to the safe design of this type of structures because many such structures are expected to survive cyclic load applications. Such situation is vulnerable to structural failures in resonant vibration should the frequency of the applied cyclic loads coincides with any natural frequencies of the plate found in the modal analysis. Solutions for these natural frequencies of plates of given geometry and material properties requires the solution of the shape of the deformed plates at various modes, and it will also provide engineers with possible shapes of the plate under each of these modes of vibration. Solids of plane geometry, such as thin plates are common appearance in machines and structures. Thin plates can be as small as printed electric circuit boards with micrometers in size or as large as floors in building structures. Like flexible cables, thin flexible plates are normally flexible and be vulnerable to transverse vibration. In some cases, these plates may rupture due to resonant vibrations, resulting in significant loss of property, and even human lives.

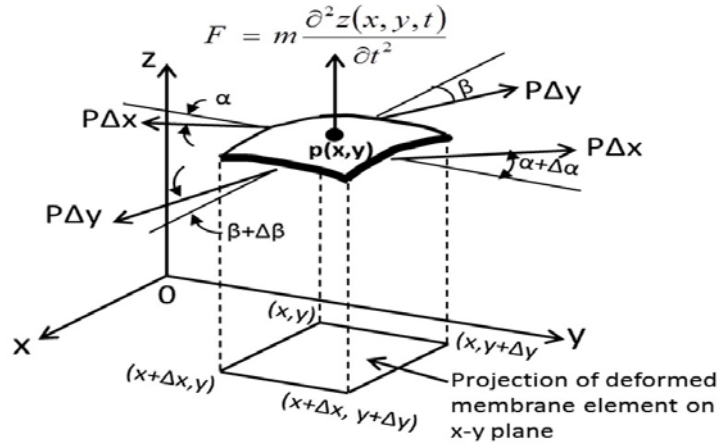


Figure 1. A free-body diagram of forces in an element of vibrating membrane

This section will derive appropriate partial differential equations (PDEs) that allow engineers to assess the amplitudes in free vibration of thin plates that are flexible enough to be simulated to thin membranes Ran [1]

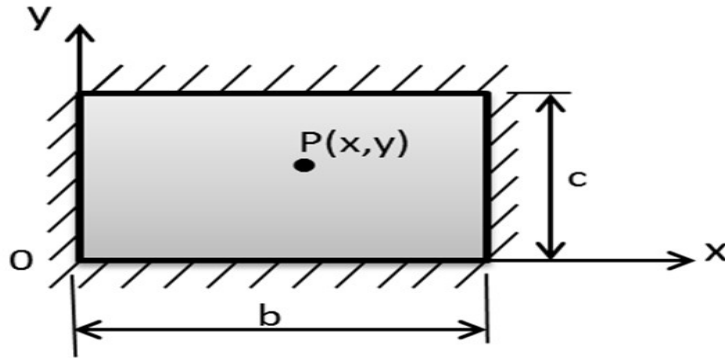


Figure 2. Plan view of a flexible thin plate undergoing a transverse vibration

The magnitudes of a transverse vibrating thin plate such as a computer mouse pad, induced by a slight instantaneous disturbance in the z-direction in Figure 2. We will have the following PDE and the given appropriate initial condition for the solution of the magnitudes of the vibrating plate at given time t, i.e. $z(x, y, t)$ as second order partial differential equations which describe rate of change in three coordinate directions of function $z(x, y, t)$ of the form:

$$\frac{\partial^2 z(x, y, t)}{\partial t^2} = \lambda^2 \left[\frac{\partial^2 z(x, y, t)}{\partial x^2} + \frac{\partial^2 z(x, y, t)}{\partial y^2} \right] \quad (1)$$

subject to initial conditions

$$\begin{cases} z(x, y, t)_{t=0} = f(x, y) \\ \frac{\partial z(x, y, t)}{\partial t} \Big|_{t=0} = g(x, y) \end{cases} \quad (2)$$

Where $\lambda = \sqrt{\frac{Pg}{m}}$ in which P = tension in the cable and m = mass per unit length which needs to be computed with given conditions. The mass per unit length of the cable is $m = \frac{M}{L}$ where M = total mass of the cable with $M = \rho V$ with V being the volume of the cable. Function $f(x, y)$

describes the cable at the initial position before the vibration take place while $g(x, y)$ describes the velocity of the plate across the plane of the plate at the inception of the vibration.

Many researchers published some works in solving this type of classical differential equation, Irvine [2] describes the in-plane and out-of-plane small amplitude free vibration of a suspended elastic cable with small sag, Leonard [3] present the finite element method has also been used for forced vibration response analysis, Rega [4] parametric analysis of large amplitude free vibrations of a suspended cable was considered, Ni et al. [5] developed a hybrid pseudo-force/Laplace transform method for transient response of suspended cables. Homotopy Perturbation Method (HPM) has been a promising numerical technique in solving partial differential equations which describe different fields of science, physical phenomena, engineering, mechanics and soon. homotopy perturbation method was proposed by He [6] for solving linear and nonlinear differential equations and integral equations. Many researchers used HPM to approximate the solutions of partial differential equations and integral equations. Vahidi et al. [7] solved nonlinear DEs, which yields the Maclaurin series of the exact solution, Chang and Liou [8] developed a third-order explicit approximation to find the roots of the dispersion relation for water waves that propagate over dissipative media, Zhou and Wu [9] solved the nonlinear PB equation describing spherical and planar colloidal particles immersed in an arbitrary valence and mixed electrolyte solution, Özi and Akçı [10] obtained periodic solutions for certain non-smooth oscillators using iterated homotopy perturbation method combined with modified Lindstedt Poincaré technique, Yazdi [11] solved nonlinear vibration analysis of functionally graded plate. Al-Saif and Abood [12] used homotopy perturbation method for solving K (2, 2) equations, Aswhad and Jaddoa [13] obtained the approximate solutions of Newell whitehead segel and fisher equations using the Adomian decomposition Method, Babolian et al. [14] solved advection problem, vibrating beam equation linear and nonlinear PDEs and the system of nonlinear PDEs and Adil et al. [15] studied general second-order partial differential equations using homotopy perturbation method. However, the fact that the HPM solves many applied mathematical problems without any transformation, discretization or restrictive assumptions can be considered as a clear advantage of this technique over the some numerical methods was established by Mohyud and Noor [16]. Moreover, several techniques including the method of characteristic, Riemann invariants, combination of waveform relaxation and multi-grid, periodic multi-grid wave form, variational iteration e.t.c encounter the inbuilt deficiencies and involve huge computational work. Thus, the homotopy perturbation algorithm was formulated to address the computational shortcoming while efficiency and accuracy are still mentained He [17].

In this work, we examined the feasibility of employing the HPM to formulate four steps algorithm for the numerical solution of three dimentional second-order PDE that occurred in a plate vibration and to investigate the behavious of functions $f(x, y)$ which describe the cable at the initial position couple with $g(x, y)$ that describes the velocity of the plate across the plane of the plate at the inception of the vibration.

2. HOMOTOPY PERTURBATION METHOD (HPM)

In this section, we present a brief description of the HPM, to illustrate the basic ideas of the homotopy perturbation method, this method is a coupling between the traditional perturbation method and homotopy, which is a highly interesting and useful concept in topology, and deforms continuously to a simple problem which is easily solved. We consider the following differential equation employed in Chun and Sakhivel [18].

$$A(u) - f(\gamma) = 0 \quad \gamma \in \Omega \quad (3)$$

with boundary conditions:

$$B\left(u, \frac{\partial u}{\partial \gamma}\right) = 0 \quad \gamma \in \Omega \quad (4)$$

where A is general differential operator, B is a boundary operator, $f(\gamma)$ a known analytic function and ∂u is the boundary of the domain Ω . The operator A can be generally divided into two parts of L and N where L is linear part, while N is the nonlinear part in the DE, Therefore Eq.(3) can be rewritten as follows:

$$L(u) + N(u) - f(\gamma) = \quad (5)$$

By using homotopy technique, one can construct a homotopy

$$Z(\gamma, m): \Omega \times [0,1] \mapsto R \quad (6)$$

which satisfies

$$H(z, m) = (1 - m)[L(z) - L(u_0)] + m[L(z) + N(z) - f(\gamma)] = 0 \quad (7)$$

or

$$H(z, m) = L(z) - L(u_0) + mL(u_0 + m[N(z) - f(\gamma)]) = 0 \quad (8)$$

where $m \in [0, 1]$, $\tau \in \Omega$ and m is called homotopy parameter and u_0 is an initial approximation for the solution of Eq.(3) which satisfies the boundary conditions obviously, using Eq.(7) or Eq.(8), we have the following equation:

$$H(z, 0) = L(z) - L(u_0) = 0 \quad (9)$$

$$H(z, 1) = L(z) + N(z) - f(\gamma) = 0 \quad (10)$$

Assume that the solution of (7) or (8) can be expressed as a series in m as follows:

$$Z = z_0 + mz_1 + m^2z_2 + m^3z_3 + \dots = \sum_{i=0}^{\infty} m^i z_i \quad (11)$$

set $m \rightarrow 1$ results in the approximate solution of (3).

Consequently,

$$u(\gamma) = \lim_{m \rightarrow 1} Z = z_0 + z_1 + z_2 + z_3 + \dots = \sum_{i=0}^{\infty} z_i \quad (12)$$

It is worth to note that the major advantage of He's homotopy perturbation method is that the perturbation equation can be freely constructed in many ways and approximation can also be freely selected

It is well known that series (12) is convergent for most of the cases and also the rate of convergence is dependent on $L(z)$. The comparisons of equal powers of m give solutions of

various orders. In sum, according to Liu [19], He's HPM considers the solution $u(x)$ of the homotopy equation in a series of m as

$$z(x) = \sum_{i=0}^{\infty} m^i z_i = z_0 + m z_1 + m^2 z_2 + m^3 z_3 + \dots \quad (13)$$

and the method considers the nonlinear $N(z)$ as

$$N(u) = \sum_{i=0}^{\infty} m^i H_i = H_0 + m H_1 + m^2 H_2 + m^3 H_3 + \dots \quad (14)$$

Where H_n are the so-called He's polynomials [17] which can be calculated by using the formula

$$H_n(z_0, z_1, \dots, z_n) = \frac{1}{n!} \frac{\partial^n}{\partial m^n} \left(N \left(\sum_{i=0}^{\infty} m^i z_i \right) \right)_{m=0} \quad (15)$$

where $n = 0, 1, 2, 3, \dots$

2.1. Homotopy Perturbation Algorithm (HPA)

In this section, we consider Eq. (1) and Eq. (2) couple with Eq. (15). We formulate a four steps algorithm using MAPLE 18 Mathematical software command to solve Eq. (1) as follows:

```

restart:
Step 1: z(x, y, 0) := f(x, y);
z_t(x, y, 0) := g(x, y);
z_0 := z(x, y, 0) + t * z_t(x, y, 0);
N := ℝ+;
λ := √P/m;
Step 2: for i from 0 to 0 do
A := (Diff(z_0, [t, t]) + λ * (Diff(z_0, [x, x]) + Diff(z_0, [y, y])));
B := -Int(A, t, t);
z_{i+1} := value(B);
end do
Step 3: for i from 1 to N do
A := (λ * (Diff(z_i, [x, x]) + Diff(z_i, [y, y])));
B := -Int(A, t, t);
z_{i+1} := value(B);
end do
Step 4: Z := sum(z_j, j = 0, 1, ... N + 1);
z(x, y) := eval(Z, t = 0);
z(x, t) := eval(Z, y = 0);
z(t, y) := eval(Z, x = 0);
output: see tables (1,2,3)

```

(16)

where N is the computational length.

3. NUMERICAL EXPERIMENT

In order to assess the accuracy of the formulated algorithm (16) for the numerical solution of the three dimensional second-order PDE that occurred in a plate vibration, we have introduced three test cases to investigate the nature of function $f(x, y)$ and subject to initial condition in [1] when vibration of the pad induced by a slight instantaneous disturbance lateral to the pad from a static equilibrium condition (i.e., zero velocity) in which $g(x, y) = 0$ and compare the approximate solutions with the analytical solutions.

$$\frac{\partial^2 z(x, y, t)}{\partial t^2} = \lambda^2 \left[\frac{\partial^2 z(x, y, t)}{\partial x^2} + \frac{\partial^2 z(x, y, t)}{\partial y^2} \right] \quad (17)$$

subject to initial conditions

$$\begin{cases} z(x, y, t)_{t=0} = f(x, y) \\ \frac{\partial z(x, y, t)}{\partial t} \Big|_{t=0} = g(x, y) \end{cases} \quad (18)$$

when the pad has fixed edges with initial sagging that can be described by functions

$$f(x, y) = \begin{cases} (10 - x^2)(5 - y^2) \\ 10 \sin(x) + 5 \cos(y) \\ e^{(10x+5y)} \end{cases} \quad (19)$$

vibration of the pad induced by a slight instantaneous disturbance lateral to the pad from a static equilibrium condition (i.e., zero velocity)

$$g(x, y) = 0 \quad (20)$$

and

$$\lambda = \sqrt{\frac{Pg}{m}} = \sqrt{\frac{(0.51 \text{ lb}_t) \left(\frac{32.0 \text{ ft}}{\text{s}^2} \right)}{\frac{0.00155 \text{ lb}_m}{\text{in}^2}}} \left(\frac{12 \text{ in}}{\text{ft}} \right) = 353.05 \text{ in/s} \quad (21)$$

Compute the above parameters into algorithm (16), we have the following numerical results tables:

Table 1. $f(x, y) = (10 - x^2)(5 - y^2)$, $g(x, y) = 0$, $\lambda = 353.05$ $N = 3$ **Case 1**

$z(x, y)$.		When $t = 0$		$z(x, t)$.		When $y = 0$		$z(t, y)$.		When $x = 0$	
x	y	Analytical Solution	HPA Solution	x	t	Exact Solution	HPA Solution	t	y	Exact Solution	HPA Solution
0	0	50.00000	50.00000	0	0	50.000000	50.000000	0	0	50.000000	50.000000
0.1	0.1	49.85010	49.85010	0.1	0.1	107.02700	107.02700	0.1	0.1	106.97780	106.97780
0.2	0.2	49.40160	49.40160	0.2	0.2	327.54200	327.54210	0.2	0.2	327.34200	327.34200
0.3	0.3	48.65810	48.65810	0.3	0.3	859.84750	859.84740	0.3	0.3	859.39741	859.39741
0.4	0.4	47.62560	47.62560	0.4	0.4	1951.1134	1951.1133	0.4	0.4	1950.3130	1950.3130
0.5	0.5	46.31250	46.31250	0.5	0.5	947.37817	947.37812	0.5	0.5	3946.1281	3946.1283
0.6	0.6	44.72960	44.72960	0.6	0.6	7293.5485	7293.5486	0.6	0.6	7291.7485	7291.7486
0.7	0.7	42.89010	42.89010	0.7	0.7	12533.399	12533.399	0.7	0.7	12530.949	12530.949
0.8	0.8	40.80960	40.80960	0.8	0.8	20309.573	20309.573	0.8	0.8	20306.372	20306.372
0.9	0.9	38.50610	38.50610	0.9	0.9	31363.580	31363.580	0.9	0.9	31359.530	31359.530

1.0	1.0	36.00000	36.00000	1.0	1.0	46535.800	46535.800	1.0	1.0	46530.800	46530.800
-----	-----	----------	----------	-----	-----	-----------	-----------	-----	-----	-----------	-----------

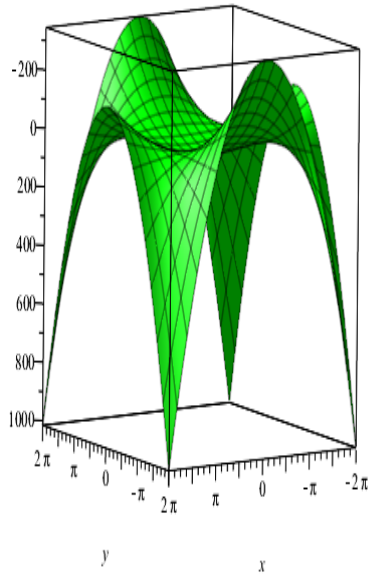
Table 2. $f(x, y) = 10 \sin(x) + 5\cos(y)$, $g(x, y) = 0$ and $\lambda = 353.05$ $N = 10$ **Case 2**

$z(x, y)$.		When $t = 0$		$z(x, t)$.		When $y = 0$		$z(t, y)$.		When $x = 0$	
X	y	Analytical Solution	HPA Solution	X	t	Exact Solution	HPA Solution	t	y	Exact Solution	HPA Solution
0	0	5.0000000	5.0000000	0	0	5.0000000	5.0000000	0	0	5.0000000	5.0000000
0.1	0.1	5.9733549	5.9733549	0.1	0.1	20.092790	20.09279	0.1	0.1	16.66497	16.66497
0.2	0.2	6.8870261	6.8870262	0.2	0.2	49.804244	49.80424	0.2	0.2	105.0698	105.0698
0.3	0.3	7.7318845	7.7318845	0.3	0.3	1116.0813	1116.081	0.3	0.3	670.1484	670.1484
0.4	0.4	8.4994883	8.4994883	0.4	0.4	8168.9733	8168.973	0.4	0.4	4229.799	4229.798
0.5	0.5	9.1821681	9.1821681	0.5	0.5	58887.972	58887.97	0.5	0.5	26382.33	26382.33
0.6	0.6	9.7731028	9.7731029	0.6	0.6	4.191-E05	4.182-E05	0.6	0.6	1.62-E05	1.63-E05
0.7	0.7	10.266387	10.266388	0.7	0.7	2.931-E06	2.931-E06	0.7	0.7	9.79-E05	9.78-E05
0.8	0.8	10.657094	10.657095	0.8	0.8	2.002-E07	2.002-E07	0.8	0.8	5.72-E06	5.72-E06
0.9	0.9	10.941318	10.941319	0.9	0.9	1.313-E08	1.313-E08	0.9	0.9	3.18-E07	3.18-E07
1.0	1.0	11.116222	11.116223	1.0	1.0	8.117-E08	8.117-E08	1.0	1.0	1.63-E08	1.63-E08

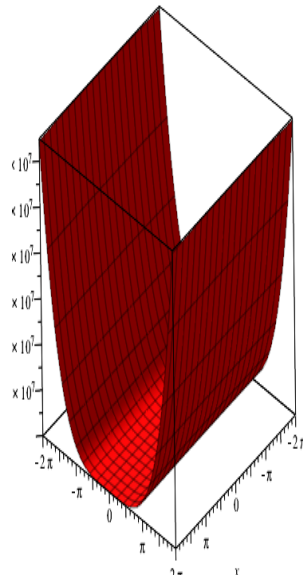
Table 3. $f(x, y) = e^{(10x+5y)}$, $g(x, y) = 0$ and $\lambda = 353.05$ $N = 15$ **Case 3**

$z(x, y)$.		When $t = 0$		$z(x, t)$.		When $y = 0$		$z(t, y)$.		When $x = 0$	
X	y	Analytical Solution	HPA Solution	X	t	Exact Solution	HPA Solution	t	y	Exact Solution	HPA Solution
0	0	1.000000	1.000000	0	0	1.000000	1.000000	0	0	1.000000	1.000000
0.1	0.1	4.481689	4.481689	0.1	0.1	6.182-E08	6.182-E08	0.1	0.1	3.75 -E06	3.76 E06
0.2	0.2	20.08553	20.08554	0.2	0.2	1.571-E17	1.571-E17	0.2	0.2	5.77-E16	5.78-E16
0.3	0.3	90.01713	90.01714	0.3	0.3	2.331-E23	2.331-E23	0.3	0.3	5.20-E22	5.20-E22
0.4	0.4	403.4288	403.4289	0.4	0.4	6.933-E27	6.933-E27	0.4	0.4	9.38-E26	9.39-E26
0.5	0.5	1808.042	1808.042	0.5	0.5	2.492-E31	2.492-E31	0.5	0.5	2.04-E30	2.05-E30
0.6	0.6	8103.084	8103.084	0.6	0.6	2.376-E34	2.377-E34	0.6	0.6	1.18-E33	1.19-E33
0.7	0.7	36315.50	36315.51	0.7	0.7	9.107-E36	9.108-E36	0.7	0.7	2.75-E35	2.76-E35
0.8	0.8	1.628-E05	1.628-E05	0.8	0.8	1.794-E39	1.795-E39	0.8	0.8	3.29-E37	3.28-E37
0.9	0.9	7.294-E05	7.294-E05	0.9	0.9	2.129-E41	2.128-E41	0.9	0.9	2.36-E39	2.35-E39
1.0	1.0	3.269-E06	3.269-E06	1.0	1.0	1.694-E43	1.695-E43	1.0	1.0	1.14-E41	1.14-E41

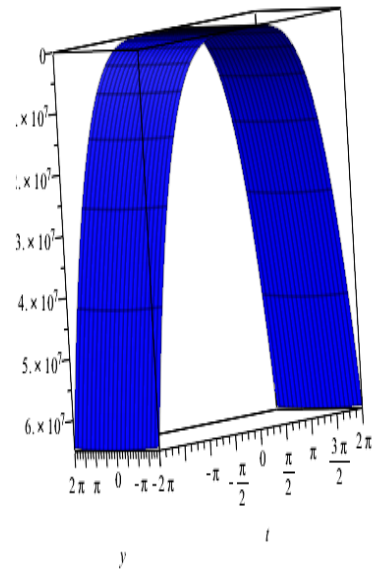
4. GRAPHS REPRESENTATION



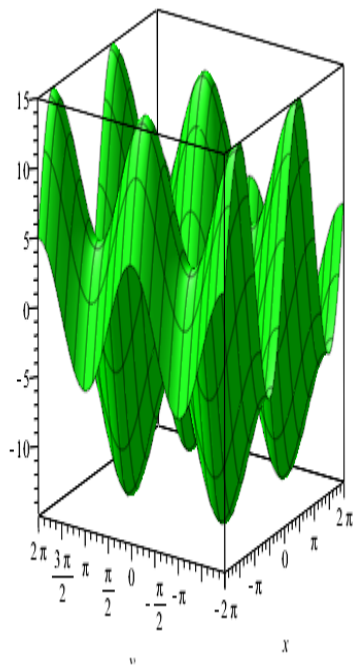
Graph 1. Numerical solution at $z(x, y)$ for $f(x, y) = (10 - x^2)(5 - y^2)$.



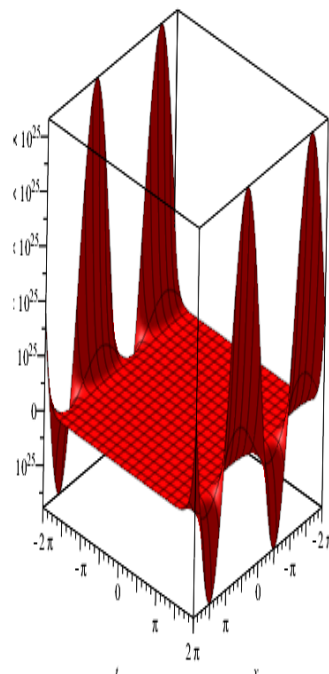
Graph 2. Numerical solution at $z(x, t)$ for $f(x, y) = (10 - x^2)(5 - y^2)$.



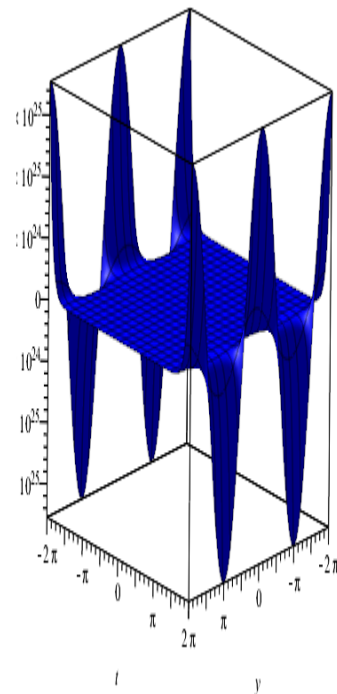
Graph 3. Numerical solution at $z(t, y)$ for $f(x, y) = (10 - x^2)(5 - y^2)$.



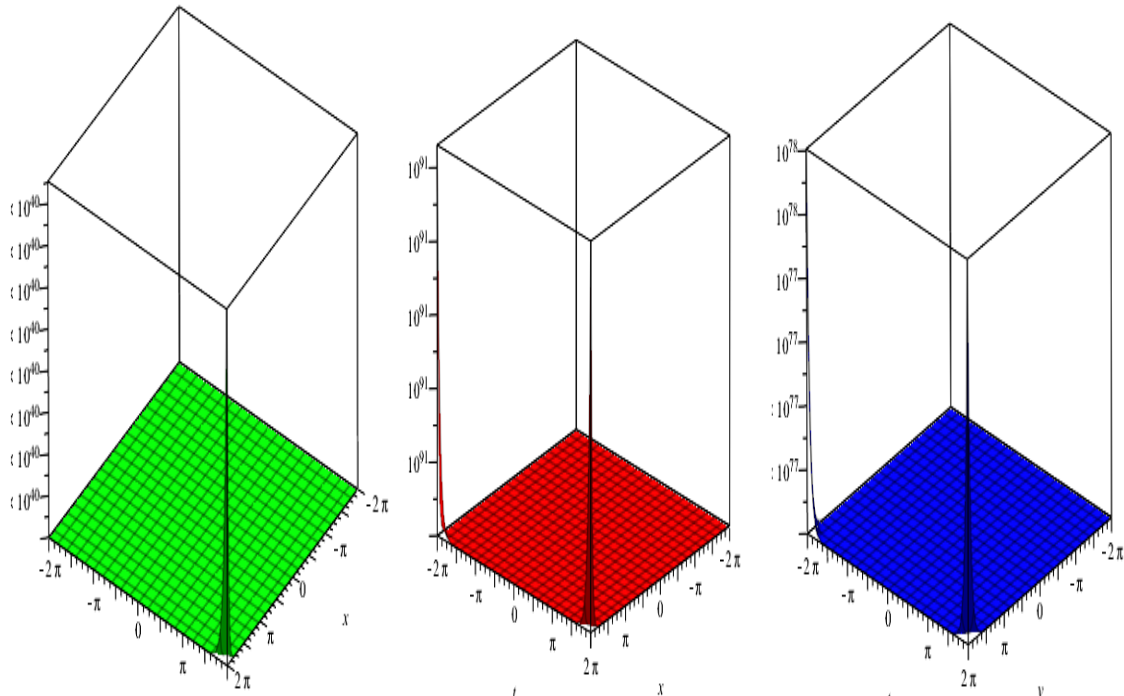
Graph 4. Numerical solution at $z(x, y)$ for $f(x, y) = 10 \sin(x) + 5 \cos(y)$.



Graph 5. Numerical solution at $z(x, t)$ for $f(x, y) = 10 \sin(x) + 5 \cos(y)$.



Graph 6. Numerical solution at $z(t, y)$ for $f(x, y) = 10 \sin(x) + 5 \cos(y)$.



Graph 7. Numerical solution at $z(x, y)$. **Graph 8.** Numerical solution at $z(x, t)$. **Graph 9.** Numerical solution at $z(t, y)$.
 for $f(x, y) = e^{(10x+5y)}$ for $f(x, y) = e^{(10x+5y)}$ for $f(x, y) = e^{(10x+5y)}$

5. DISCUSSION AND CONCLUSIONS

5.1. Discussion

Modal shapes of thin plates require numerical solutions of $Z(x, y, t)$ which is a very tedious job. It will also be a great deal of laborious efforts to obtain numerical solution to graphical representations of these shapes. Consequently, the objective of this study is to formulate fast, easy, and accuracy algorithm to simulate the task ahead. Thus, the objective was accomplished through the formulated algorithm using MAPLE 18 mathematical software in which the plots are shown in graphs 1 to 9 for the geometric behaviours of thin plates vibration when functions $f(x, y)$ (algebraic, trigonometric and exponential) at a static equilibrium condition $g(x, y) = 0$ which was examined. The corresponding numerical solutions for the three test cases are presented in Tables 1 to 3. Moreover, the graphs modal shapes also indicate where the peak amplitudes of vibration of the flexible plate or the nature of frequency of the wave would occur, from which the design engineers should take precaution for not placing delicate attachments at these locations to avoid possible damages due to excessive deformation of the plate structure.

5.2. Conclusion

In this paper, we formulate a four steps algorithm using homotopy perturbation method for the numerical solution of three dimensional second-order PDE which occurred in a plate vibration. The method is applied in a direct way without any transformation, discretization or restrictive assumptions. Also, we have tested the HPA on three different implementations which are shown the efficiency and accuracy of the proposed method. The approximate solutions are in good agree with analytical solutions (see tables 1 to 3). It may be concluded that the HPA is powerful

and efficient in finding the numeric-analytic solutions for a wide class of problems in applied sciences and engineering.

REFERENCES

- [1] Ran Hsu Tai (2018) "Applied Engineering Analysis", published by John Wiley & Sons, (ISBN 9781119071204) Applied Engineering Analysis pp:71-78.
- [2] Irvine M, (1981) "Cable Structures", The MIT Press, Cambridge, New York pp: 23-45.
- [3] Leonard J.W, (1988) "Tension Structures", McGraw-Hill Book Company, New York.
- [4] Rega .G, Vestroni F and Benedettini F, (1984) "Parametric analysis of large amplitude free vibrations of a suspended cable", International Journal of Solids and Structures 20(2), pp:95–105.
- [5] Ni.Y.Q, Lou.W.J and Ko,J.M, (2000) "A hybrid pseudo force/Laplace transform method for non-linear transient response of a suspended cable", Journal of Sound and Vibration 238(2), pp:189–214.
- [6] He, J.-H. (1999), "Homotopy perturbation technique", Computer methods in applied mechanics and engineering, 178, 257
- [7] Vahidi, A., Babolian, E., & Azimzadeh, Z. (2011), "An improvement to the homotopy perturbation method for solving nonlinear Duffing's equations", Bulletin of the Malaysian Mathematical Sciences Society pp: 23-34
- [8] Chang, H.-K., and Liou, J.-C. (2006), "Solving wave dispersion equation for dissipative media using homotopy perturbation technique", Journal of waterway, port, coastal, and ocean engineering, 132.
- [9] Zhou, S., and Wu, H. (2012) "Analytical solutions of nonlinear Poisson–Boltzmann equation for colloidal particles immersed in a general electrolyte solution by homotopy perturbation technique", Colloid and Polymer Science, 290, 1165.
- [10] Özi, s, T., and Akçı, C. (2011) "Periodic solutions for certain non-smooth oscillators by iterated homotopy perturbation method combined with modified Lindstedt Poincaré technique", Meccanica, 46, 341.
- [11] Yazdi, A. A. (2013) "Homotopy perturbation method for nonlinear vibration analysis of functionally graded plate", Journal of Vibration and Acoustics, 135, 021012.
- [12] Al-Saif, A. and Abood, D. A. (2011) "The Homotopy Perturbation Method for Solving K (2, 2) Equation", J, Basrah Researches (Sciences).
- [13] Aswhad, A. A., & Jaddoa, A. F. (2016) "The Approximate Solution of Newell Whitehead Segel and Fisher Equations Using The Adomian Decomposition Method", arXiv preprint arXiv: 1602.04084.
- [14] Babolian, E., Azizi, A., & Saeidian, J. (2009) "Some notes on using the homotopy perturbation method for solving time-dependent differential equations", Mathematical and Computer Modelling, 50, 213.
- [15] Adil M. Al-Rammahi, and Ghassan A. Al-Juaifri (2017) "A Study of General Second-Order Partial Differential Equations Using Homotopy Perturbation Method", Global Journal of Pure and Applied Mathematics. ISSN 0973-1768 Volume 13, Number 6, pp. 2471–2492
- [16] Mohyud-Din S.T and Noor M.A (2009) "The HPM for Solving Partial Differential Equations" Downloaded from PubFactory at 09/06/2016 12:45:36AM via ReadCube/Labtiva.
- [17] He,J.H, (2004) "Comparison of homotopy perturbation method and homotopy analysis method", Applied Mathematics and Computation 156, pp527-539.
- [18] Chun, C. and Sakthivel, R. (2010) "Homotopy perturbation technique for solving twopoint boundary value problems. Comparison with other methods", Computer Physics Communications, 181, 1021.
- [19] Liu H.-K, (2011) "Application of homotopy perturbation methods for solving systems of linear equations," Applied Mathematics and Computation, vol.217, no.12, pp.5259–5264.



International Journal of Engineering and Innovative Research

<http://dergipark.gov.tr/ijeir>

TÜRKİYE’NİN AKDENİZ BÖLGESİNE AİT RÜZGÂR EKSERJİSİNİN ÇOK KATMANLI YAPAY SİNİR AĞI İLE MODELLENMESİ

Durmuş Fatih Mengi^{1*}, Sedat Metlek²

¹Uşak Üniversitesi, Makine Mühendisliği Bölümü, Uşak, Türkiye.

² Mehmet Akif Ersoy Üniversitesi, Teknik Bilimler Meslek Yüksekokulu, Mekatronik Programı, Burdur, Türkiye.

*Sorumlu Yazar: drfatihmengi@gmail.com

(Received: 30.04.2020; Revised: 15.05.2020; Accepted: 30.06.2019)

ÖZET: Bu çalışmada Türkiye’nin Akdeniz Bölgesi içerisinde yer alan, enlem ve boylam çizgilerinin kesiştiği 21 noktanın rüzgâr ekserji analizi yapay sinir ağı ve klasik hesaplama yöntemleri ile kıyaslanmıştır. Bu amaç doğrultusunda NASA’dan elde edilen, 1981 ile 2018 yılları arasındaki aylık ortalama yüzey sıcaklığı, yüzey basıncı ve rüzgâr hızı değerleri kullanılmıştır. NASA’dan alınan veriler ışığında örnek bir rüzgâr türbini modeli oluşturulmuş, üretebileceği maksimum enerji ve ekserji değerleri klasik hesaplama yöntemleri ile hesaplanmıştır. Çalışmanın sonucunda yapay sinir ağı ile elde edilen değerler ve klasik hesaplama yöntemleri ile elde edilen değerler kıyaslanmış, %0,00024 ortalama karesel hata oranı ile başarılı sonuçlar elde edilmiştir. Böylece özellikle rüzgâr enerji santrali yatırımı yapacak yatırımcıların ve diğer karar alıcıların ilk etapta ihtiyaç duyduğu, ekserji analiz sonuçları çok az veri ile hızlı bir şekilde hesaplanması sağlanmıştır.

Anahtar Kelimeler: Rüzgâr Enerjisi, Ekserji Analizi, Enerji Potansiyeli, Yapay Sinir Ağları.

MODELING BELONGS TO TURKEY'S MEDITERRANEAN COAST WIND OF EXERGY MULTILAYER NEURAL NETWORK

ABSTRACT: In this study, 21 points where latitude and longitude intersect from in Turkey's Mediterranean Coast, wind Exergy analysis and artificial neural network were compared with conventional methods of calculation. For this purpose, monthly average surface temperature, surface pressure and wind speed values obtained from NASA between 1981 and 2018 were used. An exemplary wind turbine model has been created with the data received from NASA, and the maximum energy and exergy values it can produce have been calculated by classical calculation methods. At the end of the study, the values obtained by artificial neural network and the values obtained by classical calculation methods were compared, and accurate results were obtained with an average square error rate of 0.00024%. In this way, the exergy analysis results needed by investors and other decision makers who will invest in wind power plants in the first place have been quickly calculated with very little data.

Keywords: Wind Energy, Exergy Analysis, Energy Potential, Artificial Neural Network.

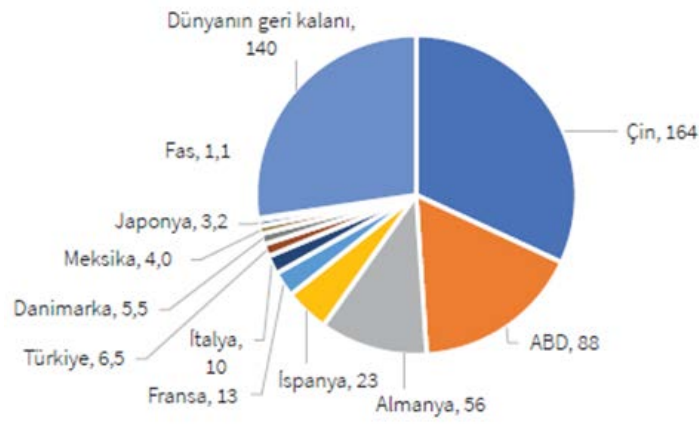
1. GİRİŞ

Teknolojinin her geçen gün kendini yenilemesi ve gelişmesine bağlı olarak artan enerji ihtiyacı dünyanın ve insanoğlunun en büyük problemlerinden birisidir. Bu sorunu çözmek için enerji konusunda çalışmalar yapılırsa da enerji açığını karşılamak için yeterli seviyede değildir. Yoğun olarak kullanılan fosil enerji kaynaklarının sebep olduğu sera gazlarının, gün geçtikçe dünya iklimine ve atmosfere verdiği zararlardan ötürü, insanoğlu temiz, sağlıklı, sürdürülebilir enerji kaynakları olarak nitelendirilen yenilenebilir enerji kaynaklarına (YEK)

doğru yönelmiştir. Yenilenebilir enerji kaynaklarından olan rüzgâr enerjisi, günümüzde en hızlı gelişime sahip olan ve en fazla yatırım yapılan, enerji kaynaklarından birisi olmuştur [1].

Kaynağı güneş olan rüzgâr enerjisi; doğal, yenilenebilir, temiz ve sonsuz bir güçtür. Güneşin dünyaya gönderdiği ışınlar yer küreyi ısıtarak bir enerji oluşturmaktadır. Günümüzde bu enerjinin yaklaşık %2'sinin rüzgâr enerjisine dönüştüğü tespit edilmiştir [2].

Birçok ülke, sürdürülebilir enerji sistemine geçiş konusunda örnekler sunmuştur. Bunlardan biriside Danimarka'dır. Danimarka, 1980'lerin sonlarında rüzgâr ve güneş enerjisi sisteminden elde ettiği enerjiyi ülke şebekesine aktaran ilk ülkelerden birisidir. Avrupa ülkelerinden biri olan İspanya'da ise kurulu gücün yaklaşık %25'ini yenilenebilir enerji kaynakları oluşturmaktadır. Bir başka Avrupa ülkesi olan Almanya ise Dünya genelinde standartları belirleyen öncü bir ülke olmuştur. 2017 yılı itibari belli başlı ülkelerin rüzgâr enerjisinden yararlanma oranları Şekil 1'de gösterilmiştir [3].



Şekil 1. Dünyada ve bazı ülkelerdeki toplam rüzgâr enerjisi kurulu gücünün genel dağılımı [3].

Dünya'da birçok ülke ile birlikte Türkiye de yenilenebilir enerji kaynaklarına yapılan yatırımlar her geçen gün katlanarak artmaktadır. IEA (Renewables 2019) raporuna göre yenilenebilir enerji kapasitesinin artışında Türkiye, Dünyada 12. sırada yer almaktadır [4].

Literatürde rüzgâr enerjisi sistemlerinin geliştirilmesine yönelik birçok çalışma bulunmaktadır. İlk yapılan çalışmalarda, meteoroloji ölçüm istasyonlarından alınan veriler ile rüzgâr gücünün enerji potansiyeli belirlenmiş ve kurulan örnek rüzgâr santralleri ile elektrik üretimi sağlanmıştır [5].

Daha sonraki yıllarda yapılan çalışmalarda ise bilgi teknolojinin gelişmesine bağlı olarak rüzgâr enerji santralleri ile ilgili çalışmalar çok farklı boyutlara taşınmıştır. Özellikle enerjinin kullanılabilirliği kavramının bilimsel bir yorumu olan ekserji ile ilgili bazı çalışmalar dikkat çekmektedir. Birçok YEK'de olduğu gibi rüzgâr enerjisinde de ekserji analizleri yapılmış ve ekserji verimleri incelenmiştir [6].

Bilgi teknolojilerinin de popüler konularından olan yapay zekâ kavramı, enerji sektöründe de ilgi görmüş ve birçok uygulamada kullanılmıştır. Özellikle rüzgâr enerjisi konusunda rüzgâr hızı ve rüzgâr enerjisi potansiyelinin tahmin edilmesinde kullanılan bir yöntem olmuştur [7]. Bunun ile birlikte yakın geçmişte bazı yapay zekâ modelleri, ekserji analizinde de kullanılmaya başlanmıştır.

Dündar [5], Türkiye geneli ortalama rüzgâr hızları ve enerji potansiyellerinin dağılımını incelemiş ve Türkiye de rüzgâr gücünden yararlanabilecek alanları Bandırma, Bodrum, Bozcaada ve Çeşme olarak belirlemiştir. Belirlenen alanlarda WASP programı yardımı ile rüzgâr atlası istatistiklerini çıkarmıştır. Toklu [8], Elazığ için aldığı meteorolojik veriler ile bir

rüzgâr enerjisi santrali tasarlamıştır. Koroneos vd. [9], güneş enerjisi, rüzgâr enerjisi ve jeotermal enerjinin ekserji analizini yapmışlardır. Çalışmalarında mevcut enerjiden gerçek enerji kullanımını incelemektedirler. Bunun ile birlikte verimlilik bazında, yenilenebilir enerji kaynakları ile yenilenemeyen enerji kaynaklarının karşılaştırmasını yapmışlardır. Hepbaşlı ve Özgener [10], yaptıkları çalışmada Ekim 2003 sonu itibariyle Türkiye’deki rüzgâr enerjisinin gelişimini gözden geçirmişler ve Türkiye için bazı öneriler sunmuşlardır. Şahin vd. [11], rüzgâr enerjisinin enerji ve ekserji özellikleri üzerinde durmuştur. Çalışmalarında rüzgâr türbini girişindeki rüzgâr hızı, hava sıcaklığı ve basıncın, rüzgârın sıcaklığı üzerindeki etkilerini incelemiştir. Ayrıca Kanada’nın Ontario eyaletindeki 21 ölçüm istasyonundan aldıkları veriler ile 100 kW’lık bir rüzgâr üretim sistemi modelleyerek enerji ve ekserji verimlerini hesaplamışlardır. Hesaplamalar sonucunda yılın 4 ayı (Ocak, Nisan, Temmuz, Ekim) için enerji ve ekserji verimliliği haritalarını çıkarmışlardır. Hepbaşlı [12], yenilenebilir enerji kaynaklarının ekserjetik açıdan analizini ve performans değerlendirmesini yapmak için bazı termodinamik parametreleri kullanmıştır. Xydis vd. [13], Yunanistan’ın Orta Mora Yarımadasında seçilen üç ayrı bölgede yapılan ölçümlerden elde ettikleri verileri kıyaslayarak bir model oluşturmuşlardır. Aynı zamanda modelledikleri rüzgâr çiftliğinde ekserji analizi yaparak bu bölgenin rüzgâr haritasını çıkarmışlardır. Mengi [6], çalışmasında Türkiye’nin içinde bulunduğu enlem ve boylam derecelerine göre 50 metre yükseklikteki aylık ortalama rüzgâr hızı, yüzey sıcaklığı ve yüzey basınç değerlerini alarak Türkiye için rüzgâr enerjisi potansiyelini belirlemiştir. Ayrıca örnek bir rüzgâr türbini için veriler kullanarak, her bir enlem ve boylam derecesi için enerji ve ekserji analizini yapmıştır. Elde ettiği hesaplama değerlerini Türkiye haritasındaki enlem ve boylam kesişim noktalarına yerleştirerek rüzgâr hızı, enerji verimi ve ekserji verimi haritası çıkarmıştır. Başkut [14], çalışmasında, Türkiye’nin ilk rüzgâr santrali olan Çeşme- Germiyan rüzgâr santralinin 2007-2008 çalışma dönemine ait enerji ve ekserji verimini, enerji ve ekserji analizi metodunu kullanarak hesaplamıştır. Ayrıca, sıcaklık, nem ve basınç gibi meteorolojik parametrelerin verim üzerindeki etkisini incelenmiştir. Saravanan vd. [15], iz parametrelerinin (wake effect) tek dizi rüzgâr çiftliğinin ekserji analizi üzerindeki etkisini incelenmişlerdir. Tek dizi rüzgâr çiftliğinin ekserji verimliliğini tahmin etmek için güç, iz (wake) ve ekserji modeli olmak üzere üç farklı modeli kullanılmışlardır. Ehyaei vd. [16], Tahran (orta rüzgar potansiyeli) ile Manjil (yüksek rüzgar potansiyeli) olmak üzere iki şehirde nominal gücü 10 kW olan bir Bergy Excel-S rüzgar türbininin, enerji, ekserji, ekonomik, gelişmiş ekserji ve genişletilmiş ekserji analizlerini yapmışlardır. Ekonomou vd. [17], bir rüzgâr çiftliğinde üretilen toplam gücün ve en uygun rüzgâr türbini sayısını kullandıkları YSA modeli ile tahmin etmişlerdir. Geliştirdikleri modeli daha önce aynı örnek için farklı yöntemlerle yapılan üç çalışma ile kıyasladıklarında kabul edilebilir başarı oranına sahip olduğunu tespit etmişlerdir. Ata [18], rüzgâr türbinlerinin farklı yüksekliklerdeki yıllık enerji üretimlerini tahmin etmek için YSA algoritmasını kullanmıştır. Elde ettikleri tahmin sonuçlarını Kırkağaç’ta bulunan otonom rüzgâr türbini ile kıyaslamış ve başarı oranının kabul edilebilir düzeyde olduğunu belirtmiştir. Lee ve Baldick [19], yaptıkları çalışmada 52 sinir ağı modeli ve 5 gauss işlem fonksiyonu kullanarak bir model geliştirmiştir. Rüzgâr gücü verileri ve kullandıkları YSA modeli ile gelecek 48 saat için rüzgâr gücünün tahmin etmişlerdir. Mortazavi vd. [20], Pareto optimum çözüm kümesi elde etmek için çok amaçlı genetik algoritma kullanmışlardır. Kullandıkları algoritma ile 10m uzunluğundaki yatay eksenli türbinlerin, kanat profilleri için geometrik karakteristikleri belirlemiştir. Çalışmalarının sonucunda Pareto optimaldik konseptiyle ikinci yasa yaklaşımının birlikte kullanılmasının gerekliliğini vurgulamışlardır. Lydia vd. [21], yaptıkları çalışmada, Yeni Zelanda’da ki beş farklı bölgenin günlük rüzgâr hızı verilerini kullanmışlardır. Geliştirdikleri modelde rüzgâr hızı tahmini için rüzgâr türbininin güç eğrisini kullanmışlardır. Pelletier vd. [22], rüzgâr türbininin güç çıkışını etkileyen parametrelerin, bir biri ile doğrusal olmayan bir ilişkisi olduğunu belirtmektedir. Bu nedenle de rüzgâr türbini

güç eğrisi modelini yapay sinir ağı kullanarak modellemişlerdir. Manobel vd. [23], rüzgâr türbini güç eğrisinin tahmini ve her bir türbinin performansının uygun bir YSA modeli ile yüksek doğrulukta yapılabileceğini tespit etmişlerdir. Altınsoy ve Bal [24], yaptıkları çalışmada Ankara'nın bazı ilçeleri için YSA modeli kullanarak rüzgâr hızı tahmini yapılmıştır. Sonuç olarak Çubuk için %9,48, Keçiören için %7,77, Polatlı için %7,88, Bala için %6,83, Şereflikoçhisar için %8,02 ve Haymana için %5,41 ortalama karesel hata oranı ile rüzgâr hızını tahmin etmişlerdir. Lawan vd. [7], Sarawak-Sibu'daki rüzgâr hızını, YSA kullanarak tahmin etmişlerdir. Bu tahmin değerine göre de toplam enerji potansiyelini hesaplamışlardır. Zafirakis vd. [25], yaptıkları çalışmada Yunanistan'da çalışan bir rüzgâr santralinden aldıkları rüzgâr hızı ve rüzgâr enerjisi üretim ölçüm değerlerini, hem YSA hem de Destek Vektör Regresyonu (SVR) modellerini, kullanarak modellemişlerdir. Nielson vd. [26], ABD'nin Kirkwood kentinde bulunan 2,5 MW gücündeki rüzgâr türbininden elde ettikleri verileri, ileri beslemeli geri yayılım algoritmasını eğitmek için kullanmışlardır. Çalışma sonucunda yüksek doğrulukta başarı oranı elde etmişlerdir.

Literatürde de görüldüğü üzere rüzgâr gücünün hızı, enerji potansiyeli ve veriminin tahmini ile ilgili yapay zekâ konularını da içeren birçok çalışmanın yapıldığı görülmektedir. Fakat yapılan çalışmalarda rüzgâr enerjisinin ekserji analizinin, çok katmanlı yapay sinir ağı (ÇKYSA) ile modelleyebilen sınırlı sayıda çalışma olduğu tespit edilmiştir. Özellikle Akdeniz Bölgesi için yapay sinir ağı ile rüzgâr enerjisi ekserji tahmini çalışması yapılmamıştır.

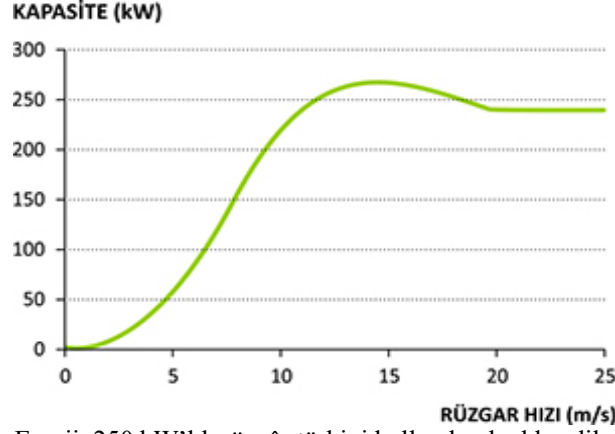
Rüzgâr enerjisinin ekserji analizinin yapılabilmesi için birçok veriye gereksinim duyulmaktadır. Özellikle herhangi bir noktaya rüzgâr enerji santrali kurulması planlandığında, santralin kurulacağı yer ile ilgili en az 5 yıllık ölçüm verilerine gereksinim duyulmaktadır. Bu verilerin elde edilmesi hem zaman hem de maddi açıdan maliyetlidir. Bu nedenle NASA'dan Türkiye'nin Akdeniz Bölgesi ile ilgili alınan basınç, sıcaklık ve rüzgâr hız bilgileri ile bir yapay sinir ağı modeli oluşturulmuştur. Oluşturulan model ile örnek bir rüzgâr türbinine ait güç eğrisi üzerinden ekserji hesaplaması yapılmış ve sonuçları ÇKYSA ile kıyaslanarak çalışmada sunulmuştur.

2. MATERYAL

Rüzgâr enerjisine dayalı çalışmaları gerçekleştirmek için birçok veriye ihtiyaç duyulmaktadır. Yapılan çalışmada Türkiye'nin Akdeniz Bölgesi içerisinde yer alan koordinat noktalarındaki, meteorolojik veriler kullanılmıştır. Bu koordinat noktalarına ait veriler; koordinat noktasının yüzey basıncı, yüzey sıcaklığı ve bu noktanın 50 metre yüksekliğindeki rüzgâr hızı değerleridir. Çalışmada kullanılan veriler NASA'nın sunmuş olduğu tablolardan elde edilmiştir.

Gerçekleştirilen çalışmada, Mengi'nin daha önce yapmış olduğu bir çalışmada kullandığı güç eğrisi kullanılmıştır [6]. Tercih edilen güç eğrisi ile NASA'nın sunmuş olduğu veriler birlikte kullanılarak, Akdeniz Bölgesindeki 21 noktanın ekserji analizi gerçekleştirilmiştir. Çalışmada kullanılan güç eğrisinin farklı hızlardaki üretmiş olduğu enerji miktarı Şekil 2'de gösterilmektedir. Şekil 2'de kullanılan eğrinin formülü ise Denklem 1'de, katsayıları da Tablo 1'de detaylı olarak gösterilmektedir.

$$E_{Potansiyel} = aV^{10} + bV^9 + cV^8 + dV^7 + eV^6 + fV^5 + gV^4 + hV^3 + iV^2 + jV + k \quad (1)$$



Şekil 2. Güç eğrisi (Mars Enerji, 250 kW'lık rüzgâr türbini kullanılarak elde edilen, kapasite-rüzgâr hızı güç eğrisi grafiği)[6].

Tablo 1. Güç eğrisinin katsayıları [6]

Katsayı	Değer
a	$-8.47015071 \times 10^{-11}$
b	$2.093134223 \times 10^{-8}$
c	$-2.201091719 \times 10^{-6}$
d	$1.287287668 \times 10^{-4}$
e	$-4.577408717 \times 10^{-3}$
f	0.1011975583
g	-1.356495025
h	10.12932888
i	-34.79795152
j	50.64102792
k	$-4.511939453 \times 10^{-2}$

Çalışmada kullanılan rüzgâr türbini, Mars Enerji firmasının 250 kW(kiloWatt)'lık türbinidir. Bu türbine ait bazı teknik bilgiler Tablo 2'de verilmiştir.

Tablo 2. Mars enerji 250kw rüzgâr türbini teknik bilgileri[6].

Türbin Yüksekliği	Kanat Çapı	Kanat Sayısı	Optimum Çalışma Hızı	Devreye Girme Hızı	Devreden Çıkma Hızı
50m	26m	3	14m/s	4m/s	25 m/s

3. METOD

3.1. Rüzgâr Enerjisi Sisteminin Termodinamik Analizi

Sabit bir hız (V) ile hareket eden bir kütle (m) hareketi süresince kinetik enerji üretir. Bu sistemlerin belirli bir referans noktasına göre sahip olduğu enerjide, kinetik enerji (KE) olarak ifade edilmektedir. Kinetik enerji Denklem 2 ile gösterilmektedir [27].

$$KE = \frac{1}{2}mV^2 \quad (2)$$

Hareket halindeki hava kütesinin türbin kanatlarına ilk çarptığı andaki hızı (V_1), türbin kanadının çıkışında ise hızı (V_0) ise rüzgâr enerjisi için genel kinetik enerji denklemi, Denklem 3 ile ifade edilmektedir [28].

$$\dot{E} = \frac{1}{2} \dot{m} (V_1^2 - V_0^2) \quad (3)$$

Burada, \dot{E} rüzgâr gücü, \dot{m} hareket halindeki hava moleküllerinin kütleli debisidir.

Hava yoğunluğu (ρ), Denklem 4 ile gösterilmektedir [27].

$$\rho = \frac{P}{RT} \quad (4)$$

P atmosfer basıncını (kPa), R ideal gaz sabitini (kJ/kgK), T ise havanın sıcaklığını (K) ifade etmektedir.

Rotor süpürme alanı (A) türbininin güç çıktısı ile doğru orantılıdır. Yatay eksenli türbin için rotor süpürme alanı, Denklem 5 ile gösterilmektedir [29].

$$A = \pi r^2 \quad (5)$$

Rüzgâr türbini tarafından üretilecek güç, rüzgârın türbine giriş hızı (V_1) ve rüzgârın türbinden çıkış hızı (V_0) arasındaki fark ile ilgilidir [30]. Bu hız değişimi sırasındaki ortalama hız Denklem 6 ile ifade edilir [28,30].

$$V_{ort} = \frac{V_1 + V_0}{2} \quad (6)$$

Bu durumda türbin kanatları üzerinden akan havanın kütleli debisi; Denklem 7 ile gösterilmektedir [27].

$$\dot{m} = \rho A V_{ort} \quad (7)$$

Denklem 3'deki genel kinetik enerji denkleminde 6 ve 7 numaralı denklemler yazılınca Denklem 8 elde edilir. Denklem 8' de gerekli matematiksel işlemler yapılarak Denklem 9 elde edilir. Betz yasası olarak bilinen C_p değeri yerine yazıldığında, kanatlar tarafından sağlanan gücün, girdi rüzgâr hızına bağlı güç denklemi, Denklem 11 ile ifade edilir [28-30].

$$\dot{E}_0 = \frac{1}{2} \left[\rho A \frac{V_1 + V_0}{2} \right] (V_1^2 - V_0^2) \quad (8)$$

$$\dot{E}_0 = \rho A V_1^3 \frac{\left(1 + \frac{V_0}{V_1}\right) \left[1 - \left(\frac{V_0}{V_1}\right)^2\right]}{2} \quad (9)$$

$$C_p = \frac{\left(1 + \frac{V_0}{V_1}\right) \left[1 - \left(\frac{V_0}{V_1}\right)^2\right]}{2} \quad (10)$$

$$\dot{E}_0 = \rho A V_1^3 C_p \quad (11)$$

Betz yasası olarak bilinen C_p incelendiğinde, $C_p = 0.59$ olarak bulunur ve rüzgâr türbininin üretebileceği maksimum güçtür [30]. Bir rüzgâr türbininin genel enerji dengesi Denklem 12 ile gösterilmektedir [30-31].

$$\sum_{in}(h + ke + pe)_{in} \dot{m}_{in} - \sum_{out}(h + ke + pe)_{out} \dot{m}_{out} + \sum_r \dot{Q}_r - \dot{W} = 0 \quad (12)$$

Denklem 12’de \dot{m}_{in} türbine giren kütlelesel hava debisini (kg/sn), \dot{m}_{out} türbinden çıkan kütlelesel hava debisini (kg/sn), h birim kütle için sahip olduğu entalpiyi (kJ/kg), \dot{W} sistemden çıkan işi (kW), \dot{Q}_r r yüzeyinden transferi gerçekleşen ısı enerjisini (kW) ifade etmektedir.

3.2. Rüzgâr Enerji Sistemlerinde Ekserji Analizi

Madde akışından dolayı oluşan genel ekserji formülü Denklem 13 ile ifade edilir.

$$\dot{E}x = \dot{E}x_k + \dot{E}x_p + \dot{E}x_{akış} + \dot{E}x_{kimyasal} \quad (13)$$

Burada; $\dot{E}x_k$, kinetik ekserji, $\dot{E}x_p$, potansiyel ekserji, $\dot{E}x_{akış}$, akış ekserjisi ve $\dot{E}x_{kimyasal}$, kimyasal ekserjidir [32].

Sistemin ürettiği elektrik kinetik enerji farkından kaynaklandığı için üretilen enerji Denklem (14a) ve (14b)’deki gibi elde edilmektedir [31-32].

$$\dot{E}x_k = \dot{E}_{üretilen} \quad (14a)$$

$$\dot{E}x_k = KE = \frac{1}{2} \rho A (V_1 - V_2)^3 C_p \quad (14b)$$

Akış ekserjisi de Denklem 15 ile ifade edilmektedir [32].

$$\dot{E}x_{akış} = \dot{m}(\Delta h - T_0 \Delta s) \quad (15)$$

Denklem 15’de \dot{m} , havanın kütlelesel debisini, Δh entalpi değişimini ve Δs ise entropi değişimini (kJ/kgK) ifade etmektedir. Entalpi’deki değişim ise Denklem 16’da verilmiştir [28,32].

$$\Delta h = C_{p,h}(T_2 - T_1) \quad (16)$$

Denklem 16’deki; $C_{p,h}$ havanın spesifik ısısı, T_1 türbin girişindeki hava sıcaklığı ve T_2 ise türbin çıkışındaki hava sıcaklığıdır. Türbin çıkışındaki hava sıcaklığı Denklem 17 ile hesaplanmaktadır [32].

$$T_2 = 35.74 + 0.6215T_{atm} - 35.75(V_1^{0.16}) + 0.4274T_{atm}(V_1^{0.16}) \quad (17)$$

Denklem 17’de, T_2 türbin çıkışındaki sıcaklığı (°F), T_{atm} atmosfer sıcaklığı (°F) ve V_1 ise türbin girişindeki rüzgâr hızını (mph) ifade eder. Birim dönüşümü yapılırsa, rüzgâr hızının birimi(m/sn) ve atmosfer sıcaklığının birimi de (°C) olarak düzenlenir ise Denklem 18 elde edilir [32].

$$T_2 = 13,126 + 0.6215T_{atm} - 13,948(V_1^{0.16}) + 0,48615T_{atm}(V_1^{0.16}) \quad (18)$$

Sistemdeki entropi üretimi ise Denklem (19a) ve (19b) ile ifade edilir [11,31].

$$\Delta \dot{S} = \Delta \dot{S}_{sistem} + \Delta \dot{S}_{çevre} \quad (19a)$$

$$\Delta \dot{S} = \dot{m} T_{atm} \left(C_p \ln \left(\frac{T_2}{T_1} \right) - R \ln \left(\frac{P_2}{P_1} \right) - \frac{\dot{Q}_{kayıp}}{T_{atm}} \right) \quad (19b)$$

T_1 giriş sıcaklığı, T_2 çıkış sıcaklığıdır. R ise hava için belirlenmiş olan ideal gaz sabitini ifade etmektedir. Rüzgâr, türbin girişinde P_1 , türbin çıkışında ise P_2 basıncını uygular. Türbin çıkışındaki basınç Denklem 20 ile hesaplanır [11,31,32].

$$P_2 = P_1 \pm \frac{\rho}{2} V_1^2 \quad (20)$$

Hava molekülleri rüzgâr türbinine belirli bir giriş hızı ile çarparken belirli bir çıkış hız ile türbini terk eder. Girişteki hız bilinmemektedir fakat çıkış hızı ise Denklem 21 ile hesaplanmaktadır [11,31,32].

$$V_2 = \sqrt[3]{\frac{2(E_{potansiyel} - E_{üretilen})}{\rho A C_p}} \quad (21)$$

Yukarıdaki denklemde $E_{potansiyel}$ değeri, rüzgâr türbinin oluşturacağı maksimum güç olarak kabul edilir. $E_{potansiyel}$ değeri seçilen örnek rüzgâr türbininin katalogundaki, kapasite-rüzgâr hızı eğrisinden hesaplanır [6]. Türbinde meydana gelebilecek ısı kayıpları ihmal edilebilir düzeyde olmasına rağmen istenilirse Denklem 22 ile hesaplanabilmektedir [31-32].

$$\dot{Q}_{kayıp} = \dot{m} C_p \left(T_{atm} - \frac{T_1 + T_2}{2} \right) \quad (22)$$

Toplam ekserji ise Denklem 23 ile hesaplanmaktadır [31-32].

$$\dot{E}_x = \dot{E}_{üretilen} + \dot{m} C_p (T_2 - T_1) + \dot{m} T_{atm} \left(C_p \ln \left(\frac{T_2}{T_1} \right) - R \ln \left(\frac{P_2}{P_1} \right) - \frac{\dot{Q}_{kayıp}}{T_{atm}} \right) \quad (23)$$

Rüzgâr türbininin (RT) enerji ve ekserji verimleri ise sırasıyla Denklem 24 ve 25'de sunulmuştur [6].

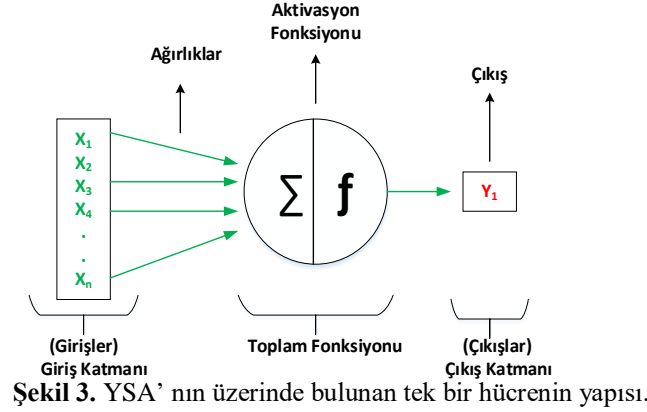
$$\eta_{RT} = \frac{\dot{E}_0}{E_{Potansiyel}} \quad (24)$$

$$\psi_{RT} = \frac{\dot{E}_x}{E_{Potansiyel}} \quad (25)$$

3.3. Yapay Sinir Ağları

Yapay Sinir Ağları (YSA), yapay zekanın popüler alt konularının birisidir. Multidisipliner olması nedeniyle birçok uygulamada da kullanılmaktadır [34-36]. Bu kadar çok tercih edilmesinin sonucunda da sürekli yeni YSA modelleri geliştirilmektedir. YSA' lar genel mantık olarak insanların algılama ve karar verme gibi düşünsel süreçlerini taklit eden bir yapıya sahiptir. Biyolojik sinir hücrelerinden esinlenerek geliştirilen YSA' lar, birbirine bağlı hücrelerden oluşmaktadır. Bu hücreler kendilerine gelen bilgiyi çözümleyebilen ve kendinden sonrasına aktarabilen bir yapıya sahiptir. YSA' ya herhangi bir konu ile ilgili yeterli sayıda

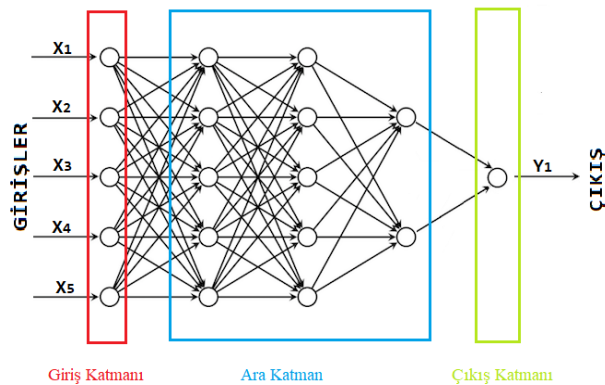
giriş ve çıkış bilgileri verildiğinde, YSA kendi iç yapısında giriş ile çıkış arasında bir bağıntı kurabilir. Ağa bu şekilde giriş ve çıkış bilgilerinin verilmesi işlemine ağı eğitilmesi denilmektedir. Ağı eğitilmesinden sonra, eğitildiği konu ile ilgili daha önce görmediği bir örnek verilirse, ağ bazı çıkarımlarda bulunabilir. YSA' lar bu çıkarım yeteneği sayesinde birçok alanda kullanılmaktadır [36-38]. Yazılımsal olarak geliştirilen yapay sinir ağının, tek bir hücresi Şekil 3'de gösterilmektedir. Bu yapıda giriş katmanı, algılayıcılardan ya da veri tabanından gelen bilgilerin doğrudan ağı sunulduğu katmandır.



Giriş katmanından gelen bilgiler, belirlenen ağırlıklar ile çarpılarak toplam fonksiyonuna aktarılmaktadır. Toplam fonksiyonundan elde edilen değer, belirlenen aktivasyon fonksiyonu ile tekrar hesaplanarak, hücrenin çıkış değeri elde edilmektedir. Denklem 26'da yaygın olarak kullanılan toplam fonksiyonu gösterilmektedir.

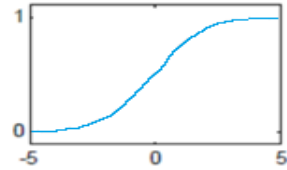
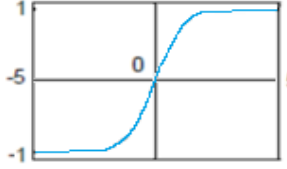

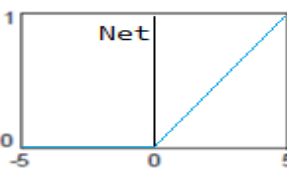
$$Net = \sum_{i=1}^{i=j} X_i W_i \quad (26)$$

Denklem 26'daki \$X_i\$, girdi katmanındaki her bir girişi, \$W_i\$ ise bu girişe ait ağırlığı ifade etmektedir. Bir yapay sinir ağı genellikle birçok sinir hücresinden oluşmaktadır. Bu sinir hücrelerinin birbirinden bağımsız olarak farklı tipte toplama fonksiyonu olabileceği gibi tüm hücrelerde aynı tip toplama fonksiyonuna sahip olabilir. Toplama fonksiyonundan elde edilen değerler belli aralıklara indirgemek için aktivasyon fonksiyonuna aktarılmaktadır. Yaygın olarak kullanılan aktivasyon fonksiyonları ve bunların indirgendiği aralıklar Tablo 3'de gösterilmektedir. Tasarlanan YSA'nın yapısında Şekil 4'de gösterildiği gibi birden fazla sinir hücresi bulunuyorsa, aktivasyon fonksiyonundan çıkan değerler bir diğer hücreye giriş olarak aktarılmaktadır. En son çıkış katmanında bulunan hücrelerin, aktivasyon fonksiyonundan çıkan değerler, YSA'nın çıkışını vermektedir.



Şekil 4. YSA Yapısı.

Tablo 3.Aktivasyon Fonksiyonları.

Fonksiyon Adı	Fonksiyon İçeriği	Grafik
Sigmoid	$y = \frac{1}{1 + e^{-Net}}$	
Tanjant Hiperbolik	$y = \frac{e^{Net} - e^{-Net}}{e^{Net} + e^{-Net}}$	
Adım Fonksiyonu	$y = \begin{cases} 1 & Net \geq 0 \\ 0 & Net < 0 \end{cases}$	
Relu	$y = \max(0, Net)$	

YSA' nın üretmiş olduğu değer çıkış katmanından elde edildikten sonra, olması gereken değer ile karşılaştırılır. Bu karşılaştırmada genellikle Denklem 31'deki gösterilen Ortalama Karesel Hata Fonksiyonu kullanılmaktadır.

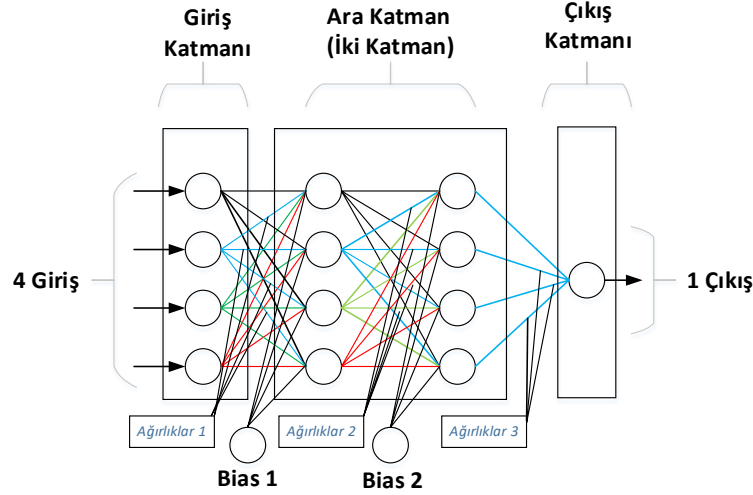
$$\text{Ortalama Karesel Hata} = \frac{1}{n} \sum_{i=1}^n (g_i - y_i)^2 \quad (31)$$

Denklem 31'de; g_i i . değer için gerçek çıktı değerini, y_i i .değer için ağı üretmiş olduğu çıktı değerini, n ağı eğitilmesi için ağa verilen örnek sayısını ifade etmektedir.

Literatürde yapay sinir ağlarının, ileri beslemeli, geri beslemeli, adaline/madaline gibi lineer ve lineer olmayan sistemler için geliştirilmiş birçok modeli bulunmaktadır. Çalışmada doğrusal olmayan olaylardan elde edilen veriler kullanıldığı için çok katmanlı geri beslemeli yapay sinir ağı modeli kullanılmıştır.

3.3.1. Çok katmanlı ileri beslemeli yapay sinir ağı (Feedforward Neural Networks)

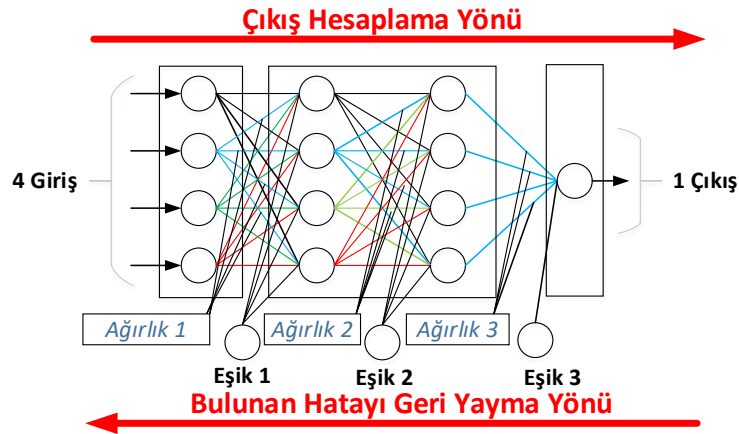
Çok katmanlı ileri beslemeli yapay sinir ağı, doğrusal çözümü bulunmayan sistemler için geliştirilmiş bir yapay sinir ağı modelidir. Yapısı itibari ile giriş katmanı, ara katman ve çıkış katmanından oluşmaktadır. Giriş katmanından giren bilgi sadece ara katmandan geçerek çıkış katmanına doğru hareket etmektedir. Bu yapıda tüm katmanlar birbirine tam bağlıdır ve ara katman sayısı birden çok olabilir. Şekil 5'de çok katmanlı ileri beslemeli ağ yapısı gösterilmektedir. Şekil 5'de gösterilen bağlantı ağırlıkları eğitim esnasında değiştirilebilir fakat çıkıştan girişe doğru bağlantı ağırlıkları değiştirilmez. Sadece ağ ileri doğru giderken ağırlıklar güncellenir.



Şekil 5. Çok katmanlı ileri beslemeli yapay sinir ağı modeli.

3.3.2. Çok katmanlı geri beslemeli yapay sinir ağı (Back forward Neural Networks)

Bu model, ağı tüm çıkışından elde edilen hatanın, çıkış katmanından giriş katmanına doğru ağırlıklarının güncellenmesi prensibine dayanmaktadır. Geri beslemeli YSA modelleri genellikle doğrusal olmayan sınıflama, eğri uyurma ve tahmin problemlerinde yüksek başarımlara sahiptir. Bu nedenle birçok uygulamada tercih sebebidir. Şekil 6'da iki ara katmanlı geri beslemeli bir YSA modeli gösterilmektedir. Bu yapıda çıkıştan elde edilen hatanın, ağırlıklara yansıtılması için bir geri yayılım algoritması kullanılmaktadır.



Şekil 6. Geri beslemeli yapay sinir ağı modeli.

Geril Yayılım Algoritması

Çok katmanlı geri beslemeli YSA modelinde, giriş katmanından gelen değerler ara katlananlardan geçerek çıkış katmanına gider ve ağı bir çıkış değeri üretir. Bu değer üretildikten sonra Denklem 32'ye göre bir hata değeri hesaplanır.

$$E(m) = B(m) - \zeta(m); \quad m = 1, \dots, m \quad (32)$$

Denklem 32'de $B(m)$ beklenen çıkış değerini, $\zeta(m)$ ağı çıkış değerini, $E(m)$ ağı hata değerini, m ise çıktı katmanındaki m . Proses elemanını ifade etmektedir. Çıktı katmanındaki tüm proses elemanlarından elde edilecek toplam hata, Denklem 33 ile elde edilmektedir.

$$TH = \frac{1}{2} \sum_m E(m)^2 \quad (33)$$

Denklem 33'deki TH toplam hatayı, $E(m)$ ise ağırlık hatası değerini ifade etmektedir. Toplam hata değeri hesaplandıktan sonra TH değeri iki aşamada, çıkış katmanından giriş katmanına doğru ağırlıklara yansıtılmaktadır.

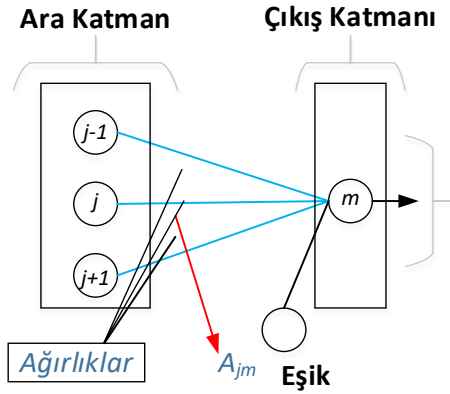
Bu aşamada ilk olarak çıkış katmanı ile ara katman arasındaki ağırlıklar güncellenmektedir. İkinci aşamada ise ara katman ile giriş katmanı arasında ağırlıklar güncellenmektedir.

1. Aşama: Çıkış katmanı ile ara katman arasındaki ağırlıkların güncellenmesi.

Şekil 7'de gösterildiği gibi, herhangi bir t zamanında (t . iterasyonda) ara katmanındaki j . proses elemanını çıkış katmanındaki m . proses elemanına bağlayan bağlantının ağırlığındaki değişim miktarına ΔA^a ve m .çıkış ünitesinin hatasına δ_m denilirse, ilk olarak δ_m değerini Denklem 34 ile hesaplamak gerekmektedir [35].

$$\delta_m = f'(NET). E_m \quad (34)$$

Denklem 34'deki $f'(NET)$ aktivasyon fonksiyonun türevini ifade etmektedir



Şekil 7. Ara katman ile çıkış katman arası.

$$\Delta A_{jm}^a(t) = \eta \delta_m \zeta_j^a + \alpha \Delta A_{jm}^a(t-1) \quad (35)$$

Ağırlıktaki değişim miktarı olan ΔA^a ise Denklem 35'e göre hesaplanmaktadır. Denklem 35'de ki, η öğrenme katsayısını, α momentum katsayısını ifade etmektedir. Ağırlıkların değişim miktarı Denklem 35'e göre hesaplandıktan sonra t . iterasyonda ki yeni ağırlık değerleri Denklem 36 ile hesaplanmaktadır.

$$A_{jm}^a(t) = A_{jm}^a(t-1) + \Delta A_{jm}^a(t) \quad (36)$$

Şekil 7'de gösterilen eşik değeri ünitesinin de güncellenmesi gerekmektedir. Çıkış katmanında bulunan proses elemanlarının eşik değeri β^c ile gösterilirse, buradaki değişim miktarı Denklem 37'ye göre hesaplanmaktadır.

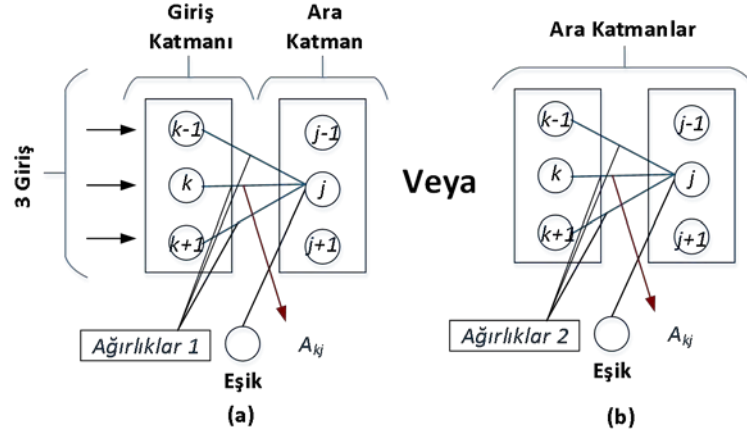
$$\Delta \beta_m^c(t) = \eta \delta_m + \alpha \Delta \beta_m^c(t-1) \quad (37)$$

Eşik değerinin t . iterasyonda ki ağırlığının yeni değeri Denklem 38'e göre hesaplanmaktadır.

$$\beta_m^c(t) = \beta_m^c(t-1) + \Delta\beta_m^c(t) \quad (38)$$

2. *Aşama*: Giriş katmanı ile ara katman arasındaki veya ara katmanlar arasındaki ağırlıkları güncellemesi.

Çıktı katmanı ile ara katman arasındaki ağırlıkların güncellenmesinde, her ağırlık için çıktı katmanındaki sadece bir proses elemanının hatası işleme alınmıştır. Çıktı katmanındaki bu hataların oluşmasında, Şekil 8.(a)'da gösterildiği gibi girdi katmanı ve ara katman arasındaki ağırlıkların etkisinin olduğu gibi eğer Şekil 8.(b)'de gösterildiği gibi birden çok ara katman varsa onlarında arasındaki ağırlıkların etkisi de bulunmaktadır.



Şekil 8.(a) Giriş ile ara katman (b) İki ara katman.

Çıkış katmanına gelen bütün bilgiler, girdi katmanı ve önceki ara katmanlardan gelmektedir. Bu nedenle çıktı katmanındaki proses elemanların hepsinden elde edilen hata, Şekil 8(a) ve (b)'de gösterilen ara katman ile girdi katmanı arasındaki (veya ara katmanlar arasındaki) ağırlıklara dağıtılmaktadır.

İlk olarak Denklem 39'da δ_j^a ile gösterilen hata hesaplanmaktadır.

$$\delta_j^a = f'(NET) \cdot \sum_m \delta_m A_{kj}^i \quad (39)$$

Sonrasında ΔA_{kj}^i ile gösterilen ağırlıklarda ki değişim miktarı ise Denklem 40 ile bulunmaktadır.

$$\Delta A_{kj}^i(t) = \eta \delta_j^a C_k^i + \alpha \Delta A_{kj}^i(t-1) \quad (40)$$

Ağırlıkların yeni değerleri ise Denklem 41 ile hesaplanmaktadır

$$A_{kj}^i(t) = A_{kj}^i(t-1) + \Delta A_{kj}^i(t) \quad (41)$$

Şekil 8.(a) ve (b)'de gösterilen eşik değerleri β^a ile ifade edilirse, eşik değerindeki değişim miktarı Denklem 42 ile gösterilmektedir.

$$\Delta\beta_j^a(t) = \eta\beta_j^a + \alpha\Delta\beta_j^a(t-1) \quad (42)$$

t. iterasyonda ki yeni eşik değeri ise Denklem 43 ile hesaplanmaktadır.

$$\beta_j^a(t) = \beta_j^a(t-1) + \Delta\beta_j^a(t) \quad (43)$$

Bu işlemler sonucunda ileri doğru çalışan YSA, geriye doğru da çalıştırılarak tüm ağırlıkların güncellenmesi sağlanacaktır. Tasarlanan geri beslemeli YSA istenilen hata değerine ulaşıncaya kadar ya da tasarımcının belirlemiş olduğu iterasyon sayısına kadar bu işlemler tekrarlanacaktır. Bu tekrarlama işlemlerinin en sonunda da ağ eğitilmiş olacaktır. Bundan sonraki adımda, eğitilen ağa daha önce görmediği veriler gönderilerek, ağın test edilmesi sağlanacaktır.

4. BULGULAR

Çalışmada Nasa'dan alınan Akdeniz Bölgesindeki, enlem ve boylamların kesiştiği 21 noktaya ait, 1981 ile 2018 yılları arasındaki sıcaklık, hız ve basınç bilgileri kullanılmıştır [33]. Tablo 3'de sadece bu 37 yıllık veriler kullanılarak elde edilen, ekserji, maksimum enerji, üretilen enerji, enerji verimi ve ekserji verimlerinin ortalama değerleri gösterilmektedir.

Tablo 3. 1981 ile 2018 yılları arasındaki Akdeniz bölgesine ait koordinatların, sıcaklık, hız ve basınç değerleri alınarak hesaplanan enerji, ekserji ve verim değerlerinin ortalamaları.

Koordinat	Ekserji (W)	Maksimum Enerji (W)	Üretilen Enerji (W)	Enerji Verimi	Ekserji Verimi
36-29	10,311	40,277	15,018	0,352	0,239
36-30	6,761	32,016	10,158	0,296	0,194
36-31	14,244	48,462	20,218	0,380	0,262
36-32	6,146	30,943	9,304	0,274	0,177
36-33	8,799	37,025	12,990	0,335	0,225
36-34	12,826	46,114	18,400	0,369	0,253
36-35	15,294	51,872	21,746	0,397	0,276
36-36	11,223	42,580	16,283	0,369	0,252
37-29	5,862	30,898	8,972	0,272	0,175
37-30	5,018	29,212	7,788	0,247	0,156
37-31	7,543	35,787	11,211	0,284	0,188
37-32	10,358	43,547	15,291	0,332	0,222
37-33	11,047	45,393	16,251	0,341	0,230
37-34	7,102	34,792	10,748	0,290	0,189
37-35	5,849	29,828	8,911	0,285	0,185
37-36	6,453	31,156	9,747	0,299	0,196
37-37	13,141	50,230	19,115	0,373	0,256
38-30	10,304	42,647	15,180	0,342	0,230
38-31	10,866	44,703	15,986	0,340	0,228
38-36	10,626	45,545	15,757	0,333	0,223
38-37	10,162	44,144	15,103	0,329	0,219

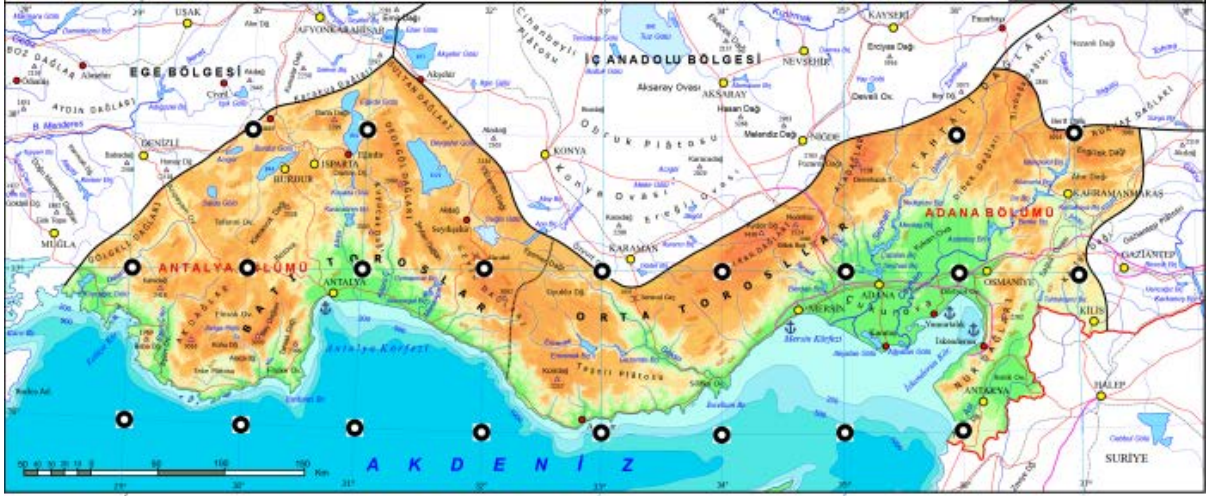
Tablo 3'de verilen maksimum enerji, rüzgâr türbininin teorik olarak üretebileceği en yüksek enerjidir. Bu değer rüzgâr türbininin güç eğrisinden türetilen 10. dereceden bir polinom olan $E_{Potansiyel}$ fonksiyonudur. Tablo 3'deki üretilen enerji terimi ise türbine ilk giriş hızının kinetik enerjisi sonucu meydana gelen enerjidir.

Tablodaki ekserji ve enerji verimleri incelendiğinde ise ekserji veriminin, enerji verimine oranla daha az olduğu görülmektedir. Bunun sebebi ise üretilen enerjinin bir kısmının sürtünmelerden, bir kısmının da mekaniksel kayıplardan kaynaklanmasıdır. Bu kayıplar sonucunda elde kalan enerji kullanılabilir enerji olarak tanımlanan ekserji verimi terimini ifade etmektedir.

Tablo 3'deki ekserji sonuçları incelendiğinde, Akdeniz Bölgesindeki kullanılabilir enerjinin en yüksek olduğu yerin kıyı şeridi boyunca uzanan 36. enlem de olduğu görülmektedir.

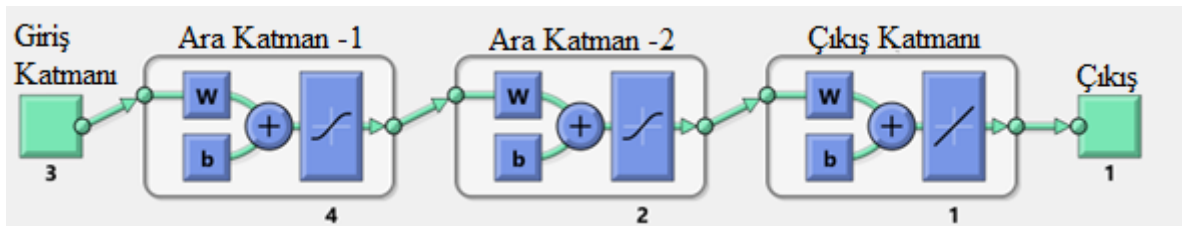
Akdenizin iç kısımlarındaki koordinat noktalarında ekserji değerleri düşmekte fakat yüksek kesimlerdeki koordinat noktalarında ekserji değerlerinin fazla olduğu görülmektedir. Bu bilgiler ışığında Akdeniz Bölgesinin kıyı ve yüksek kesimlerinin rüzgâr enerjisi açısından kullanılabilirliği yüksektir.

Şekil 9'da gösterilen enlem ve boylamların kesiştiği her bir noktaya ait 456 adet veri bulunmaktadır. Çalışmada 21 adet kesişim noktası kullanıldığı için toplam 9576 adet veri kullanılmıştır.



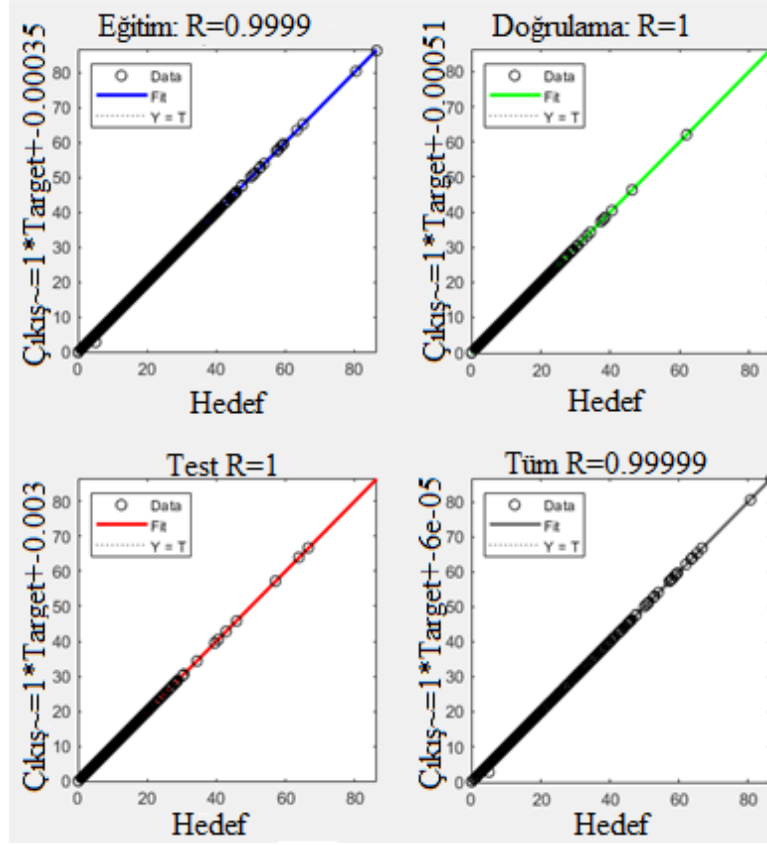
Şekil 9. Akdeniz bölgesinde bulunan noktalar.

Elde edilen sıcaklık, hız ve basınç verileri ile ekserji hesaplaması yapılmıştır. Sonraki aşamada çok katmalı geri beslemeli bir yapay sinir ağı modeli oluşturulmuştur. Oluşturulan modelin yapısı Şekil 10'de gösterilmektedir. Bu modelde ekserji hesaplamasında kullanılan sıcaklık, basınç ve hızdan oluşan üç adet veri, giriş olarak kullanılmıştır. Bu nedenle veri sütunlarının her biri, giriş katmanındaki bir nörona doğrudan aktarılmaktadır.



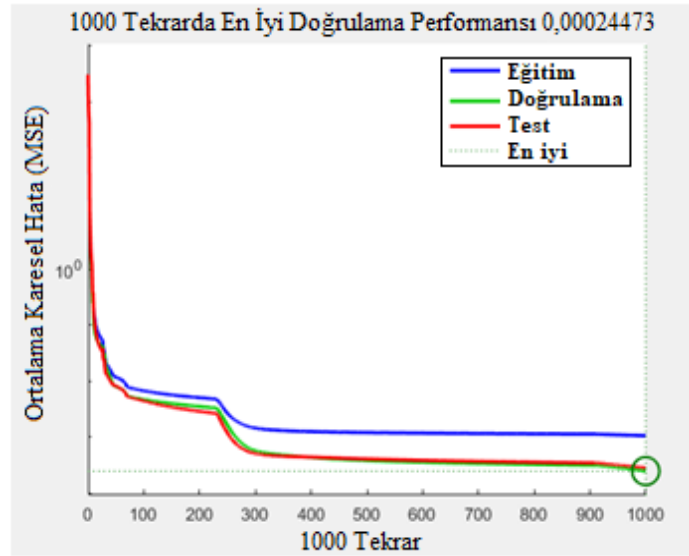
Şekil 10. Hazırlanan YSA yapısı.

Tasarlanan modelde giriş katmanından sonra iki adet ara katman bulunmaktadır. İlk ara katmanda 4 nöron, ikinci ara katmanda ise 2 nöron bulunmaktadır. İlk ara katman ve ikinci ara katmanda tanjant hiperbolik aktivasyon fonksiyonu kullanılmıştır. Sistemin çıkışında ise sadece ekserji değeri olacağı için tek bir çıkış bulunmaktadır. Eldeki verilerin %80 eğitim, %10'u test ve %10'u da doğrulama verisi olarak kullanılmıştır. Bu veriler kullanılarak sistem test edildiğinde Şekil 11'de gösterilen regresyon sonuçları elde edilmiştir. Şekil 11 incelendiğinde bütün noktaların regresyon doğrusunun üzerine yerleştiği görülmektedir.



Şekil 11. Regresyon analiz sonuçları.

Sistemin başarısını ölçmek için ortalama karesel hata formülü kullanılmış olup sistemin genel hata oranı Şekil 12’de gösterilmektedir. Buradan da anlaşılacağı üzere Ekserji hesaplamasının sonucunda elde edilen değerler ile kullanılan modelinin üretmiş olduğu değerler kıyaslandığında, aradaki hatanın 0,00024’e kadar düştüğü görülmektedir. Bu durumda kullanılan modelinin çok yüksek oranda başarı elde ettiğini ispatlamaktadır.



Şekil 12. Hata değeri grafiği.

Çalışma farklı aktivasyon fonksiyonları ve farklı ara katman yapıları ile test edildiğinde bu değerden biraz daha yüksek hata oranı elde edilmiştir.

5. TARTIŞMA VE SONUÇ

Bir rüzgâr enerji santrallerinin kurulacağı bölgede daha önce bir santral kurulmadıysa ve özellikle ilk kez o bölgede kurulacaksa, o bölge için enerji ve ekserji analizi yapmak çok önemlidir. Bu nedenle ilk olarak santral kurulacak yerin, enerji ve ekserji açısından verimli olup olmadığını tespit etmek için uzun zaman harcanan, alan ölçümleri yapılmaktadır. Sonrasında da bu ölçüm verilerine dayanan birçok hesaplama yapılmaktadır. Bu hesaplamalar içerisinde bazı varsayımlarda da bulunmak gerekebilmektedir. Yapılan hesaplama sonucuna göre de olumlu ya da olumsuz karar verilmektedir.

Yukarıda da anlatıldığı gibi karar verme sürecince birçok ara işlem ve hesaplamanın yapılması zorunludur. Bu işlemlerde oldukça zaman alan ve çok bilinmeyenli denklemlerden oluşan karmaşık bir işlemdir. Bu işlemler içerisinde de yine bazı varsayımlarda bulunmak gerekmektedir. Fakat özellikle yatırımcılar ve karar alıcılar için, zamanı optimum şekilde kullanarak hızlı ve doğru karar verebilmek son derece önemlidir. Bu nedenle yukarıda anlatılan işlem kalabalığından ve birçok ölçüm verisi için zaman harcamaktansa, daha az veri ile yüksek doğrulukta bilgi sahibi olmak karar alıcılar için çok daha önemli olabilmektedir.

Bu sebeple gerçekleştirilen çalışmada sadece sıcaklık, hız ve basınç verileri kullanarak geri beslemeli bir yapay sinir ağı modeli geliştirilmiştir. Geliştirilen modelin eğitilmesinde 1981 ile 2018 yılları arasında, Akdeniz Bölgesinde bulunan 21 noktadan alınan veriler kullanılmıştır. Geliştirilen YSA modelinin sonuçları ile klasik ekserji analizinden elde edilen sonuçlar kıyaslanmış olup, %99,9'un üzerinde başarı oranı ile ekserji değerleri tahmin edilmiştir.

Böylece Akdeniz Bölgesindeki koordinat noktaları verilen yerler için saniyeler içerisinde yüksek başarı oranı ile doğru sonuçlar üretilebilmektedir. Çalışmanın sonucunda Akdeniz Bölgesi için yatırımcıların ve karar alıcıların ilk etapta ihtiyaç duydukları ekserji sonuçlarına çok az veri ile ulaşabilmeleri mümkün hale getirilmiştir. Bundan sonraki çalışmada, uygulamada kullanılan güç eğrisinin katsayılarının YSA ile de hesaplanması hedeflenmektedir. Bunun dışında bir diğer hedefte çalışmanın tüm Türkiye uygulanmasıdır.

KAYNAKLAR

- [1] Karık, F., Sözen, A., İskender, Ü., (2015). Türkiye’de Rüzgar Enerjisinde Mevcut Durum. Gazi Mühendislik Bilimleri Dergisi (GMBD), 1, 2, 219–233. <https://dergipark.org.tr/tr/pub/gmbd/issue/29232/312919>
- [2] Kavcıoğlu, Ş., (2019). Yenilenebilir Enerji ve Türkiye, Finansal Araştırmalar ve Çalışmalar Dergisi, 11, 21, 209–227. <https://doi.org/10.14784/marufacd.623399>
- [3] Rüzgâr ve güneş Türkiye ’ de enerji dönüşümünü nasıl hızlandırabilir: Küresel örnekler., (2018). https://www.shura.org.tr/wp-content/uploads/2019/01/SHURA_Rüzgar-ve-Güneş-Türkiyede-Enerji-Dönüşümünü-Nasıl-Hızlandırabilir-Küresel-Örnekler.pdf.
- [4] IEA., (2019). Renewables 2019 – Analysis. <https://www.iea.org/reports/renewables-2019>
- [5] Dündar, C., (1997). Bandırma Bodrum Bozcaada ve Çeşme Bölgeleri Rüzgar Enerjisi Potansiyellerinin Belirlenmesi, Yüksek Lisans Tezi, Hacettepe Üniversitesi, İstanbul.
- [6] Mengi, D. F., (2013). Rüzgar Enerjisi Potansiyelinin Enerji ve Ekserji Haritasının İncelenmesi, Yüksek Lisans Tezi, Süleyman Demirel Üniversitesi Fen Bilimleri Enstitüsü, Isparta.
- [7] Lawan, S. M., Abidin, W. A. W. Z., Masri, T., (2019). Implementation of a topographic artificial neural network wind speed prediction model for assessing onshore wind power potential in Sibü, Sarawak, Egyptian Journal of Remote Sensing and Space Science. <https://doi.org/10.1016/j.ejrs.2019.08.003>
- [8] Toklu M., (2002). Rüzgar Enerjisi ve Elazığ Şartlarında Bir Rüzgar Santrali Tasarımı. Yüksek Lisans Tezi, Fırat Üniversitesi, Fen Bilimleri Enst., Elektrik Eğitimi ABD., Elazığ..
- [9] Koroneos, C., Spachos, T., Moussiopoulos, N., (2003). Exergy analysis of renewable energy sources, Renewable Energy. [https://doi.org/10.1016/S0960-1481\(01\)00125-2](https://doi.org/10.1016/S0960-1481(01)00125-2)

- [10] Hepbasli, A., Ozgener, O., (2004). A review on the development of wind energy in Turkey, *Renewable and Sustainable Energy Reviews*, 8, 257–76. <https://doi.org/10.1016/j.rser.2003.10.006>
- [11] Şahin, A. D., Dincer, I., Rosen, M. A., (2006). New Spatio-Temporal Wind Exergy Maps, *Journal of Energy Resources Technology*, 128, 3, 194–202. <https://doi.org/10.1115/1.2213271>
- [12] Hepbasli, A., (2008). A key review on exergetic analysis and assessment of renewable energy resources for a sustainable future, *Renewable and Sustainable Energy Reviews*, 12, 593–661. <https://doi.org/10.1016/j.rser.2006.10.001>
- [13] Xydis, G., Koroneos, C., Loizidou, M., (2009). Exergy analysis in a wind speed prognostic model as a wind farm sitting selection tool: A case study in Southern Greece. *Applied Energy*, 86, 2411–2420. <https://doi.org/10.1016/j.apenergy.2009.03.017>
- [14] Başkut.Ö., (2010). Rüzgar Güç Tesislerinin Ekserji Analizi, Yüksek Lisans Tezi, Ege Üniversitesi, İzmir.
- [15] Saravanan, A. J., Karthikeyan, C. P., Samuel, A. A., (2011). Exergy Analysis of Single Array Wind Farm Using Wake Effects, *Engineering*, 03,09, 949–958. <https://doi.org/10.4236/eng.2011.391177>
- [16] Ehyaei, M. A., Ahmadi, A., Rosen, M. A., (2019). Energy, exergy, economic and advanced and extended exergy analyses of a wind turbine, *Energy Conversion and Management*, 183,183, 369381. <https://doi.org/10.1016/j.enconman.2019.01.008>
- [17] Ekonomou, L., Lazarou, S., Chatzarakis, G. E., Vita, V., (2012). Estimation of wind turbines optimal number and produced power in a wind farm using an artificial neural network model, *Simulation Modelling Practice and Theory*, 21, 21–25. <https://doi.org/10.1016/j.simpat.2011.09.009>
- [18] Ata, R., (2008). Otonom bir Rüzgar Türbininin Farklı Yüksekliklerdeki Enerji Eldesinin YSA ile Analizi, *Gazi Üniversitesi Mühendislik Mimarlık Fakültesi Dergisi*, 23, 3, 523–529. <https://dergipark.org.tr/pub/gazimmfd/issue/6677/88513>
- [19] Lee, D., Baldick, R., (2014). Short-Term Wind Power Ensemble Prediction Based on Gaussian Processes and Neural Networks, *IEEE Transactions On Smart Grid*, 5,1, 501–510. <https://doi.org/10.1109/TSG.2013.2280649>
- [20] Mortazavi, S. M., Soltani, M. R., Motieyan, H., (2015). A Pareto optimal multi-objective optimization for a horizontal axis wind turbine blade airfoil sections utilizing exergy analysis and neural networks, *Journal of Wind Engineering and Industrial Aerodynamics*, 136, 62–72. <https://doi.org/10.1016/j.jweia.2014.10.009>
- [21] Lydia, M., Suresh Kumar, S., Immanuel Selvakumar, A., Edwin Prem Kumar, G., (2015). Wind resource estimation using wind speed and power curve models, *Renewable Energy*, 83, 425–434. <https://doi.org/10.1016/j.renene.2015.04.045>
- [22] Pelletier, F., Masson, C., Tahan, A., (2016). Wind turbine power curve modelling using artificial neural network, *Renewable Energy*, 89, 207–214. <https://doi.org/10.1016/j.renene.2015.11.065>
- [23] Manobel, B., Sehnke, F., Lazzús, J. A., Salfate, I., Felder, M., Montecinos, S., (2018). Wind turbine power curve modeling based on Gaussian Processes and Artificial Neural Networks, *Renewable Energy*, 125, 1025–1020. <https://doi.org/10.1016/j.renene.2018.02.081>
- [24] Altınoy, M., Bal, G., (2019). Uzun Dönem Rüzgar Hızı Tahmininde Yapay Sinir Ağlarının Kullanımı ve Performans İncelemesi, *Mesleki Bilimler Dergisi (MBD)*, 8, 1, 21–28. <https://dergipark.org.tr/en/pub/mbd/issue/45578/539436>
- [25] Zafirakis, D., Tzanes, G., Kaldellis, J. K., (2019). Forecasting of Wind Power Generation with the Use of Artificial Neural Networks and Support Vector Regression Models, *Energy Procedia*, 159, 509–514. <https://doi.org/10.1016/j.egypro.2018.12.007>
- [26] Nielson, J., Bhaganagar, K., Meka, R., Alaeddini, A., (2020). Using atmospheric inputs for Artificial Neural Networks to improve wind turbine power prediction. *Energy*, 190. <https://doi.org/10.1016/j.energy.2019.11627>
- [27] Çengel, A. Y., Michael, A. B., (2008). *Termodinamik Mühendislik Yaklaşımıyla*, (A. Pınarbaşı (Ed.); 5th ed.). İzmirGüven Kitabevi.
- [28] Yüksel, Y. E., Öztürk, M., (2016). Eysel Uygulamalar için Birleşik Rüzgar-Güneş-Hidrojen Sisteminin Termodinamik Analizi., *El-Cezeri Fen ve Mühendislik Dergisi*, 3, 3, 401–416. <https://doi.org/10.31202/ecjse.258567>
- [29] Uğuz, S., (2005). Rüzgar Enerjisi ile Elektrik Üretimi, Yüksek Lisans Tezi, Gazi Üniversitesi, Ankara.
- [30] Kökey, I., (2013). Rüzgar Enerjisi Potansiyelinin Belirlenmesi ve Rüzgar Enerji Satrallerinin Performans Değerlendirmesinde Ekserji Analizinin Önemi, <https://www.researchgate.net/publication/324680303%0ARÜZGAR>
- [31] Dincer, I., Rosen, M. A., (2007). *Exergy: energy, environment and sustainable development* (1st ed.), Elsevier Science, UK.
- [32] Koçer, A. A., (2013). Elektrik Üretimi İçin Güneş Havuzu Destekli Çoklu Üretim Sisteminin Termodinamik Analizi, Yüksek Lisans Tezi, Süleyman Demirel Üniversitesi, Isparta.
- [33] Nasa. “Türkiye'nin Akdeniz Bölgesi için meteorolojik veriler”, [25.10.2019]. Available: <https://power.larc.nasa.gov/data-access-viewer/>.



- [34] Bař, N., (2006). Yapay sinir ađları yaklaşımı ve bir uygulama, Yayınlanmış Yüksek Lisans Tezi, Fen Bilimleri Enstitüsü, Mimar Sinan Üniversitesi, İstanbul.
- [35] Elmas, Ç., (2003) Yapay sinir ađları, Seçkin Yayıncılık, Ankara.
- [36] Haton, J.P., ve Haton, M.C., (1991). Yapay zekâ. (Çev. A. Ekmekçi ve A. Türker). İletişim Yayınları, İstanbul.
- [37] Pirim, A., (2006). Yapay zeka. Journal of Yaşar University, 1, 1, 81-93. Retrieved from <https://dergipark.org.tr/tr/pub/jyasar/issue/19113/202842>.
- [38] Metlek, S., ve Yılmaz, T., (2019). Analysis of Perceived Service Quality and Customer Satisfaction in the Aviation Sector with Artificial Neural Networks, 2. Uluslararası Teknoloji ve Bilim Konferansı (Techno-Science),853-864, Burdur, Türkiye.



International Journal of Engineering and Innovative Research

<http://dergipark.gov.tr/ijeir>

ANALYSIS OF A SIMULATED FLAT PLATE SOLAR COLLECTOR SYSTEM USING SOLIDWORKS FLOW SIMULATOR INTERFACE

Eghosa Omo-Oghogho^{1*} , Ejuvwedia Godwin Sadjere¹ 

¹ Department of Mechanical Engineering, University of Benin, P.M.B 1154, Ugbowo, Nigeria.

*Corresponding Author: eghosa.omo-oghogho@uniben.edu

(Received: 26.04.2020; Revised: 01.06.2020; Accepted: 15.06.2020)

ABSTRACT: One of the promising source of renewable energy is solar energy. Water heating by solar energy for domestic use is one of the most successful and feasible applications of solar energy. Other areas of application of solar energy include solar drying, electricity generation using photovoltaic cells, solar cooling and refrigeration, solar still (or solar distillation) and solar cooking. In this study flat plate solar collector was simulated, a temperature of $58^{\circ}C$ and an efficiency of 51% was achieved respectively. Solar radiation being abundantly present in Nigeria is one area of focus among the renewable energy resources and this can be harnessed for heating water for both domestic and industrial purposes.

Keywords: Simulation, Solid works, Solar Collector, Flow Simulator, Ambient Condition.

1. INTRODUCTION

Solar flat plate collector is a type of solar thermal systems, it provides environmental friendly heat for industrial water heating, commercial building, space heating, hospital water, household water and the heating of swimming pools. Such systems collect the suns energy to heat a fluid. The heated water is then stored in a tank similar to a convectional gas or electric water tank and some systems use an electric pump to circulate the fluid through the collectors [1].

The analysis of thermal collectors is able to be done experimentally and by simulating the heat transfer phenomena within the system. Sopian et al. [2] conducted an experimental study on the thermal performance of a solar flat plate collector having a wooden case, no glass cover (unglazed) and a solar water heater integrated with a storage system.

Several studies which compare experimentally results with Computational Fluid Dynamics (CFDs) results are shown by [3, 4].

Farahat et al [5] and Chamoli [6] used MATLAB to optimize a flat plate collector considering its exergy analysis in order to improve the efficiency of the collectors by decreasing the losses. Garg and Rani [7] calculated the overall heat loss coefficient and the collector efficiency under different conditions such as the absence of cover, with single and double glazing under different ambient conditions, tilt angles, wind speeds, emissivity of both glass cover and absorber plate.

Pillai and Agarwal [8] discussed the influence of various parameters on the efficiency of solar collectors and concluded that at low solar insolation in the range of $200-600 \text{ W/m}^2$ with double glazed collectors are superior to single glazed collectors. Anderson et al [9] examined the performance by changing the colors of solar collector. Based on the transmittance-absorptance

result of various colored collectors the hypothetical performances of these collectors were calculated using the Hottel-Whillier-Bliss 1-D steady-state model given by Duffie and Beckmann [10].

This research helps to analyze and simulate the flat plate solar collector, in this study the computational tool is SolidWorks which gives many design opportunities. The design of the collector and the thermal simulation were made in the same environment by adding flow simulation tab.

2. MATERIALS AND METHOD

This simulation was done using Solidworks as a simulation tool. The initial conditions, boundary conditions and the control condition are shown in Tables 1, 2, 3, 4, 5, 6, 7, 8, 9, 10, 11, 12 and were selected based on the thermodynamic analysis done.

Flow Simulator software was the subprogram attached to Solidworks for the simulation of the flat plate solar collector. The initial/ambient conditions were selected based on the design consideration and parameters gotten from the thermodynamic analysis of the collector system.

Table 2, 3 and 4 are the ambient condition selected on the Flow Simulator bearing in mind the design and thermodynamic parameters gotten. Table 5, 6, 7, 8, 9, 10 are the control platforms on the Flow Simulator after the ambient conditions have been meet.

Table 1. Initial conditions selected for the ambient state.
Ambient conditions generated from Solidworks

Thermodynamic parameters	Static Pressure: 101325.00 Pa Temperature: 299.1 K
Velocity parameters	Velocity vector Velocity in X direction: 0.500 m/s Velocity in Y direction: 0.020 m/s Velocity in Z direction: 0.020 m/s
Solid parameters	Default material: Copper Initial solid temperature: 303.00 K Radiation Transparency: Opaque
Turbulence parameters	Turbulence intensity and length Intensity: 2.00 % Length: 0.007 m

Table 2 Initial conditions selected for inlet mass flow rate.
Inlet Mass Flow 1

Type	Inlet Mass Flow
Faces	Face<2> at Plate and tubes-1
Coordinate system	Face Coordinate System
Reference axis	X
Flow parameters	Flow vectors direction: Normal to face Mass flow rate: 0.014 kg/s Fully developed flow: No Inlet profile: 0
Thermodynamic parameters	Temperature: 299.1K
Turbulence parameters	Turbulence intensity and length Intensity: 2.00 % Length: 0.007 m
Boundary layer parameters	Boundary layer type: Turbulent

Table 3. Initial conditions selected for static pressure conditions.
Static Pressure 1

Type	Static Pressure
Faces	Face<6> at Plate and tubes-1
Coordinate system	Face Coordinate System
Reference axis	X
Thermodynamic parameters	Static pressure: 101325.00 Pa Temperature: 299.1 K
Turbulence parameters	Turbulence intensity and length Intensity: 2.00 % Length: 0.007 m
Boundary layer parameters	Boundary layer type: Turbulent

Table 4. Control conditions for temperature (1).
GG Av Temperature (Fluid) 1

Type	Global Goal
Goal type	Temperature (Fluid)
Calculate	Average value
Coordinate system	Global coordinate system
Use in convergence	On

Table 5. Control conditions for temperature (2).
GG Av Temperature (Fluid) 2

Type	Global Goal
Goal type	Temperature (Fluid)
Calculate	Average value
Coordinate system	Global coordinate system
Use in convergence	On

Table 6. Control conditions for temperature (3).
GG Av Temperature (Fluid) 3

Type	Global Goal
Goal type	Temperature (Fluid)
Calculate	Average value
Coordinate system	Global coordinate system
Use in convergence	On

Table 7. Control conditions for mass flow rate.
GG Mass Flow Rate 1

Type	Global Goal
Goal type	Mass Flow Rate
Coordinate system	Global coordinate system
Use in convergence	On

Table 8. Control conditions for net radiant flux (solar).
GG Av Net Radiant Flux (solar) 1

Type	Global Goal
Goal type	Net Radiant Flux (solar)
Calculate	Average value
Coordinate system	Global coordinate system
Use in convergence	On

Table 9. Control conditions for the temperature (solid).
GG Av Temperature (Solid) 1

Type	Global Goal
Goal type	Temperature (Solid)
Calculate	Average value
Coordinate system	Global coordinate system
Use in convergence	On

Table 9 presents the selected flat plate solar collector size on the design interface on Solidworks using the Flow Simulator program.

Table 10. Size of computational domain.

X min	-0.483 m
X max	1.265 m
Y min	-0.275 m
Y max	1.082 m
Z min	-1.282 m
Z max	0.398 m

The basic mesh dimensions applicable to the X, Y and Z coordinates of the flat plate solar collector was presented in Table 10. This was necessary in the simulation of the collector system, coarse mesh with large elements require less computation time which may result to inaccurate results. Mesh convergence obtained on X, Y and Z coordinates were 17, 12 and 17. The process was followed by mesh refinement which resolved the model with finer mesh sizes for accurate results.

Table 11. Basic Mesh Dimensions.

Number of cells in X	17
Number of cells in Y	12
Number of cells in Z	17

The mesh properties employed in modelling of the flat plate solar collector are presented in Table 11. This shows the values of the total cell count, fluid cells, solids cells, etc as shown in Table 12. This mesh analysis was gotten after using the mesh dimensions and the sizes of the computational domain.

Table 12. Analysis of Mesh.

Total cell count	79740
Fluid cells	20139
Solid cells	13480
Partial cells	46121
Trimmed cells	0
Heat transfer analysis	Heat conduction in solids
Flow type	Laminar and turbulent
Time- dependent analysis	Off
Gravity	On
Radiation	On
Humidity	50.0%
Default Wall Roughness	1.0 micrometer

3. RESULTS AND DISCUSSION

The collector system where simulated using Flow Simulator on Solidworks interface, the input parameters were estimated from system design and thermodynamic analysis and some of the input parameters are designed conditions set by the Flow Simulator considering ambient and boundary conditions.

Table 13. Input/output parameters.

Name	Input	Output
Pressure [Pa]	101291.63	107615.07
Temperature [K]	299.08	331
Density (Fluid) [kg/m ³]	1.15	995.74
Velocity [m/s]	0	6.790
Velocity (X) [m/s]	-4.487	5.470
Velocity (Y) [m/s]	-5.760	2.214
Velocity (Z) [m/s]	-4.716	3.292
Mass Fraction of Steam []	0	0.0041
Mass Fraction of Air []	0	0.9959
Mass Fraction of Water []	0	1.0000
Volume Fraction of Water []	0	1.0000
Temperature (Fluid) [K]	299.08	315.56
Temperature (Solid) [K]	299.13	327.88
Mass Fraction of Condensate []	0	0
Mass Fraction of Vapour []	0	0
Volume Fraction of Vapour []	0	0
Density (Solid) [kg/m ³]	2600.00	8960.00
Mach Number []	0	0.02
Vorticity [1/s]	0.031	1037.197
Shear Stress [Pa]	0	1.80
Relative Pressure [Pa]	-33.37	6290.07
Prandtl Number []	0.6956699	5.8635293
Efficiency [%]	0	0.51
Relative Humidity [%]	0	20.02
Heat Transfer Coefficient [W/m ² /K]	0.001	6620.796
Surface Heat Flux [W/m ²]	-520.709	18453.624
Heat Flux [W/m ²]	0.032	1450886.891
Overheat above Melting Temperature [K]	-1053.927	-765.702

Table 13 shows the input parameters and the output parameters used during the simulation of the flat plate solar collector on the Solidworks interface. The output parameters are then compared with results gotten from the collector thermodynamic analysis results, which is then validated using the developed model with the experimental results.

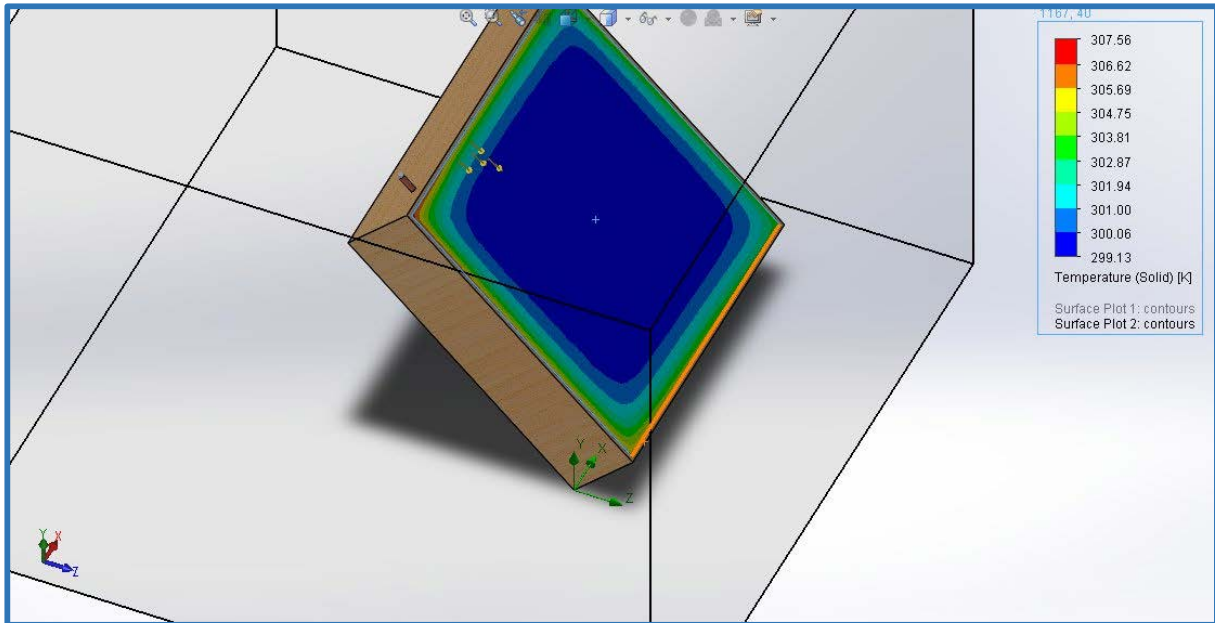


Figure 1. Glass Temperature after Simulation.

Figure 1 indicates that the glass did not lose much heat to the atmosphere, it acts as a thermal cover to protect the flat plate solar collector against heat loss. The blue colour around the mid area indicates that there was no heat loss around that region, as it moves towards the edge of the collector it shows a mixture of colour showing little heat loss at the edge.

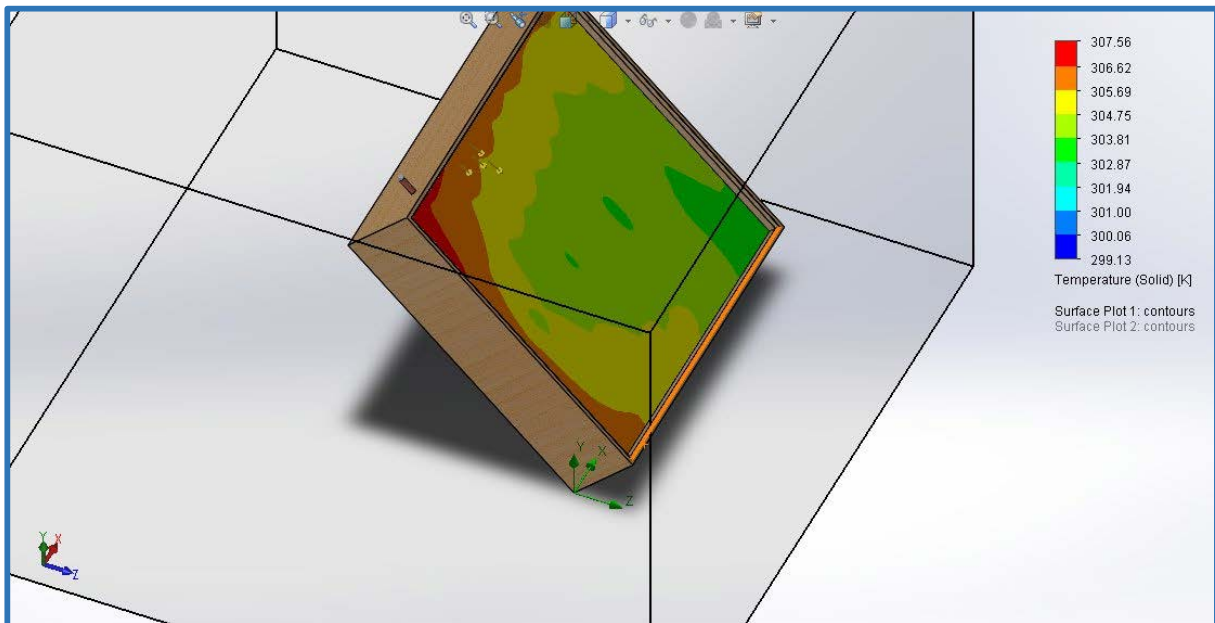


Figure 2. Plate Temperature after Simulation.

Figure 2 indicates that the plate temperature after simulation shows a mixture of colours and also show red which is the colour code form the maximum temperature achieved at the inlet temperature of $299.13^{\circ}C$, it acts as a thermal cover to protect the flat plate solar collector against heat loss. This means the absorber plate efficiently passed the heat to the heat pipe.

Table 14. Temperatures gotten from simulation without preheat.

Day	Inlet temp (K)	10am Outlet Temp (K)	11am Outlet Temp (k)	12:00NOON outlet temp (K)	1:00PM outlet temp (K)	2:00PM outlet temp (K)	3:00PM outlet temp (K)
17th Jan	295	305	313	321	324	326	328
16th Feb	295	303	310	318	320	322	325
16th Mar	295	303	310	316	319	322	324
15th Apr	295	300	304	310	305	304	304
15th May	295	300	303	302	305	302	302
11th Jun	295	297	302	299	297	300	299
17th Jul	295	297	301	300	299	297	301
16th Aug	295	299	302	306	308	310	310
15th Sep	295	302	302	305	310	312	315
15th Oct	295	304	308	318	320	322	322
14th Nov	295	304	310	318	318	324	326
10th Dec	295	305	310	319	322	325	330

Table 14 shows the temperature that was gotten from the simulation, the inlet water was allowed to flow into the system from 10am to 3pm. At an interval of one hour, it was also observed that the temperature was highest for January, December and lowest for June, July respectively.

Table 15. Temperatures gotten from simulation with preheat.

Day	Inlet temp (K)	12:00NOON outlet temp (K)	1:00PM outlet temp (K)	2:00PM outlet temp (K)	3:00PM outlet temp (K)
17th Jan	295	343	343	344	348
16th Feb	295	338	338	339	341
16th Mar	295	333	332	333	333
15th Apr	295	327	325	326	323
15th May	295	322	322	320	318
11th Jun	295	320	319	317	314
17th Jul	295	321	320	319	316
16th Aug	295	325	324	324	322
15th Sep	295	330	330	330	330
15th Oct	295	336	336	337	338
14th Nov	295	341	342	343	346
10th Dec	295	344	344	346	350

Table 15 shows the temperature that was gotten after preheating the flat plate solar collector from 9am to 12noon. It shows an increase in temperature when compared to the temperatures gotten without preheating.

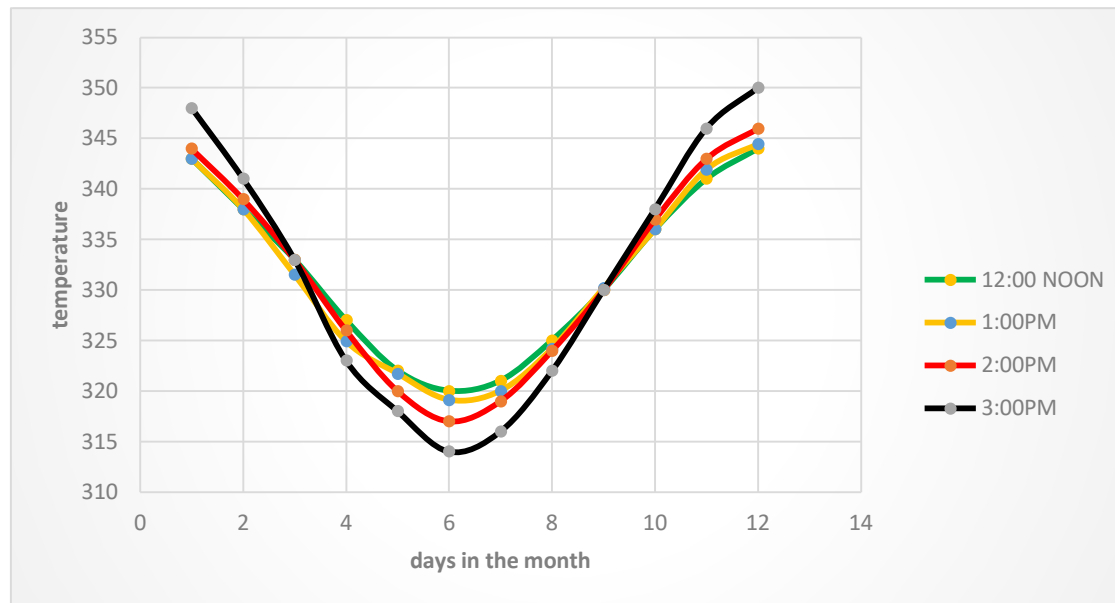


Figure 3. A graph of temperature against days in the month.

The graph shown in figure 3 indicates that the outlet temperatures increases in the beginning of the year with the first few months (dry season) and it goes down towards the middle of the year (raining season) and rises again towards the last few months of the year (dry season).

4. CONCLUSION

The flat plate solar collector was simulated using SolidWorks, an output temperature of 58°C and an efficiency of 51% was achieved respectively. The obtained temperature can be used for domestic and some industrial applications. The analysis was done for both preheat and without preheat, preheat occurs when the flat plate collector system is place outside under open sky for direct contact with the sun for some hours before passing water through the system. The condition for without preheat involves passing water from the supply tank into the collector without allowing the flat plate solar collected to be heated before opening the water supply tank.

REFERENCES

- [1] Dimitrios P. (2001): Solar water heating systems study reliability, quantitative survey and life cost method, MSC. Thesis, Department of Mechanical Engineering, University of Strathelyde in Glasgow.
- [2] Sopian, K., Syahri, M., Abdullah, S., Othman, M.Y. and B. Yatim, B (2004)" Performance of a non-metallic unglazed solar water heater with integrated storage system", Renewable Energy, volume 29: pp 1421–1430.
- [3] Selmi, M., Al-Khawaja, M.J., and Marafia, A. (2008) "Validation of CFD simulation for flat plate solar energy collector" Renewable Energy, volume 33: pp 383-387.
- [4] Vettrivel, H and Mathiaragan, P (2013) Experimental Study on a Flat Plate Solar Collector, International Journal of Mechanical Engineering and Research, volume 3(6): pp 641-646.
- [5] Farahat, S., Sarhaddi, F. and Ajam H., (2009) "Exergetic optimization of flat plate solar collectors", Renewable Energy, volume 34, pp1169–1174.
- [6] Chamoli, S., (2013) Exergy analysis of a flat plate solar collector, Journal energy South. Afr., vol.24 no.3 Cape Town.
- [7] Garg, H.P. and Rani, U. (2016) Loss Coefficients from Solar Flat-Plate applied Energy, volume 7, pp 109 - 117.
- [8] Agarwal, V.K. and Larson D.C. (200) Calculation of top heat loss coefficient of a flat-plate solar collector. Solar Energy, volume 27, pp 69-71.
- [9] Anderson T., Duke M., and Carson J. (2010) The effect of color on the thermal performance of building integrated solar collectors, Solar Energy Materials and solar cells, volume 94, pp 350-354.
- [10] Duffie J. and Beckmann W. (2013) solar engineering of thermal processes, 3rd edition (Wiley Interscience, New York).



THREE-DIMENSIONAL MODAL ANALYSIS OF BEAMS WITH TRIANGULAR AND HEXAGONAL CROSS-SECTIONS USING DIFFERENT CERAMIC MATERIALS

Savas Evran^{1*} 

¹Canakkale Onsekiz Mart University, Faculty of Çanakkale Applied Sciences, Department of Energy Management, Çanakkale, Turkey.

*Corresponding Author: sevrans@comu.edu.tr

(Received: 23.05.2020; Revised: 05.06.2020; Accepted: 15.06.2020)

ABSTRACT: This study deals with the investigation of the effects of cross-sections and ceramic materials on the free vibration behavior of beams. Fundamental frequency analyses were performed using finite element software ANSYS based on Taguchi's L8 orthogonal array with two control factors. Ceramic material types were used as the first control factor consisting of four levels such as Zirconia (ZrO_2), Silicon nitride (Si_3N_4), Alumina (Al_2O_3), and Silicon carbide (SiC) while cross-sections of beams were considered as the second control factor including two levels such as triangle and hexagon. To optimize the ceramic materials and the cross-sections, analysis of signal-to-noise (S/N) ratio was used. Important control factors and their percent contributions on numerical fundamental free vibration response were performed using analysis of variance (ANOVA). According to ANOVA results, the percent contribution ratios of the control factors on fundamental frequency of the beams are found as 67.45 for ceramic material and 31.50 for the cross-section of beams.

Keywords: Modal analysis, Cross-section, Ceramic, Finite element approach.

1. INTRODUCTION

Beam structures with various cross-sections can be broadly utilized in different engineering applications, such as different types of bridges, columns, and frames, amongst many others. In general, beams have been made using metal and ceramic materials. The ceramic materials have superb characteristics for heat resistance whereas the metal materials have superb strength and toughness [1]. Especially, three-dimensional free vibration characteristic of beams has attracted several engineering designers and researchers because of their widespread applications. In literature, various studies including free vibration analyses can be seen. Balhaddad and Onipede [2] presented a study about modal analysis of pre-twisted beams using three-dimensional approach. Evran [3] presented the modal analysis of the functionally graded tapered beams which having three layers using finite element software ANSYS and Taguchi method. Giunta et al. [4] reported modal analysis of sandwich beams with three-dimensions. Fang et al. [5] presented modal analysis of rotating functionally graded beams under cantilever boundary conditions in three dimensions. Evran [6] investigated the free vibration characteristic of layered functionally graded beams in three dimensions using numerical and statistical methods. In modal analysis, ANSYS software was used for finite element approach. Evran and Yilmaz [7] evaluated the impacts of ceramic and metal materials on the modal analysis of layered beams using finite element and Taguchi methods. Alshorbagy et al. [8] presented a study including modal analysis of a beam designed from functionally graded materials using the finite element approach. Yilmaz and Evran [9] investigated the first mode frequency characteristic of beams made from functionally graded materials in axial direction using experimental and numerical

methods. As can be seen from above literature, there are many studies regarding free vibration. In this study, fundamental frequency analysis of the beams with triangular and hexagonal cross-sections were performed using different ceramic materials.

2. MATERIALS AND METHODS

In numerical analysis, beams with different cross sections were used, and each beam was made of different ceramic materials such as Zirconia (ZrO₂), Silicon nitride (Si₃N₄), Alumina (Al₂O₃), and Silicon carbide (SiC). Poisson's ratio for each material was taken to be constant and it was used as 0.3. Young module and density data for ceramic materials were given in Table 1.

Table 1. Ceramic Materials Properties [10].

Material Type	Properties	
	E (GPa)	ρ (kg/m ³)
Zirconia (ZrO ₂)	151.00	3000
Silicon nitride (Si ₃ N ₄)	322.27	2370
Alumina (Al ₂ O ₃)	380.00	3800
Silicon carbide (SiC)	427.00	3210

The statistical analysis was performed using Minitab software. Numerical frequency analyses for the first mode were conducted under L8 orthogonal array which has two control factors, based on Taguchi method. The first control factor includes four levels while the second control factor consists of two levels. The first control factor was accepted as ceramic materials while the second control factor was taken as cross-sections of the beams and they were determined as triangle and hexagonal. The control factors and their levels were listed in Table 2.

Table 2. Control factors and levels.

Control Factors	Symbol	Levels			
		Level 1	Level 2	Level 3	Level 4
Ceramic Material	A	ZrO ₂	Si ₃ N ₄	Al ₂ O ₃	SiC
Cross-Section of Beam	B	Triangle	Hexagon		

In order to find the optimum levels of ceramic materials and the cross-sections of the beams for the maximum free vibration behavior, “the larger is better” quality characteristic was used based on Taguchi method. This quality characteristic was identified in Equation 1 [11].

$$\left(\frac{S}{N}\right)_{HB} = -10 \cdot \log \left(n^{-1} \sum_{i=1}^n (y_i^2)^{-1} \right) \tag{1}$$

in here, n shows the number of numerical free vibration analysis in a trial and y_i symbolizes ith data evaluated, for this study.

3. FINITE ELEMENT SOLUTION

3-D finite element solutions for free vibration analysis of the beams with triangular and hexagonal cross-sections were performed using finite element software ANSYS. Numerical analyses were carried out as modal analysis for the first mode. In the analysis, 3-D model element type called as SOLID186 was used. The element type is 3-D 20-Node Structural Solid and it demonstrates quadratic displacement performance and is defined by twenty nodes which have three degrees of freedom every nodes: translations for the nodal x, y, and z directions [12].

UX, UY, and UZ were used as degrees of freedom. Therefore, $UX = UY = UZ$ was used as 0 for clamped boundary conditions. Length and diameter of cantilever beams were used as 100 in mm and 10 in mm. The cross-sections of beams were demonstrated in Figure 1.

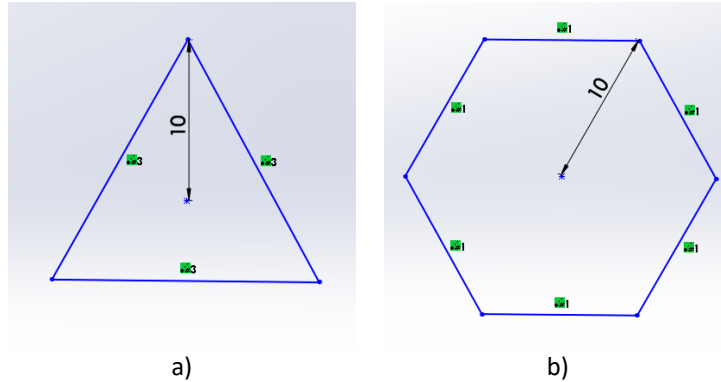


Figure 1. The cross-sections a) triangle and b) hexagon.

The beams were modelled under free and clamped boundary conditions. Sweep mesh type was employed for mesh operation. Cantilever beam and homogenous structural solid geometry for SOLID186 element were shown in Figure 2.

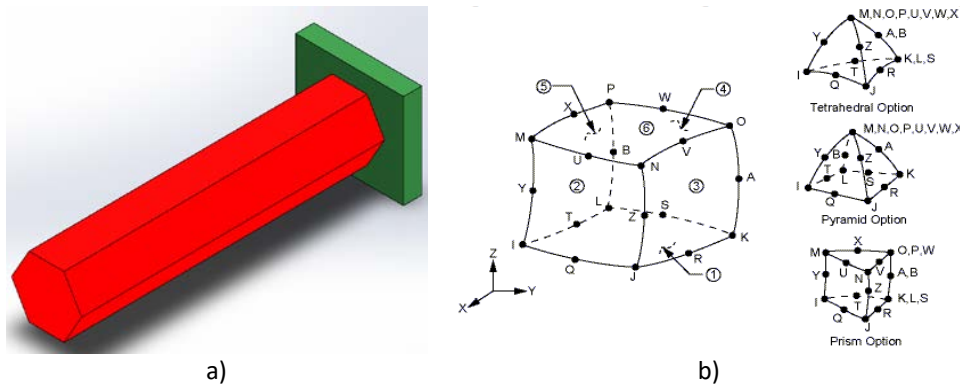


Figure 2. a) Cantilever beam and b) SOLID186 homogenous structural solid geometry [12].

4. RESULTS AND DISCUSSIONS

In order to optimize the levels of ceramic materials and the cross-sections of beams on free vibration, modal analyses were conducted using L8 orthogonal array based on Taguchi method. S/N ratio data were calculated for the finite element results using the statistical method. Results obtained for finite element and S/N ratio were tabulated in Table 3.

Table 3. Frequency and S/N ratio results for L8 orthogonal array.

Run	Designation	Control Factors		Results	
		Ceramic Type	Cross-Section	Frequency (Hz)	S/N ratio (dB)
1	A ₁ B ₁	ZrO ₂	Triangle	1395.30	62.8934
2	A ₁ B ₂	ZrO ₂	Hexagon	1793.21	65.0726
3	A ₂ B ₁	Si ₃ N ₄	Triangle	2293.38	67.2095
4	A ₂ B ₂	Si ₃ N ₄	Hexagon	2947.40	69.3888
5	A ₃ B ₁	Al ₂ O ₃	Triangle	1966.71	65.8748
6	A ₃ B ₂	Al ₂ O ₃	Hexagon	2527.57	68.0541
7	A ₄ B ₁	SiC	Triangle	2268.31	67.1140
8	A ₄ B ₂	SiC	Hexagon	2915.18	69.2933
Overall Mean (\bar{T}_{α})				2263.38	

Finite element approach was carried out for the fundamental frequency of each beam using ANSYS software. Results obtained for eight analyses were given in Figure 3 as visually.

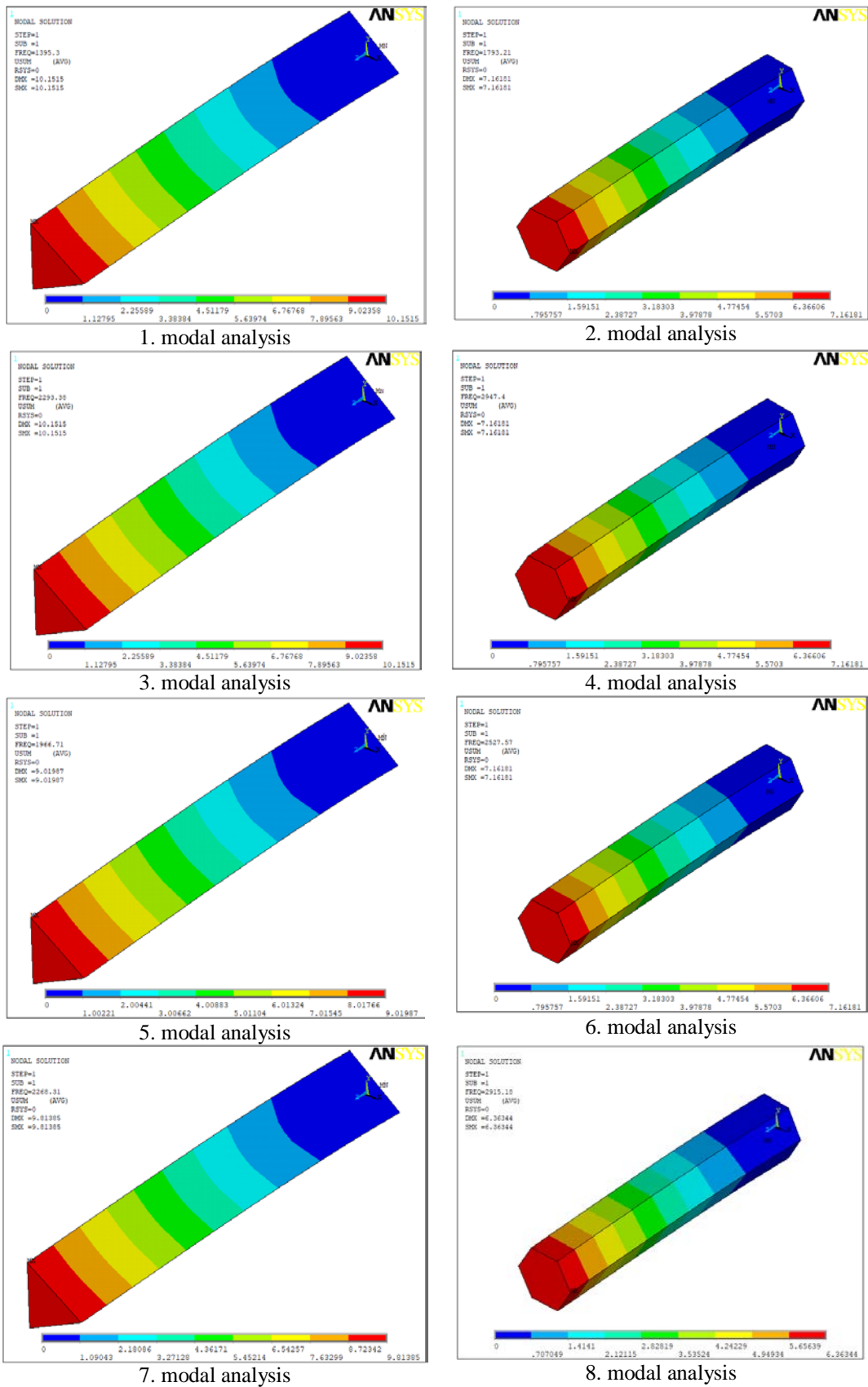


Figure 3. Fundamental frequency analysis for finite element approach.

4.1. Examination of Optimal Levels

In order to examine the optimal levels of control factors such as ceramic material types and cross-sections of the beams, average finite element data and their S/N ratio data for each level of all control factors based on numerical fundamental frequency and S/N ratio data were calculated using Minitab statistical software. Results found were presented in Table 4.

Table 4. Response table for S/N ratio and frequency.

Level	S/N ratio in dB		Mean in Hz	
	A	B	A	B
1	63.98	65.77	1594	1981
2	68.30	67.95	2620	2546
3	66.96		2247	
4	68.20		2592	
Delta	4.32	2.18	1026	565
Rank	1	2	1	2

As can be seen from Table 4, optimum levels of ceramic material types and cross-section of the beams are found as second levels. Therefore, the maximum numerical fundamental frequency result was obtained hexagonal beam made of Silicon nitride. In order to see the impacts of every levels of control factors on the numerical fundamental free vibration analysis, average S/N ratio data for each level of control factors were plotted and were presented in Figure 4.

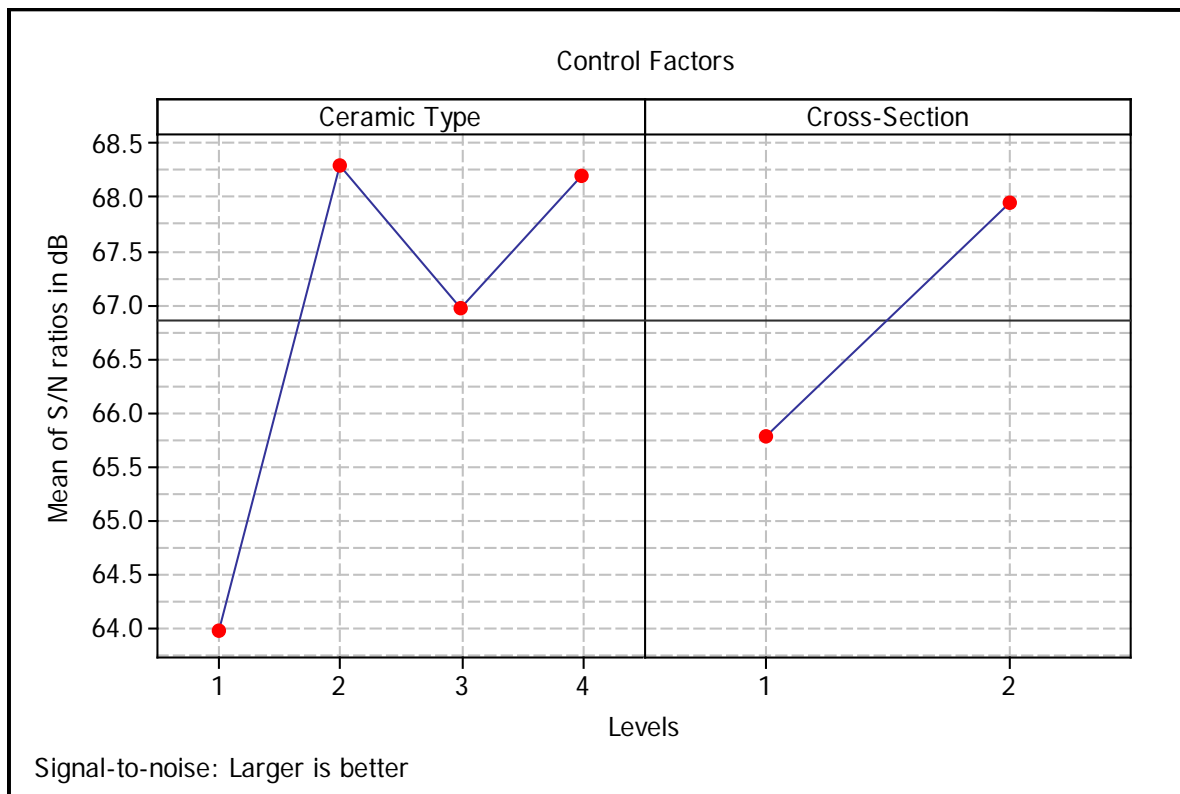


Figure 4. Impacts of ceramic materials and cross sections at different levels.

It can be seen from Figure 4 that free vibration of beams increases from the first level to the second level whereas decrease from the second level to third level. However, free vibration of beams increases from the third level to the fourth level. For the cross-sections of beams, free vibration increases from level 1 to level 2.

4.2. Analysis of Variance

Analysis of variance (ANOVA) was employed to see impact ratios of control factors on fundamental frequency results and to obtain significant control factors at 95 % confidence level using Minitab statistical software. Result solved for R-Sq = 98.95% and R-Sq (adj) = 97.55% were illustrated in Table 5.

Table 5. ANOVA for fundamental free vibration.

Source	DF	Seq SS	Adj MS	F	P	% Effect
A	3	1366543	455514	64.210	0.003	67.45
B	1	638258	638258	89.970	0.002	31.50
Error	3	21282	7094			1.05
Total	7	2026083				

Table 5 indicates that the control factors have powerful impacts on free vibration of the beams owing to $P < 0.05$ data. Also, the percent contribution ratios of control factors on fundamental frequency of the beams are found as 67.45 for ceramic material and 31.50 for the cross-section of beams.

4.3. Estimation of Optimum Fundamental Frequency

Prediction of optimal fundamental frequency was carried out using the significant control factors including the optimal levels for the maximum response. According to analyses of signal-to-noise and variance, the optimal result for the free vibration characteristic at the maximum level was found using control factors called A and B at the second levels. The predicted mean of free vibration characteristic for the first mode can be computed using Equation 2 [11].

$$\mu_\alpha = \bar{A}_2 + \bar{B}_2 - \bar{T}_\alpha \tag{2}$$

For Equation 2, \bar{A}_2 and \bar{B}_2 were calculated to be 2620 Hz and 2546 Hz, respectively following analysis of signal-to-noise. These data for means were presented in Table 4. Also, \bar{T}_α is the overall mean for Taguchi L8 orthogonal array with two control factors and this data was given as 2263.38 Hz in Table 3. Substituting numerical data of different terms in Equation 2, μ_α is computed to be 2902.62 Hz. Confirmation analysis and the population at the 95 % confidence intervals were computed following Equation 3 and Equation 4 [11], respectively.

$$CI_{CA} = \left(F_{\alpha;1;n_2} V_{error} \left[\frac{1}{n_{eff}} + \frac{1}{R} \right] \right)^{0.5} \tag{3}$$

$$CI_{POP} = \left(\frac{F_{\alpha;1;n_2} V_{error}}{n_{eff}} \right)^{0.5} \tag{4}$$

$$n_{eff} = \frac{N}{(1 + T_{DOF})} \tag{5}$$

where, $\alpha = 0.05$ describes the risk and $n_2 = 3$ points to the error value for degree of freedom in ANOVA in Table 5. $F_{0.05;1;3}$ is taken to be 10.13 [11] and this data was given in F ratio table associated with 95 % confidence interval. $V_{error} = 7094$ implies the error value for variance according to ANOVA data. R was utilized the sample size of confirmation numerical analysis of free vibration for the first mode and this value is operated as 1. T_{DOF} symbolizes the total number of degrees of freedom for the powerful control factors in ANOVA and this value was

employed to be 4. N implies the total number of finite element analysis and it was determined to be 8 for Taguchi’s L8 orthogonal array as shown in Table 3. Thus, n_{eff} was found to be 1.6. CI_{CA} and CI_{POP} were analyzed as $341.72 \pm$ and ± 211.93 , respectively. The expected confidence interval for confirmation numerical analysis [11] is:

$$\text{Mean } \mu_{\alpha} - CI_{CA} < \mu_{\alpha} < CI_{CA} + \text{Mean } \mu_{\alpha}$$

The population connected to the 95 % confidence interval [11] is:

$$\text{Mean } \mu_{\alpha} - CI_{POP} < \mu_{\alpha} < CI_{POP} + \text{Mean } \mu_{\alpha}$$

The fundamental frequency for the first mode and predictive results for the optimum level using predicted confidence intervals were listed in Table 6.

Table 6. Optimum response.

Designation	Numerical Result	Predictive Result	Predicted Confidence Intervals for 95% Confidence Level
A ₂ B ₂	2947.40 Hz	2902.62 Hz	2560.9 < μ_{α} < 3244.34 for CI_{CA} 2690.69 < μ_{α} < 3114.55 for CI_{POP}

5. CONCLUSIONS

Impacts of the cross-sections and ceramic materials on the fundamental free vibration behavior of beams were analyzed using 3-D finite element model based on ANSYS software. The numerical analyses were performed using Taguchi’s L8 orthogonal array which has two control factors. The levels of the first control factor were assumed as triangular and hexagonal cross-sections while the levels of the second control factor were considered as ceramic materials such as Zirconia (ZrO₂), Silicon nitride (Si₃N₄), Alumina (Al₂O₃), and Silicon carbide (SiC). The significant levels and percent contribution rate of the cross-sections and ceramic materials on fundamental frequency analysis were carried out using ANOVA while the effects of the control factors were performed using S/N ratio analysis. The following conclusions are noted from this study:

- The maximum fundamental frequency result was obtained using hexagonal cross-section of beam designed from silicon nitride.
- The percent contribution ratios of control factors on numerical fundamental free vibration of the beams were found as 67.45 for ceramic material and 31.50 for cross-section of beams.
- Ceramic materials and the cross-sections were carried out to be the significant control factors owing to $P < 0.05$.
- The maximum impact was occurred in free end of beams while the minimum impact was determined in clamped end.
- The free vibration behavior of the beams with triangular cross-sections are smaller compared to the beams which have hexagonal cross-sections.
- Estimated optimum fundamental frequency at 95 % confidence intervals was obtained to be $2560.9 < \mu_{\alpha} < 3244.34$ for CI_{CA} and $2690.69 < \mu_{\alpha} < 3114.55$ for CI_{POP} .

REFERENCES

[1] Shen, H.-S. Functionally Graded Materials : Nonlinear Analysis of Plates and Shells. Boca Raton; New York; London, CRC Press, 2009.
 [2] Balhaddad, A.S., Onipede, D. (1998). "Three-Dimensional Free Vibration of Pretwisted Beams". AIAA Journal, 36, 1524-1528.


- [3] Evran, S. (2018). "Numerical First Mode Frequency Analysis of Axially Layered Functionally Graded Tapered Beams". *Ömer Halisdemir Üniversitesi Mühendislik Bilimleri Dergisi*, 7, 399-406.
- [4] Giunta, G., Metla, N., Koutsawa, Y., Belouettar, S. (2013). "Free Vibration and Stability Analysis of Three-Dimensional Sandwich Beams Via Hierarchical Models". *Composites Part B: Engineering*, 47, 326-338.
- [5] Fang, J., Zhou, D., Dong, Y. (2017). "Three-Dimensional Vibration of Rotating Functionally Graded Beams". *Journal of Vibration and Control*, 24, 3292-3306.
- [6] Evran, S. (2018). "Natural Frequency Analysis of Layered Functionally Graded Beams". *Anadolu University of Sciences & Technology-A: Applied Sciences & Engineering*, 19, 83-94.
- [7] Evran, S., Yılmaz, Y. (2017). "The Effects of Layer Arrangements on Fundamental Frequency of Layered Beams in Axial Direction". *Sakarya Üniversitesi Fen Bilimleri Enstitüsü Dergisi*, 21, 968-977.
- [8] Alshorbagy, A.E., Eltaher, M.A., Mahmoud, F.F. (2011). "Free Vibration Characteristics of a Functionally Graded Beam by Finite Element Method". *Applied Mathematical Modelling*, 35, 412-425.
- [9] Yılmaz, Y., Evran, S. (2016). "Free Vibration Analysis of Axially Layered Functionally Graded Short Beams Using Experimental and Finite Element Methods". *Science and Engineering of Composite Materials*, 23, 453-460.
- [10] Talha, M., Singh, B.N. (2010). "Static Response and Free Vibration Analysis of Fgm Plates Using Higher Order Shear Deformation Theory". *Applied Mathematical Modelling*, 34, 3991-4011.
- [11] Ross, P.J. *Taguchi Techniques for Quality Engineering*, McGraw-Hill International Editions, 2nd Edition, New York, USA, 1996.
- [12] ANSYS Help, Version 13.



International Journal of Engineering and Innovative Research

<http://dergipark.gov.tr/ijeir>

DETERMINATION OF ATTITUDES AND QUALIFICATIONS OF CIVIL ENGINEERING STUDENTS FOR USE OF VOCATIONAL SOFTWARE

Melda Alkan Çakıroğlu¹ 

¹Isparta University of Applied Sciences, Faculty of Technology, Department of Civil Engineering, Isparta, Turkey.

*Sorumlu Yazar: meldacakiroglu@isparta.edu.tr

(Received: 15.05.2020; Revised: 03.06.2020; Accepted: 15.06.2020)

ABSTRACT: It is extremely important for candidate engineers of today to be raised as equipped engineers who have grasped the importance of technology throughout their education life and who use it effectively and efficiently, are aware of the responsibilities brought by their profession, can generate practical and analytical solutions when faced with problems, constantly follow the developments in their professional field, are aware of lifelong learning, can apply their knowledge acquired during their academic life to life, and briefly who can fulfill the requirements of the age of technology. In a sense, candidate engineers need to have the knowledge, skills and self-confidence to effectively use technology during the education process so that they will be able to fulfill all the aforementioned requirements. In this context, in terms of professional development, it is important for candidate engineers to have an insight about computer software related to their professional fields and improve themselves continuously in this regard. By the courtesy of computer software packages, which have developed rapidly in recent years, design and analysis of an engineering system can be done by software packages based on theoretical principles on the basis of standards and regulations. In this context, the fact that the engineer candidates can use the package programs related to their professional fields is an important factor in terms of employment. The aim of this study was to gain insight into the knowledge and awareness of Civil Engineering students about the package programs related to their professional fields, which programs will also contribute to their employment after graduation, and to learn their interest in using these programs. In accordance with this aim, the idea to conduct this descriptive study emerged in order to determine the attitudes and skills of the students from the Department of Civil Engineering, Faculty of Technology, Isparta University of Applied Sciences to using the package programs related to their professional field and knowing programming languages. In this study, a survey was conducted on a total of 311 students studying at the Department of Civil Engineering, Faculty of Technology, Isparta University of Applied Sciences during the academic year 2018-2019 to measure their knowledge and usage of package programs. The analyses were performed by SPSS statistical package program, and tests such as frequency analysis, variance analysis, t-test and reliability analysis were used to analyze data. In the light of the data obtained, it was investigated whether the attitudes of the students to using package programs showed any significant differences by variables, including class level, gender, purpose of using computer and using package programs.

Keywords: Civil Engineering, Technology, Computer, Professional Software, Package Program, Program Languages.

1. INTRODUCTION

Technological advances force companies to hire employees well-trained in the field of computer. University education is one of the most important opportunities to have an education and gain knowledge in this field before stepping into the business life [27]. When today's conditions are examined and based on estimations regarding scientific and technological advances that can be seen in the near future, it is clear that the new generation Civil Engineers should be trained as engineers who can think, produce solutions to problems, are open to

innovations and interpret such innovations [14]. Use and dissemination of information technologies in areas such as engineering education that use, produce and, in short, reform technology is inevitable [2].

Computer programs, developed in recent times that analyze and design are among the most important factors that led to the analysis phase [1]. The possibilities offered by the computer package programs have shown their effect especially in the field of engineering. Computer technology and special technical software are so developed that engineers and computers have become an inseparable duo [11]. Today, software designed for construction companies, capable of managing all field activities, project management, financial and operational activities, has started to be used in the construction sector [22].

Since computer package programs make it possible to design, plan, analyze and report processes in a fast and practical way, designers of software offer training and enhancement support, programs are able to constantly upgrade themselves according to new developments, and have visual features, the use of package programs has become widespread. Now, many engineering problems can be solved with advanced computer package programs. Therefore, it would be useful to look at students' knowledge, skills and attitudes for use of these programs in order to enable them to use the computer package programs related to their professional fields in an appropriate and effective manner throughout and after their engineering education.

When the literature is examined, it is seen that the researchers are working on engineering education and these studies are increasing day by day. Studies conducted on this subject matter include, among others, engineering education [6], civil engineering education [38], [4], [5], [37], [26], [7], three-phase laboratory teaching and learning methodology in the engineering education [10], efficacy of e-learning and traditional learning in the construction safety education [16], use of computer in engineering and architecture education [30], [28], [18] importance of the computer-assisted education in professional development [15], efficacy of health and safety training in the construction industry using traditional tools and computer-assisted technologies (H&S) [13], computer software and communication technologies in the construction industry [39] and [22], Building Information Model in the construction industry (BIM) [12] and [29], use of the PpcProject software in the Software Project Management for educational purposes [32], use of three-dimensional (3D) and Virtual reality (VR) models in the civil engineering education [33], examination of advantages offered by Autodesk Developer Network (ADN) and Academic Partnership (AP) programs in terms of university education [35].

In this study conducted by [3], a questionnaire was applied to the fourth grade students studying in Civil Engineering departments of Çukurova University, Erciyes University and Gazi University in order to determine the deficiencies of civil engineering education, and as a result of questions posed in order to ascertain competence of students terms of "Level of Use in Package Programs and Software", it was concluded that the students were competent in using MS Office and AutoCAD software but they found themselves incompetent in the use of structure analysis package programs. In the study conducted by [21], a questionnaire was applied to the senior students of the Civil Engineering Department of Gazi University Faculty of Engineering in order to determine factors involved in selection of the graduation project and the project process and it was found out that very few students used programming language in their projects and majority of students did not want to use software programs. According to [26], it has been suggested that classes for teaching package programs becoming increasingly widespread at universities may lead to an extremely wrong and dangerous thought in students

that theoretical knowledge and classes are unnecessary and may, in turn, help engineers with a poorly developed theoretical foundation who are good at inputting data into package programs graduate from universities, causing a decrease in the quality of engineering services. In this study, it is emphasized that the necessary limit should be set for use of package programs in education programs, importance should be attached to the selection of package programs taught and the fact that these programs cannot replace the thought of engineering and an awareness should be raised in students. Improving students' ability to write programs in at least one computer language would be more beneficial in terms of improving the quality of engineering services.

This study emerged from the understanding that it would be beneficial for the employment of students to explore their interest and desire to learn package programs and to show the extent to which they benefited from computer technology. In this context, a questionnaire study was conducted in order to measure attitudes and skills of the students from the Department of Civil Engineering, Faculty of Technology, Isparta University of Applied Sciences for using the package programs related to their professional field.

The study, answers to the following questions were sought:

Among students of Civil Engineering:

1. What is their level of learning the computer software related to their field of profession?
2. What is their level of knowledge and skills about learning package programs?
3. What do they think about the inclusion of package programs in teaching?

2. STUDY GROUP

The study group of the research consists of 709 students studying in Civil Engineering Department, Faculty of Technology of Isparta University of Applied Sciences in the fall semester of 2018-2019 academic year. In this study, no sample selection was made and students in all classes were included in the research. However, only those who volunteer were included in the research for participation and no measurement tool was applied to those not wishing to take part. Demographic data of 311 students who participated in the study is given in Table 1.

Table 1. Demographic information of the students that participating in the research.

Variables	Categories	f	%
Gender	Male	244	78.5
	Female	67	21.5
Age	17-21	128	41.2
	22-26	169	54.3
	27-31	8	2.6
	32-36	6	1.9
Education	1. Education	179	57.6
	2. Education	132	42.4
Class	1. Class	55	17.7
	2. Class	44	14.1
	3. Class	97	31.2
	4. Class	115	37.0
	TOTAL	311	100.0

3. METHOD

In this study, the answer for the question "What are knowledge and skills of Civil Engineering Department students for using a package program in their field of profession and their attitudes towards learning?" was sought. Therefore, as a method, it was decided to use numerical data in order to reach large sample groups and to enable statistical evaluation in a short period of time. The study was limited to students studying at the Civil Engineering Department, Faculty of Technology of Isparta University of Applied Sciences.

Also, it was assumed that, during the study;

1. The students who answered the questionnaire would give sincere and objective answers to questions.
2. The sample would represent the population.

Permission was obtained from the Dean's Office of the Faculty of Technology of Isparta University of Applied Sciences for the application of the questionnaire. During the study, a questionnaire study focused on the students' learning and using competencies of the package program was planned and, at the stage of determining the questions of the questionnaire, related literature was screened and questionnaires conducted by [19], [20], [36], [8], [25], [9], [31], [23], [24] were reviewed and used for the purpose of preparing questions.

The questions were presented to the opinions of 2 experts from the Departments of Computer and Civil Engineering in order to assess the scope validity, robustness and safety of the questions, and questions found to be unnecessary in terms of scope, language and expression were removed following an examination based on feedbacks received from the experts and the questionnaire was given its final shape.

Questionnaire study is composed of 3 parts and 42 items with the first part being aimed at determining the personal details of participants (class, education, age, gender), the second part being aimed at measuring competence in terms of computer program use and learning level of computer programs, the third part being aimed at their perspectives about learning the use of the package program in the field of profession, their expectations of the software they want to learn, their suggestions on effective use of package programs in education and their attitudes for use of programs. Path three of the study consists of five point likert scale type options such as (1) I certainly agree, (5) I do not agree at all, which have a neutral central point and are considered to be the most practical method of measurement. The answers given to each item of the questionnaire were classified in the IBM SPSS Statistics 23.0 software program and represented by numerical values.

Frequency and percentage values were calculated to interpret the demographic part of the questionnaire. Since the part relating to questions "What are your wishes you would like to achieve when learning the package program? and "What is your opinion about use of package programs in your field of profession and teaching of it as a lesson?" is of the five-point Likert type, assessment range of their arithmetic mean was found to be 0.80. Accordingly, for the purpose of analysis of data: ranges such as 4.21-5.00 "I certainly agree", 4.20-3.41 "I agree", 3.40-2.61 "I neither agree nor disagree", 2.60-1.81 "I don't agree", 1.80-1.00 "I don't agree at all" were taken into account. Students' average scores of attitudes towards learning and using the package program were evaluated for each item based on these ranges. Findings about whether or not students' attitudes towards the use of package program showed a significant

difference according to gender were determined by t test. Findings about whether or not students' attitudes towards the use of package program in education showed a significant difference depending on the level of class were determined by ANOVA test.

The Cronbach Alpha internal consistency coefficient calculated for the reliability of the parts of the questionnaire regarding expectations from package program, usage and teaching perspective regarding the package program were calculated as 0.881 and 0.883, respectively. Accordingly, there is internal consistency between all items of the scale. According to the findings, factor analysis was conducted to determine the construct validity of the questionnaire and the factor loads ranged from 0.89 to 0.91, and the total variance under one factor was found to be 55.48. Factor loads of items included in the factor vary between 0,318 and 0,831. The factor loads of items in the questionnaire were found to be higher than 0,300. It can be said that it is sufficient in terms of construct validity. Kaiser-Meyer-Olkin (KMO) and Barlett's Test was found to be 0,915. It was ascertained that data are suitable for factor analysis.

4. RESEARCH FINDINGS

In this part, the findings obtained from the statistical analysis of the responses given to the questionnaires prepared for the use of package program by Civil Engineering Department students are given in tables. Table 2 shows students' general opinions about the items related to their expectations from package program education. Table 3 shows the general views of students regarding items concerning their standpoints about use of package programs related to their field of profession and teaching of such programs as a lesson.

Table 2. Views on the question “What are your wishes you want to be met while learning package program?”.

What are your wishes you want to be met while learning package program?		I certainly agree	I agree	I neither agree nor disagree	I don't agree	I don't agree at all
1. Provision of practical solutions by it	f	218	82	11	-	-
	%	70.10	26.40	3.50	-	-
2. Turkish is its language	f	13.80	93	56	13	11
	%	44.40	29.90	18.00	4.20	3.50
3. It's easy to install	f	166	100	30	13	2
	%	53.40	32.20	9.60	4.20	6.00
4. It is easy to learn and comprehensible	f	183	96	25	5	2
	%	58.80	30.90	8.00	1.60	0.60
5. It's compatible with the computer hardware	f	186	97	23	3	2
	%	59.80	31.20	7.40	1.00	0.60
6. It accelerates the project and design process	f	196	91	21	3	-
	%	63.00	29.30	6.80	1.00	-
7. Availability of the technical support service	f	196	85	28	1	1
	%	63.00	27.30	9.00	0.30	0.30
8. Regular updates	f	185	90	32	3	1
	%	59.50	28.90	10.30	1.00	0.30
9. It is affordable	f	214	62	27	8	-
	%	68.80	19.90	8.70	2.60	-

96.50% (300 students) stated that they wanted it to offer practical solutions while learning package program, whereas 3.50% (11 students) stated that they were undecided. 92.30% (287 students) expressed a positive opinion that it would accelerate the student project and design process and 1.00% (3 students) stated that this expression was not effective in learning the program.

Table 3. Views on the question "What is your opinion about use of package programs in your field of profession and teaching of it as a lesson?".

What is your opinion about use of package programs in your field of profession and teaching of it as a lesson?		I certainly agree	I agree	I neither agree nor disagree	I don't agree	I don't agree at all
1. It is useful to use package programs in vocational lessons.	f	198	87	24	1	1
	%	63.70	28.00	7.70	0.30	0.30
2. Theoretical and practical information can be used together with the package program.	f	164	109	36	1	1
	%	52.70	35.00	11.60	0.30	0.30
3. Package programs contribute to the learning process while practicing.	f	174	99	33	4	1
	%	55.90	31.80	10.60	1.30	0.30
4. Package program courses must be compulsory course.	f	144	83	69	13	2
	%	46.30	26.70	22.20	4.20	0.60
5. I have enough knowledge about package programs.	f	76	95	85	44	11
	%	24.40	30.50	27.30	14.10	3.50
6. I am in need of education on package programs.	f	147	102	49	10	3
	%	47,3	32,8	15,8	3,2	1
7. I keep abreast of package programs related to my field.	f	94	120	66	23	8
	%	30.20	38.60	21.20	7.40	2.60
8. I have gained basic knowledge about package programs for the first time at the university.	f	116	98	53	29	15
	%	37.30	31.50	17.00	9.30	4.80
9. I can learn to use a package program at the university.	f	119	117	58	12	5
	%	38.30	37.60	18.60	3.90	1.60
10. Even though I take package program lessons, I am unable to draw projects.	f	80	93	72	46	20
	%	25.70	29.90	23.20	14.80	6.40
11. I think that I am sufficient in terms of entering the project data into the program, analyzing and interpreting the results.	f	81	101	90	29	10
	%	26.00	32.50	28.90	9.30	3.20
12. I am more interested in classes related to package programs.	f	125	121	48	13	4
	%	40.20	38.90	15.40	4.20	1.30
13. A certain level of foreign language proficiency is required to learn the program.	f	147	115	45	3	1
	%	47.30	37.00	14.50	1.00	0.30
14. I have to have a good command of the program to advance in the professional field.	f	172	90	41	8	-
	%	55.30	28.90	13.20	2.60	-
15. I can improve myself on package programs after graduation.	f	135	105	55	11	5
	%	43.40	33.80	17.70	3.50	1.60
16. I can also learn the package program by myself without education	f	99	94	90	24	4
	%	31.80	30.20	28.90	7.70	1.30
17. I think that one is required to be knowledgeable about the package program for a job.	f	181	90	32	6	2
	%	58.20	28.90	10.30	1.90	0.60

91.70% (285 students) agreed that "It is useful to use package programs in vocational courses", 7.70% (24 students) stated that they were undecided and 0.60% (2 students) stated that they did not agree. 87.70% (273 students) expressed positive opinion for the phrase "Package programs contribute to the learning process while practicing", 10.60% (33 students) neither agreed nor disagreed and 1.60% (5 students) stated that it would not make a contribution. 73.00% (227 students) of the students agreed that "Package program courses should be compulsory course",

while 4.80% (15 students) stated that they did not agree and 22.20% (69 students) stated that they were undecided. 80.10% (249 students) stated that they needed education on package programs, whereas 4.20% (13 students) stated that they did not need education on package programs. 15.80% (49 students) stated that they were undecided. 75.90% (236 students) agreed with the phrase "I can learn to use a package program in the university" while 5.50% (17 students) stated that they did not. 18.60% (58 students) stated that they were undecided. 79.10% (246 students) stated that they were interested in the courses related to the package programs, while 5.50% (17 students) stated that they did not agree. 15.40% (48 students) stated that they were undecided. 62.00% (193 students) stated that they agreed with the item "I can learn the package program by myself without education." while 9% (28 students) stated that they did not agree with the idea that they could learn it by themselves. 28.90% (90 students) stated that they were undecided.

Table 4 shows Independent Sample t-test for the gender factor in order to measure their willingness to learn the package program according to independent variables and their skills and knowledge in using the program, whereas Table 5 shows one-way variance (ANOVA) analysis comparisons for comparison of their perspectives about learning to use the package program according to their class levels. Level of significance was taken as $p < 0.05$.

Table 4. Distribution of students' views about their willingness to learn package program and teaching of it as a lesson according to gender variable and results of t test.

Items	Gender	n	\bar{X}	S	t	p
Would you like to learn a package program relating to your field of profession?	Male	244	1.71	1.115	1.607	0.109
	Female	67	1.48	0.841		
What are your wishes you want to be met while learning package program?	Male	244	1.58	0.579	2.114	0.033
	Female	67	1.42	0.409		
What is your opinion about use of package programs in your field of profession and teaching of it as a lesson?	Male	244	1.91	0.560	-0.248	0.804
	Female	67	1.92	0.527		

When the table was examined, there were no significant differences according to gender in the opinions of students about the items in parts of "Would you like to learn a package program related to your field of profession? ($P > 0.05$) and "What is your opinion about use of package programs in your field of profession and teaching of it as a lesson?". A significant difference was found in items relating to the group "What are your wishes you want to be met while learning package program?". Male students' willingness to learn package programs is higher than female students. ($\bar{X} = 1.71$) ($\bar{X} = 1.48$) Female students' attitudes towards using package programs and teaching of it as a lesson were better than male students with a little difference. ($\bar{X} = 1.92$) ($\bar{X} = 1.91$)

Table 5. Results of the one-way variance (ANOVA) analysis comparisons for comparison of their perspective differences about learning to use the package program according to their class levels.

Items	Class	n	\bar{X}	S	f	p
How did you learn to use computer software related to your field of profession?	1. Class	55	1.843	0.1012	1.813	0.145
	2. Class	44	1.780	0.1186		
	3. Class	97	1.818	0.0999		
	4. Class	115	1.801	0.1399		
Would you like to learn a package program relating to your field of profession?	1. Class	55	1.730	1.1130	2.003	0.114
	2. Class	44	1.390	0.7540		
	3. Class	97	1.580	0.9880		
	4. Class	115	1.810	1.1840		
What are your wishes you want to be met while learning package program?	1. Class	55	1.477	0.4629	0.950	0.417
	2. Class	44	1.472	0.4923		

Items	Class	n	\bar{X}	S	f	p	
Opinion about use of package programs in your field of profession and teaching of it as a lesson	3. Class	97	1.549	0.5576	1.680	0.171	
	4. Class	115	1.602	0.6011			
	1. Class	55	1.972	0.5371			
	2. Class	44	1.985	0.5183			
		3. Class	97	1.949	0.5544		
		4. Class	115	1.821	0.5650		

Tukey HSD test was conducted to determine the group in favor of which the difference was (Table 6-8). As seen in the tables, there was no significant difference between the opinions in the items according to the class variable ($p > 0.05$).

Table 6. Results of Tukey HSD test according to students' willingness for learning the package program and the class variable.

Class	Mean Difference	p	
1. Class	2. Class	0.341	0.386
	3. Class	0.150	0.836
	4. Class	-0.081	0.966
2. Class	1. Class	-0.341	0.386
	3. Class	-0.191	0.754
	4. Class	-0.422	0.113
3. Class	1. Class	-0.150	0.836
	2. Class	0.191	0.754
	4. Class	-0.231	0.389
4. Class	1. Class	0.081	0.966
	2. Class	0.422	0.113
	3. Class	0.231	0.389

Table 7. Results of Tukey HSD test according to wishes of students they want to be met and the class variable.

Class	Mean Difference	p	
1. Class	2. Class	0.005	1.000
	3. Class	-0.072	0.866
	4. Class	-0.125	0.509
2. Class	1. Class	-0.005	1.000
	3. Class	-0.076	0.870
	4. Class	-0.130	0.545
3. Class	1. Class	0.072	0.866
	2. Class	0.076	0.870
	4. Class	-0.053	0.896
4. Class	1. Class	0.125	0.509
	2. Class	0.130	0.545
	3. Class	0.053	0.896

Table 8. Results of Tukey HSD test according to students' point of view regarding field of profession and use of package program as well as teaching of it as a lesson and the class variable.

Class		Mean Difference	P
1. Class	2. Class	-0.013	0.999
	3. Class	0.024	0.994
	4. Class	0.152	0.335
2. Class	1. Class	0.013	0.999
	3. Class	0.037	0.983
	4. Class	0.165	0.331
3. Class	1. Class	-0.024	0.994
	2. Class	-0.037	0.983
	4. Class	0.128	0.333
4. Class	1. Class	-0.152	0.335
	2. Class	-0.165	0.331
	3. Class	-0.128	0.333

4. CONCLUSION

Today, analysis and design of building systems can be carried out with computer programs including advanced analysis techniques in accordance with international and earthquake regulations. It can be said that keeping abreast of programs related to the field of profession and having a good command of such programs would give the civil engineer an important advantage in terms of employment since the technological developments are so fast that the programs in this field will increase continuously and improve themselves.

Therefore, first of all, students' knowledge, skills and attitudes should be considered in order to enable civil engineering students to use computer package programs related to their professional fields in a beneficial and effective manner throughout and after their engineering education. In this study, it is aimed to investigate the interest and willingness of students of the civil engineering department in learning package programs.

Based on the data obtained from the study, it was determined that the students did not have enough information about the use of package programs. 80.10% (249 students) stated that they needed education on package programs whereas 4.20% (13 students) stated that needed no education. 15.80% (49 students) stated that they were undecided. 75.90% (236 students) stated that they agreed with the phrase "I can learn to use package program in university" and 5.50% (17 students) stated that they did not agree with this phrase. It was observed that students had positive attitudes towards the use and learning of vocational package program applications. 91.70% (285 students) of the students stated that it would be beneficial to use package programs in vocational classes. 87.70% (273 students) found positive the statement "Package programs contributed to the learning process while practicing" and 1.60% (5 students) stated that they did not think that it would make any contribution. 79.10% (246 students) stated that they were interested in classes related to the package programs, while 5.50% (17 students) stated that they did not agree with this. 15.40% (48 students) stated that they were undecided.

In this context, in order to increase students' interests and attitudes, it is thought that it would be useful if educational institutions improved their technological infrastructure to a possible extent throughout the education and taught basic principles of software as well as basic lessons in vocational classes. However, it should be emphasized that the student needs to examine, interpret and control the results obtained from the program at all times during the education.

Acknowledgments

I would like to extend thanks sincerely to Civil Engineering Department, Dean's Office of the Faculty of Technology of Isparta University of Applied Sciences and all students participate survey which supported this study.

REFERENCES

- [1] Altın, S. (2009). Improvement requirements in civil engineering education, Proceedings Book of the First Civil Engineering Education Symposium, 1-19. http://www.imo.org.tr/resimler/ekutuphane/pdf/16664_37_18.pdf, Date of Access: 07.05.2019
- [2] Baran, T. and Kahraman, S. (2009). "Soul of the Age" in universities: Contribution to education technologies of information, First Civil Engineering Education Symposium, 111-118. Antalya, Turkey.
- [3] Bayram, S. Çelik, T.G. and Oral, L.E. (2015). Educational Qualification and Vocational Competence of Engineering Students: Civil Engineering Student Perspective, Turkish Journal of Education, Volume 4, Issue 1, 4-18.
- [4] Birinci, F. (2009). Solutions and problems, general situation education of civil engineering in Turkey, First Civil Engineering Education Symposium, 243-252. Antalya, Turkey.
- [5] Birinci, F. and Koç, V. (2007). General structure of education of civil engineering in Turkey and new approaches for development, 4th Construction Management Congress, TMMOB-IMO Istanbul Branch, 343-352.
- [6] Bosman, L. and Fernhaber, S. (2019). Applying Authentic Learning through cultivation of the entrepreneurial mindset in the engineering classroom, Education Sciences, 9, 7; doi:10.3390/educsci9010007
- [7] Cachim, P., (2015). An overview of education in the area of civil engineering in Portugal, International Scientific Conference Urban Civil Engineering and Municipal Facilities, SPbUCEMF-2015, Procedia Engineering 117, 431 – 438. doi: 10.1016/j.proeng.2015.08.191
- [8] Çağlar, İ. Dikilitaş, S. and Coşar, M. (2005). The productivity effect of the intensive usage of the computer technologies in the vocational schools, 1st. International Vocational and Technical Education Technologies Congress, 05–07 September 2005, 174-181. Istanbul, Turkey.
- [9] Çelik, F. Kocaman, F. and Önal, A.S. (2008). A research on the computer literacy levels of primary and lower-secondary teachers in Burdur, Mehmet Akif Ersoy University Journal of Faculty of Education, 8(15), 1-13.
- [10] Chowdhury, H. Alam, F. and Mustary, I. (2019). Development of an innovative technique for teaching and learning of laboratory experiments for engineering courses, Energy Procedia 160, 806-811, 2nd International Conference on Energy and Power, ICEP2018, 13–15 December 2018, Sydney, Australia, 10.1016/j.egypro.2019.02.154
- [11] Demir, N. (2011). Chief engineer, Second Civil Engineering Education Symposium, Union of Chambers of Turkish Engineers and Architects, Proceedings Book, 23-24 September 2011, Mugla University, Atatürk Cultural Center, 79-105. Muğla.
- [12] Fridrich, J. and Kubečka, K. (2014). BIM – The process of modern civil engineering in higher education, Procedia - Social and Behavioral Sciences 141, 763 – 767. WCLTA 2013, doi: 10.1016/j.sbspro.2014.05.134
- [13] Gao, Y. Gonzalez, V. and Yiu, T.W. (2019). The effectiveness of Traditional Tools and Computer-Aided Technologies for Health and Safety Training in the construction sector: A systematic review, Computers & Education <https://doi.org/10.1016/j.compedu.2019.05.003>
- [14] Genç, Numanoğlu, A. Eryılmaz, M. and Şahin, B. (2016). Distance education in civil engineering: Model lesson study with the "Moodle", Third Civil Engineering Education Symposium, 8-9 Ocak 2016, 104-111.
- [15] Güllüoğlu, S.S. (2010). The importance of computer aided education on professional development, doi: 10.5824/1309-1581.2010.002.x, AJIT-e Online Academic Journal of Information Technology, Volume: 1, Issue: 1.
- [16] Ho, C-L. and Dzeng, R-J. (2010). Construction Safety Training via e-learning: Learning effectiveness and user satisfaction, Computers & Education 55, 858–867. doi:10.1016/j.compedu.2010.03.017
- [17] IBM SPSS Statistics 23.0. <https://www-01.ibm.com/support/docview.wss?uid=swg24038592>, Date Access: 06.05.2019.
- [18] Işık, B.Ö. (2017). Contribution of computer-aided design programs to architectural education, The Journal of International Social Research, Volume: 10 Issue: 51, Issn: 1307-9581, doi: <http://dx.doi.org/10.17719/jisr.2017.1814>
- [19] İnceoğlu, M.M. (2002). An impression on basic computer education in universities, Academic Informatics 2002, 6-8 February 2002, Selcuk University, Konya, Turkey. <https://ab.org.tr/ab02/tammetin/92.doc>

- [20] İnceoğlu, M.M. (2004). The opinion of about teaching JAVA programming language of BÖTE students, XIII. National Congress on Educational Sciences, 6-9 July 2004, Inonu University, Faculty of Education, Malatya, Turkey.
- [21] Kaya, N. Yünkül, K. and Çiçek, C.T. (2017). Assessment by importance to and student preferences of graduation Projects of civil engineering sStudents, Fourth Civil Engineering Education Symposium, (IMES 2017), 161-174. Izmir, Turkey.
- [22] Keleş, A.E. and Kaya Keleş, M. (2018). Examination of computer software and information technologies whose usage increased in the construction industry, *El- Cezeri Journal of Science and Engineering*, 5(2); 610-617.
- [23] Korkut, A. (2015). Establishment of infrastructure for education and training in planning, design and arts, Namik Kemal University, Scientific Research Project Supported by Higher Education Institutions.
- [24] Korkut A. and Özyavuz, M. (2016). A research on the necessity of technology infrastructure in design training, *Journal of Tekirdag Agricultural Faculty*, 13(02).
- [25] Köse, S. Gencer, A.S. and Gezer, K. (2007). Vocational high school students' attitudes toward computer and iInternet, *Pamukkale University Journal of Education*, (1) 21.Issue, 44-54.
- [26] Oğuz, C. Altın, S. Yaman, İ.Ö. Kırçıl, M.S. Bakır, A. and Sönmez, G. (2009). Truth of Turkey in education of civil engineering, *First Civil Engineering Education Symposium*, 207-241, Antalya.
- [27] Özdemir, M.S. (2001). A study on measuring the change of computer knowledge and use profile of OGU Industrial Engineering Department Students, *Eng.&Arch.Fac.Osmangazi University*, Vol.XIV, No 1, 1-17.
- [28] Özmen, G. (2011). Computer in education of civil engineering, *Second Civil Engineering Education Symposium*, 47-53. Mugla, Turkey.
- [29] Özorhon, B. and Çağlayan, S. (2017). Determination of the content of the lessons of Building Information Modeling (BIM) planned open license program in the departments of civil engineering in Turkey, *Fourth Civil Engineering Education Symposium (in memory of Ayhan Emekli)*, *Congress Symposium Proceedings Book*, 95-106.
- [30] Palmer, S. (2000). On- and off-campus computer usage in engineering education, *Computers & Education* 34, 141-154.
- [31] Polat, H. and Güzel, E. (2011). University students' attitudes towards the use of computers and internet. *5th International Computer&Instructional Technologies Symposium*. Elazığ, Turkey.
- [32] Salas-Morera, L. Arauzo-Azofra, A. García-Hernández, L. Palomo-Romero, J.M. and Hervás-Martínez, C. (2013). PpcProject: An educational tool for software project management, *Computers & Education* 69, 181–188. <http://dx.doi.org/10.1016/j.compedu.2013.07.018>
- [33] Sampaio, A.Z. Ferreira, M.M. Rosário, D.P. and Martins, O.P. (2010). 3D and VR models in civil engineering education: Construction, rehabilitation and maintenance, *Automation in Construction* 19, 819–828. doi:10.1016/j.autcon.2010.05.006
- [34] Smirnova, Z.V. Vaganova, O.I. Gatsalova, L.B. Golubeva, O.V. and Chelnokova, E.A. (2019). Teaching package development for engineering training programs, *IOP Conf. Series: Materials Science and Engineering*, 483, 012033. doi:10.1088/1757-899X/483/1/012033
- [35] Tuchkevich, E. Rechinsky, A. Vysotskiy, A. Zolotova, J. and Tuchkevich, V. (2015). ADN and AP Programs for civil engineering students, *Procedia Engineering* 117, 1137 – 1142, *International Scientific Conference Urban Civil Engineering and Municipal Facilities, SPbUCEMF-2015*. doi: 10.1016/j.proeng.2015.08.247
- [36] Tuti, S. (2005). Investigation of the performance indicators on information and communication technologies in education, students' opinions and their perceived self-efficacy, *Hacettepe University, Division of Computer Education and Instructional Technologies, MsThesis*.
- [37] Üçüncü, O. (2009). Approaches on education of civil engineering, *First Civil Engineering Education Symposium, Congress Symposium Proceedings Book*, 375-384. Antalya, Turkey.
- [38] Yenigün, K. and Gürel, M.A. (2004). Some suggestions and evaluation of education of the civil engineering in Turkey, *1th National Congress on Engineering*, 20-21 May 2004, 149-156. Izmir, Turkey.
- [39] Yılmaz, G. Akçamete Güngör, A. and Demirörs, O. (2016). Information and communication technologies used in construction sector, *10th Turkish National Software Engineering Symposium*, October 24-26, 562-573. Canakkale, Turkey.